

## Responsive photonic polymer coatings

***Citation for published version (APA):***

van Heeswijk, E. P. A. (2019). *Responsive photonic polymer coatings*. [Phd Thesis 1 (Research TU/e / Graduation TU/e), Chemical Engineering and Chemistry]. Technische Universiteit Eindhoven.

***Document status and date:***

Published: 10/12/2019

***Document Version:***

Publisher's PDF, also known as Version of Record (includes final page, issue and volume numbers)

***Please check the document version of this publication:***

- A submitted manuscript is the version of the article upon submission and before peer-review. There can be important differences between the submitted version and the official published version of record. People interested in the research are advised to contact the author for the final version of the publication, or visit the DOI to the publisher's website.
- The final author version and the galley proof are versions of the publication after peer review.
- The final published version features the final layout of the paper including the volume, issue and page numbers.

[Link to publication](#)

***General rights***

Copyright and moral rights for the publications made accessible in the public portal are retained by the authors and/or other copyright owners and it is a condition of accessing publications that users recognise and abide by the legal requirements associated with these rights.

- Users may download and print one copy of any publication from the public portal for the purpose of private study or research.
- You may not further distribute the material or use it for any profit-making activity or commercial gain
- You may freely distribute the URL identifying the publication in the public portal.

If the publication is distributed under the terms of Article 25fa of the Dutch Copyright Act, indicated by the "Taverne" license above, please follow below link for the End User Agreement:

[www.tue.nl/taverne](http://www.tue.nl/taverne)

***Take down policy***

If you believe that this document breaches copyright please contact us at:

[openaccess@tue.nl](mailto:openaccess@tue.nl)

providing details and we will investigate your claim.

# Responsive Photonic Polymer Coatings

PROEFSCHRIFT

ter verkrijgen van de graad van doctor aan de Technische Universiteit  
Eindhoven, op gezag van de rector magnificus prof.dr.ir. P.F.T. Baaijens, voor  
een commissie aangewezen door het College van Promoties, in het openbaar te  
verdedigen op dinsdag 10 december 2019 om 16.00 uur

door

Ellen Petronella Arnolda van Heeswijk

Geboren te Lith

Dit proefschrift is goedgekeurd door de promotoren en de samenstelling van de promotiecommissie is als volgt:

Voorzitter: prof.dr.ir. E.J.M. Hensen  
1<sup>e</sup> Promotor: prof.dr. A.P.H.J. Schenning  
2<sup>e</sup> Promotor: prof.dr. D.J. Broer  
Copromotor: dr. N. Grossiord  
Leden: dr. A.C.C. Esteves  
prof.dr. C.N. Bowman  
prof.dr. C.E. Koning  
Adviseur: dr. M.G. Debije

*Het onderzoek of ontwerp dat in dit proefschrift wordt beschreven is uitgevoerd in overeenstemming met de TU/e gedragscode Wetenschapsbeoefening*

*"Anything is possible when you have  
the right people there to support you."*

- Misty Copeland

A catalogue record is available from the Eindhoven University of Technology  
Library ISBN: 978-90-386-4922-1

Copyright © 2019 by Ellen van Heeswijk

Printed by Gildeprint

The research described in this thesis was financially supported by SABIC

# Table of Content

<b>Summary</b>		VII
<b>Chapter 1</b>	Introduction	1
<b>Chapter 2</b>	Adhesion and alignment of cholesteric liquid crystalline coatings on flexible substrates	21
<b>Chapter 3</b>	Humidity-gated temperature-responsive broadband coatings	35
<b>Chapter 4</b>	Thiol-acrylic elastomer responsive photonic coatings	55
<b>Chapter 5</b>	Encapsulated single-substrate photonic reflectors	75
<b>Chapter 6</b>	Technology assessment	91
<b>Samenvatting</b>		103
<b>Acknowledgement</b>		107
<b>Curriculum Vitae</b>		111
<b>List of Publications</b>		112



# Summary

## Responsive photonic polymer coatings

Coatings are applied on nearly all daily used surfaces, providing protection or aesthetics to the substrate. However, most of these coatings are static, meaning that they are not responsive to environmental stimuli. In recent years, the demand for surfaces with stimulus-triggered responsive properties became increasingly prominent in both academic and industrial branches. Cholesteric liquid crystalline polymers, which are one dimensional photonic materials have emerged as attractive materials for the development of stimuli-responsive reflective coatings. The helical organization of the cholesteric liquid crystals causes selective reflection of light of which the wavelength can be tuned.

This thesis focusses on the fabrication of responsive photonic cholesteric liquid crystalline polymer coatings for flexible substrates that are able to change their reflective color in response to environmental changes such as temperature, humidity and solvents. First, photonic liquid crystalline coatings were prepared having good alignment and adhesion without the need for additional alignment layers, surface modifications, solvents or surfactants. For this, the cholesteric liquid crystals were aligned on the substrates by shear using an industrial scalable gap-applicator. To increase adhesion to the polymer substrates, the surface was pretreated with a photoinitiator benzophenone, allowing for covalent bonds between the substrate and the coating.

Secondly, three routes were investigated to create robust responsive photonic coatings, which could be processed using industrial relevant fabrication techniques. In the first approach, temperature-responsive coatings were fabricated using hydrogel-like photonic liquid crystals. These coatings were able to absorb and desorb water from the environment, thereby shifting the reflection band and thus the structural color. At a high environmental humidity, absorption



and desorption of water vapor from the air was regulated by temperature variations. Moreover, the width of the reflection band of a single-layer coating was increased to 400 nm, covering a substantial area of the infrared sunlight spectrum causing heat. Such materials are potentially interesting for energy-efficient indoor heat control, reflecting heat (near infrared light) during warmer periods and transmitting heat during cooler periods.

Solvent and temperature responsive reflective coating based on elastomeric cholesteric liquid crystals were fabricated as well. By using dithiols and diacrylates, liquid crystalline moieties were incorporated in the main chain, creating a less densely crosslinked network. The step growth polymerization kinetics could be monitored simply by a visible structural color change. By mask exposure or low intensity exposure to UV light followed by a post cure, responsive patterned or broad reflection band polymer network coatings were fabricated, respectively, needing no additional heating or solvents. Using a test setup for gravure printing, well aligned patterned coatings were prepared using again industrial relevant processes. These coatings showed reversible temperature responses at high temperatures (150-200°C) and swelling behavior towards several solvents.

In the last approach studied in this research photo-enforced stratification was used to form encapsulated single-substrate photonic reflectors. A single-layered coating was transformed into a cell during photopolymerization, having a non-polymerized cholesteric liquid crystalline mixture sandwiched between the substrate and a polymeric top layer. Due to the insolubility of the polymers and the non-polymerizable liquid crystalline mixture, the polymer phase-separates during polymerization to form an acrylic top-coat, providing the robustness of the coating. Since the cholesteric liquid crystals are not polymerized, large reflection band shifts were observed upon temperature changes of only a few degrees. Moreover, adhesion of the coating to the substrate was improved by providing walls to anchor the polymer top layer to the substrate.

Overall, this thesis shows that stimuli-responsive liquid crystalline photonic polymer coatings can be produced on flexible polymer substrates using industrial relevant processes. The coatings show good alignment and adhesion and several approaches were studied to introduce stimuli-responsive behavior in polymer coatings. These materials show the broad range of opportunities for liquid crystalline photonic coatings in developing stimuli-responsive materials for various applications, such as responsive paints, optical sensors, security features and smart infrared reflective windows.



# Chapter 1

## Introduction

---

This chapter is partially reproduced from: 'Environmentally responsive photonic polymers'  
E.P.A. van Heeswijk, A.J.J. Kragt, N. Grossiord, A.P.H.J. Schenning, *Chem. Commun.*, 2019,  
55, 2880-2891.

## 1.1 General introduction

Coatings provide protection or aesthetics to nearly all daily used surfaces. In recent years, the demand for surfaces with additional (stimulus-triggered) properties became increasingly prominent in many industrial branches. For example, surfaces that change their color based on variations in temperature, humidity, light or solvents are highly interesting for sensors, energy saving, rewritable paper and security features.<sup>[1-8]</sup> Many living organisms show various forms of irritability and adaptation. For instance, mammalian skin adapts to external temperature fluctuations aiding in a process called homeostasis in order to maintain internal body temperature and to function properly.<sup>[9]</sup> Other organisms use color changes for camouflage and communication.<sup>[10-12]</sup> For example, the blue damselfish *chrysiptera cyanea*, which changes from blue-green at daytime to violet at night in response to light and various beetles, which change their coloration in response to humidity.<sup>[13-15]</sup>

Environmentally triggered color changes may arise from modulations of photonic structures. These materials are generally fabricated by colloidal crystals, block copolymers or chiral nematic (*i.e.* cholesteric) liquid crystals (Ch-LC), with periodically nano-structured layers of alternating refractive indices. This periodic structure results in constructive interference of the light reflected at each interface according to Bragg's law (eq. 1.1).

$$\lambda = 2dn_{av}\cos\theta \quad \text{Eq 1.1}$$

Where  $\lambda$  is the wavelength of Bragg reflection,  $n_{av}$  is the average refractive index,  $d$  is the length of a repeating layer and  $\theta$  represents the angle of incidence light. As the equation shows, the wavelength of the photonic crystal depends on the refractive indices itself and periodicity of the layers. A responsive photonic material can thus be fabricated using a material that is able to change its refractive index or periodicity upon exposure to a stimulus.

One-dimensional anisotropic Ch-LC have emerged as attractive materials for the development of photonic stimuli-responsive systems as their color response can be programmed in a reversible manner. Ch-LC systems are obtained when chiral nematic LCs are used or when nematic LCs are doped with chiral molecules. These chiral molecules initiate a helical organization of the LCs wherein the molecular director of the successive 'layers' is displaced by a small rotation with respect to their neighboring layers (Figure 1.1a). The helical organization causes the system to reflect circularly polarized light of the same handedness in a photonic manner, while transmitting circularly polarized light with opposite handedness.

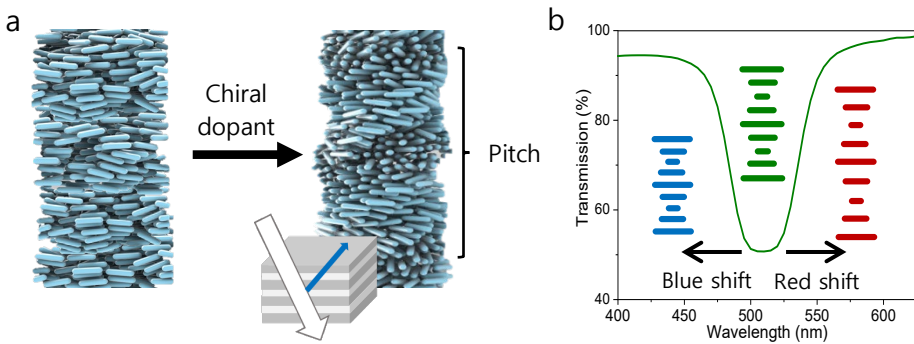


**Figure 1.1:** (a) Schematic representation of a nematic to cholesteric LC phase transition by addition of a chiral dopant.<sup>[16]</sup> The Ch-LC phase reflects one handedness of circular polarized light photonically due to the difference in extraordinary and ordinary refractive indexes of the LCs. (b) Typical transmission spectrum of a Ch-LC and simplified schematics of the Ch-LC pitches. An increase of the pitch will lead to a red shift of the reflection band whereas a decrease of the pitch results in a blue shift of the photonic coloration.

The helical pitch ( $P$ ) is defined as the length needed for a  $360^\circ$  rotation of the molecular director and equals  $2d$  in Bragg's law (Eq 1.2). The pitch length is inversely proportional to the helical twisting power ( $HTP$ ) and concentration ( $[C]$ ) of the chiral dopant added (Eq 1.3). The optical bandwidth ( $\Delta\lambda$ ) is determined by the pitch and the difference between the extraordinary ( $n_e$ ) and ordinary ( $n_o$ ) refractive index of the LCs that arises from the optical anisotropy (Eq 1.4).

$$\lambda = n_{av} * P \quad \text{Eq. 1.2}$$

$$P = \frac{1}{HTP * [C]} \quad \text{Eq. 1.3}$$

$$\Delta\lambda = (n_e - n_o) * P \quad \text{Eq. 1.4}$$

By polymerization of reactive mesogens in the Ch-LC phase, the helical alignment of the LCs is fixed and mechanical strength is provided by the network formed. Designing monomer mixtures carefully and including mesogens with different functionalities (*e.g.* monoacrylates and diacrylates), allows for tailoring of the desired final material properties. As the number of pitches is fixed by polymerization, shrinkage or expansion of the material will cause a decrease or increase in pitch length, respectively, resulting in a blue shift or red shift of the reflection band (Figure 1.1b). A loss of the reflection band will occur when the helical alignment is disrupted.

In this chapter, recent developments are discussed in the field of photonic LC materials that change coloration due to changes in the environmental stimuli: temperature, humidity and light. Irreversible responsive polymers and reversible responsive polymer films are included. Particular attention is given to the possible scalability and applications of these adaptive photonic materials.

## **1.2 Temperature-responsive Ch-LC polymers**

Irreversible as well as reversible temperature-responsive photonic polymers can be prepared by various methods. By embossing, temperature-responsive shape-memory coatings were prepared showing only one-way responsive behavior. Reversibly temperature-responsive coatings can be achieved by using Ch-LC elastomers that reversibly reorganize upon temperature fluctuations.

### **Irreversible temperature-responsive Ch-LC polymers**

Shape memory polymers are attractive to prepare one-way irreversible temperature-responsive photonic materials. They can fix a temporary shape and recover to their original shape upon heating. By embossing a glassy Ch-LC network above the glass transition temperature ( $T_g$ , ranging from 40 °C to 60 °C) and subsequently cooling, a cholesteric pitch was compressed in a temporary

alignment, resulting in a blue shift of the reflection band from 580 nm to 550 nm.<sup>[17]</sup> Upon subsequent heating above the  $T_g$  the cholesteric pitch restored to its original state within minutes, resulting in a red shift of the reflection band. By fabricating a semi-interpenetrating network of a Ch-LC polymer and poly(benzyl acrylate), the  $T_g$  was broadened (*i.e.* ranging from 10 °C to 54 °C). After embossing these films display multiple highly stable colors within the  $T_g$  range.<sup>[18]</sup>

Recently, a low density crosslinked Ch-LC shape memory polymer was coated on a flexible substrate by flexographic printing and embossed after curing by a structured rubber using a heated brass stamp (Figure 1.2a).<sup>[19]</sup> During embossing above  $T_g$  at 35 °C and cooling, the approximately 1  $\mu\text{m}$  roughness of the rubber led to a roughness increase of the coating from 0.02  $\mu\text{m}$  to 0.3  $\mu\text{m}$ , which caused severe scattering and loss of a specific reflection band (Figure 1.2b). Briefly heating the coating above the  $T_g$  restored the initial red appearance of the coating. It was found that the crosslink density (consisting of 10% diacrylic monomers) was critical for the desired mechanical properties and responsive behavior as an increase of the crosslink density led to a brittle material and a decrease of the crosslink density led to a tacky coating. These materials may be of interest as time-temperature integrators to monitor the cold chain of food and pharmaceuticals as the color change is irreversible.



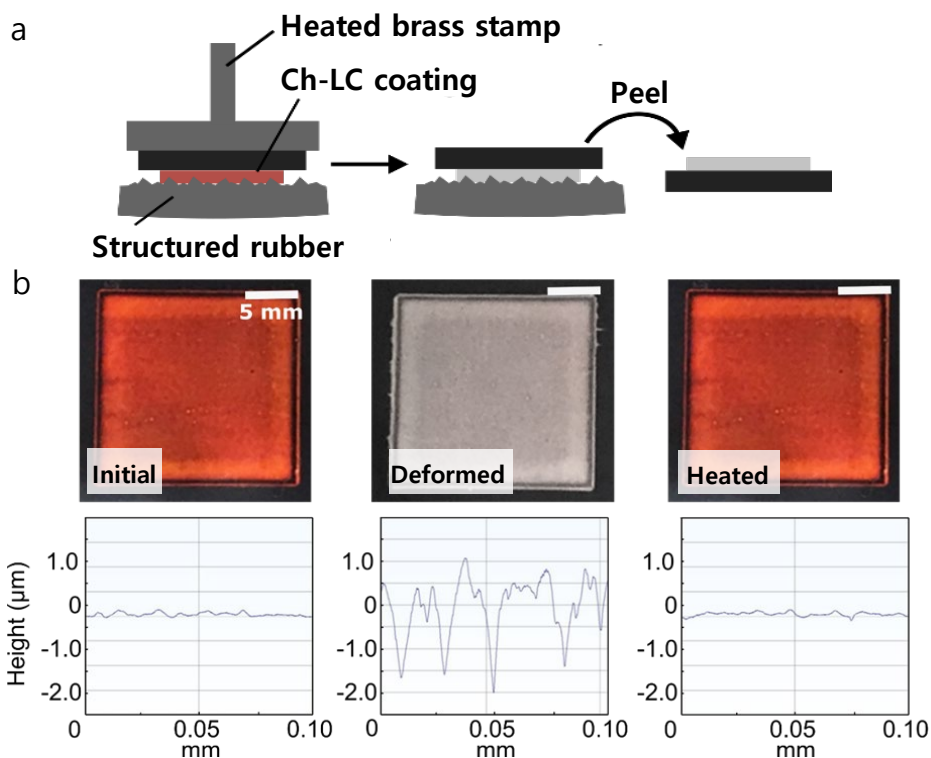


**Figure 1.2:** (a) Schematic deformation protocol consisting of pressing the Ch-LC coating into a structured rubber using a heated brass stamp and subsequently peeling it off of the rubber. (b) Photographs and height profiles of labels prior to deformation (initial) after deformation by compression and after heating. Reproduced with permission from ref. [19]

In another study, a hot-pen was used to locally evaporate a hydrogen-bonded chiral dopant from a Ch-LC network coating. After the coating was locally heated to 160 °C for 30 min, the reflection band in the heated areas was irreversibly shifted from 615 nm to 525 nm, revealing a readable written pattern. To increase the resolution and reduce the time needed for the evaporation process, the coating was irradiated with a laser beam (700 mW/cm<sup>2</sup>) for 25 s, from which the local heating was enough to evaporate the chiral dopant showing a green to orange contrast with excellent resolution.<sup>[20]</sup> These coatings could be interesting as writable photonic paper.

## Reversible temperature-responsive Ch-LC polymers

Although the intrinsically irreversible temperature-responsive behavior is sought after for *e.g.* time-temperature indicators and writable photonic paper, most envisioned applications, such as real-time sensors and thermochromic paints or windows, require a reversible color change. By using Ch-LC elastomers, these reversible temperature responses were realized. Ch-LC elastomers such as side chain LC polysiloxanes were combined with Ch-LC monomers to form a semi-interpenetrating network after UV-polymerization (Figure 1.3a). These coatings showed a reversible decrease in reflection band intensity upon heating above the cholesteric-to-isotropic transition temperature ( $T_{Ch-I}$ ) of the elastomer (Figure 1.3b). The wavelength reflected was tuned between 500 nm and 900 nm by varying the concentration of Ch-LC monomers. The reflectivity loss upon heating could be tuned by varying the crosslink density. Upon heating from 20 °C to 120 °C, 49% to 94% of the reflectivity was lost when decreasing the concentration of monomers in the mixture from 25.5% to 14.9 wt% respectively. The reflectivity was recovered upon cooling.<sup>[21]</sup>

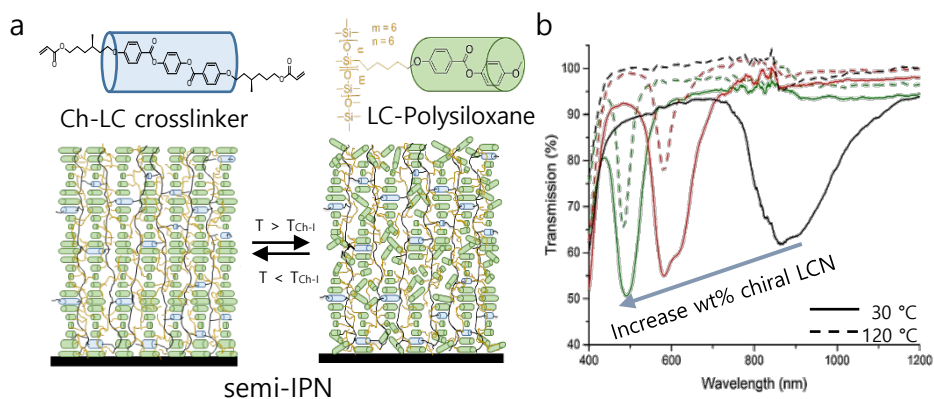


**Figure 1.3:** (a) Schematic representation of a semi-interpenetrating network (IPN) formed by a side chain LC polysiloxane through a chiral LC network (Ch-LC crosslinker). Upon heating above the  $T_{Ch-I}$  the polysiloxanes lose cholesteric order, which it gains upon cooling below  $T_{Ch-I}$ . (b) Transmission spectra showing the reversible decrease of the reflection band intensity of coatings containing various concentrations of the Ch-LC network. The solid and dashed lines represent the spectra at 30 °C and 120 °C, respectively. Ch-LC crosslinker concentrations were 14.9 wt%, 21.0 wt%, 25.5 wt% for the black, red and green curves, respectively. Adapted with permission from ref. [21]

Other temperature-responsive elastomers showed a blue shift with increasing temperature, owing to a LC phase transition. For instance, side chain LC polymers were prepared with a cholesteric to blue phase transition at 126 °C. Blue phases are distinct thermodynamic LC phases that appear over a narrow temperature range at the  $T_{\text{ch-l}}$  of highly chiral LCs.<sup>[22]</sup> Getting closer to the blue phase the cholesteric pitch became shorter and thus blue shifted. Wavelength shifts between 525 nm and 406 nm were obtained this way.<sup>[23]</sup> Larger shifts are found for LC elastomer materials with a smectic to cholesteric transition. Since the smectic LC phase does not have a helical structure, the pitch can be considered as infinitely long. Approaching the smectic-to-cholesteric phase transition temperature ( $T_{\text{s-ch}}$ ) from the Ch-LC phase will therefore result in a very large red shift of the reflection band. This is why a mixture of a side chain Ch-LC polymer combined with a low molecular weight chiral dopant having this transition resulted in a polymer film that shifted reversibly from 1250 nm to 2350 nm upon cooling from 57 °C to 17 °C.<sup>[24]</sup> Another material having a  $T_{\text{s-ch}}$  was obtained by coating short oligomers of reactive LCs. This yielded coatings that could shift between 1195 nm and 701 nm or between 754 nm to 484 nm, covering the visible light range.<sup>[25]</sup> These large blue shifts upon heating do not only make these materials potentially attractive for decorative and sensing applications, but also as energy saving infrared regulating smart windows. Furthermore, these materials can be coated using conventional coating techniques, such as, for example, blade-coating which increase their potential for large scale production.

A drawback of these materials is that they are relatively soft and prone to damage. To fabricate a more mechanically robust system, Ch-LC droplets can be embedded inside a hard polymer network. The composition of these Ch-LC droplets can be chosen in such a way that they show a color change from red to blue upon heating within the cholesteric phase, after which they become isotropic upon further heating. The transition temperature can be controlled by varying the Ch-LC ink composition. This concept was first patented in 1975 by Robert Parker Research and has been used to fabricate all kinds of thermometers, such as

forehead strips, color changing labels and mood rings.<sup>[26]</sup> Such polymer dispersed LC systems show great potential for scalability using flexible substrates and a roll-to-roll process. Liang *et al.*, showed the successful fabrication of meter scale temperature-responsive foils using dispersed LC droplets.<sup>[27,28]</sup> However, although these systems are based on LC phase transitions, no aligned Ch-LC was obtained and therefore, these particular systems are based on scattering mechanisms instead of photonic reflection.

### 1.3 Humidity-responsive Ch-LC polymers

Optical humidity sensors can be fabricated by incorporating hydrophilic polymers containing polar or charged moieties in various photonic structures. This creates reversible photonic polymer films that can swell and deswell depending on the humidity of the environment.

#### Reversible humidity-responsive Ch-LC polymers

Humidity-responsive coatings based on hydrogen-bond containing Ch-LC networks are able to absorb water from their environment after the hydrogen bonds are treated with potassium hydroxide (KOH) solution to create hygroscopic polymer salts.<sup>[29]</sup> The helical pitch of the Ch-LC network increases because of the water absorption, shifting the reflected light to longer wavelengths. A visible color shift from green to yellow was observed when the relative humidity (RH) was increased from 3% to 83%. Patterns were realized by illumination through masks or inkjet printing of  $\text{Ca}^{2+}$  containing solutions. Upon water uptake, inhomogeneous swelling occurred, creating various colors in one sample. The creation of photonic images, make these materials potentially suitable for customizable aesthetics, data encryptions and anti-counterfeit labels.<sup>[30,31]</sup> Fully camouflaged films were prepared using inkjet printing of  $\text{Ca}^{2+}$  ion aqueous solutions on a coating after removal of nonreactive monomers and a base treatment using a 1M KOH solution. By replacing monovalent potassium ions by a bivalent calcium ion, swelling was inhibited, since it re-established the

connection between the carboxylate anions (Figure 1.4a). Patterns appear after breathing or water dipping. As illustrated in Figure 1.4b, higher concentrations of  $\text{Ca}^{2+}$  ensured a lower degree of swelling of the coatings when exposed to water or vapor, enabling formation of camouflaged multi-colored images (Figure 1.4c).<sup>[30]</sup>

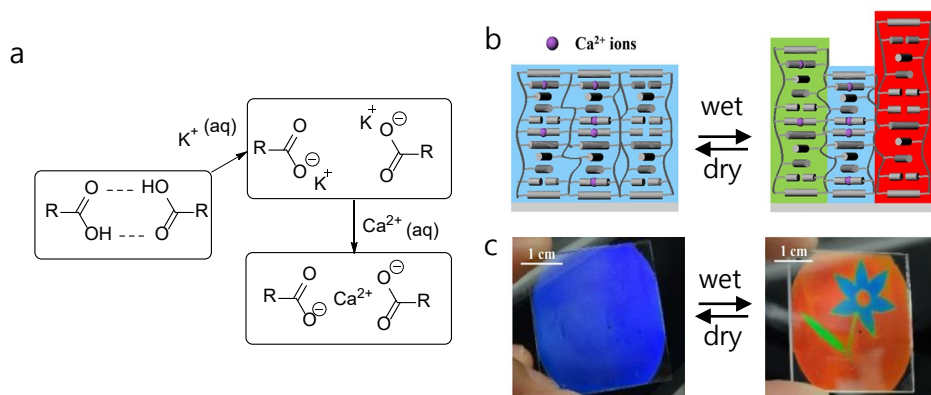


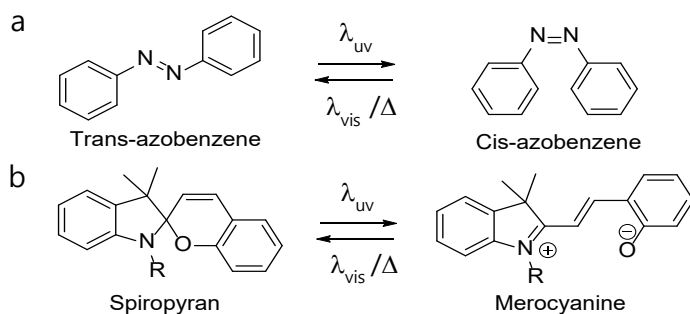
**Figure 1.4:** (a) Hydrogen bonds are disrupted by treatment with  $\text{K}^+$  ions, upon saturating the coating with  $\text{Ca}^{2+}$  swelling with water is inhibited due to the re-establishment of the connection between the carboxylate anions. (b) The coating is patterned by saturating different spots to different levels. In the wet state, areas with lower amounts of  $\text{Ca}^{2+}$  ions swelled more compared to more saturated areas, giving rise to full color patterning while staying indistinguishable from each other in a dry blue colored state. (c) Image of an inkjet-printed full color flower pattern which appeared in the wet state, but was hidden in the dry state. Adapted with permission from ref. [30]

A similar effect was achieved using a co-assembly of acid-hydrolyzed photonic cellulose nanocrystals and waterborne polyurethane.<sup>[32]</sup> After writing on the films with a 0.025 M NaCl solution, patterns were visualized by exhaling. Choosing different inks such as water and 0.1 M NaCl, the patterns could also be made temporary (irreversibly removed upon drying) or more durable (still visible when dried), respectively. By washing the film with water, patterns were erased and could be written again, making these materials promising as rewritable paper. Similar research on free standing films showed that by including 10 wt% to 30 wt% polyethylene glycol, larger reversible shifts of approximately 435 nm could be achieved when increasing the RH from 30% to 100%. Simultaneously the intensity of the reflection band was decreased.<sup>[33]</sup> This results in the ability to

obtain a broader spectrum of colors, ranging from green to red and even to colorless materials at high RH.

### 1.4 Light-responsive Ch-LC polymers

Infiltrating photonic polymers with photochromic dyes enables the ability to create reversible light-responsive materials. Well-known photo-responsive moieties are azobenzenes and spiropyrans. These moieties can undergo an isomerization upon light irradiation causing change in size and conformation of the photochromic dye. By using azobenzenes, a cis-trans isomerization is observed,<sup>[34]</sup> whereas spiropyrans give rise to the open-ring isomer merocyanine upon UV-illumination (Scheme 1.1).<sup>[35]</sup>



**Scheme 1.1:** (a) Cis-trans isomerization of azobenzene. (b) Ring opening isomerization of spiropyran to merocyanine.

### Reversible light-responsive Ch-LC polymers

Photo-responsive Ch-LC films were prepared by a  $\text{SiO}_2$  inverse opal, filled with non-reactive nematic LC, including an azobenzene based LC.<sup>[36,37]</sup> Upon illumination with UV light, the azobenzene moieties isomerize from trans to cis, causing a nematic-to-isotropic transition of the LC inside the voids of the inverse opal film. In the nematic phase, the LCs were aligned parallel to the voids surface forming random bipolar orientations with respect to each other. Since the dielectric constants of the LC spheres were random, requirements for Bragg diffraction were not met, leading to light scattering. In the isotropic phase

however, the dielectric constant became equal for all voids and a reflection peak due to Bragg diffraction appeared (Figure 1.5a). After several seconds, a clear reflection band became visible, which disappeared after the illumination was stopped or the illuminated wavelength was changed to the visible light, causing the LCs to realign in the nematic phase (Figure 1.5b). Since thermotropic LCs were used, a phase-transition to the isotropic phase was also obtained by heating (from 25 °C to 40 °C), making these systems dual-responsive.<sup>[37]</sup>

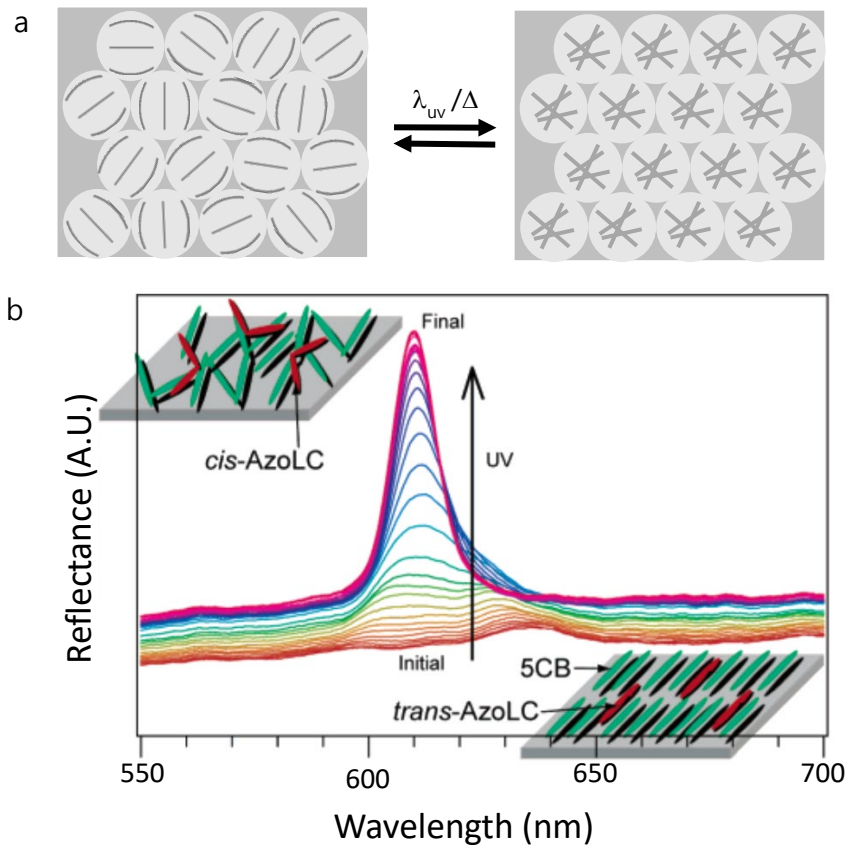


**Figure 1.5:** (a) Schematic representation of the random bipolar (left) and isotropic (right) alignment. (b) Reflection spectra of a mixture of 5CB and AzoLC-infiltrated inverse opal films. Upon illumination with UV light, a peak appears due to the disruption of the nematic alignment, which is caused by the cis-isomers. Adapted with permission from ref. [35]

Zhao *et al.* used a similar approach in which the inverse opal film itself was prepared from polymerizable LCs including an azobenzene-based LC.<sup>[38]</sup> Upon light exposure, the alignment of the polymers is disrupted and the order of the inverse opal film is reduced. Therefore, these films behave in an opposite way to the SiO<sub>2</sub> filled with LCs, meaning that upon UV illumination (5 min, 365 nm, 50 mW/cm<sup>2</sup>) the reflection band nearly disappears and recovers during visible light illumination (15 min, 530 nm, 20 mW/cm<sup>2</sup>). An intensity contrast of more than 77% was reached. Again, a dual-responsive system was created, since the reversible phase-transition could also be induced by temperature.

Another approach to inhibit Bragg reflection in an ordered system is to match refractive indices of the individual layers. To achieve this, glass substrates were spin-coated with alternating layers of azobenzene polymers LCs and poly(vinyl alcohol).<sup>[39–41]</sup> Photonic reflectance was lost after annealing at 80 °C, because of the thermal-induced out-of-plane molecular orientation of the azobenzene polymer, causing a very small difference in refractive indices between the different layers.<sup>[39]</sup> The out-of-plane orientation of the azobenzene polymer was also obtained using visible light of 436 nm (60 mW/cm<sup>2</sup>) for 1 hour (Figure 1.6a, 1.6b).<sup>[40]</sup> In both cases, the azobenzene polymers could reorient to an in-plane random orientation leading to an increase in reflectivity from approximately 20% to 80% using 365 nm UV light between 8 mW/cm<sup>2</sup> and 40 mW/cm<sup>2</sup> for 5 minutes. The reflectivity increase can be improved by approximately 10% after illumination of 5 minutes by copolymerizing high refractive non-photo-responsive LC groups, which prevents interruption of light penetration needed for the photo-response.<sup>[40,41]</sup> Patterned coatings were prepared by illumination through a mask, which were stable for more than a few weeks at room temperature and ambient light (Figure 1.6c). Moreover, reflected color and intensity could be tuned by layer thickness, in which thicker layers enable reflectance at longer wavelengths, and bilayer numbers, in which an increase in layers ensured an increase in intensity of the reflection band. The reversibility, scalability and pattern-ability make these



materials potential candidates for photo-rewritable paper and cell-free, self-standing reflective color display devices without backlight.

In order to shift the reflected wavelength instead of increasing or decreasing its intensity, an inverse opal structure was created based on azobenzene containing polymers. Upon irradiation with linearly polarized light, the out-of-plane orientation of the azobenzene moieties parallel to the incident light increased. Therefore, the effective refractive index of the azobenzene polymers was decreased by 0.034 according to calculations. As a result, the photonic bandgap was blue shifted with increasing irradiation time, obtaining a maximum shift of 40 nm after 25 minutes illumination with 488 nm light at fixed intensity of 100 mW/cm<sup>2</sup>.

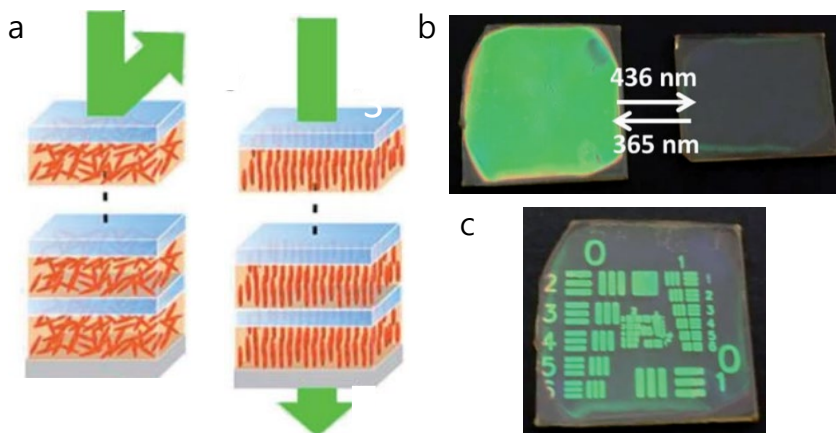


**Figure 1.6:** (a) Schematic representation of the changes in molecular orientation of the azobenzene polymers, showing the in-plane random orientation after exposure to 365 nm light (left) and the out-of-plane orientation after exposure to 436 nm light (right). (b) Photographs of the coating for both the in-plane random and out-of-plane orientation of the azobenzene polymers. (c) Photograph of a patterned coating, prepared by illumination through a mask. Adapted with permission from ref. [40]

## 1.5 Industrial feasibility

Academic research has shown beautiful examples of adaptive photonic LC polymer coatings that autonomously respond to environmental stimuli such as

temperature, humidity and light, similar to environmentally adaptive photonic structures found in nature. Across these LC polymers, various mechanisms are responsible for the structural color change, including Ch-LC polymers that show a shape memory, hydrogel-like Ch-LC that can swell and deswell and LC polymers that can undergo a phase transition or change in order. In this section the feasibility and challenges of the materials in future applications are discussed.

Irreversible responsive Ch-LC shape memory polymers can be processed in their monomer state via blade-coating or printing after which they are polymerized. The shape memory effect is triggered by an embossing step. These processing techniques are suitable for large-scale production. Further development of these materials regarding industrialization would be to process them via roll-to-roll compatible processes on various substrates, as was demonstrated by the coatings prepared using the flexographic printing test setup. Among the polymers that can swell and deswell, photonic hydrogels are the most commonly used to create adaptive photonic polymers. By using temperature or humidity as a stimulus, large responses with respect to reflectivity as well as central wavelength position can be achieved. These features are of interest for potential applications such as sensors, aesthetics and rewritable paper. However, these hydrogels are limited to (biomedical) applications that involve wet environments, since they require water. Responsive photonic polymers can also be fabricated that operate without a swelling solvent. Elastomeric (semi-interpenetrating networks) will be prone to damage, leaving for instance fingerprints upon touching. For commercial applications, this may require the need of, for instance, a protective coating or the need to coat the LC elastomer on the interior of a double pane window. A more commercially established technique is the use of LC droplets embedded in a polymer binder, which provides mechanical robustness. This technology is already used for temperature sensors for decades and recently also steps in the direction of smart windows have been taken.<sup>[26,27]</sup> For many applications the responsive properties of photonic LC materials need to be fine-tuned. For example, for smart window applications in buildings, greenhouses and car interiors,

temperature-responsive IR reflecting polymers could be of interest to minimize indoor heating, with fast response times in the order of minutes or even seconds. In most light-responsive photonic polymers, high energy UV light is required and thereby the lifetime of the materials is potentially limited due to degradation. Thus, obtaining polymers responsive to lower energy light (*e.g.* ambient sunlight) is a highly desirable goal in this field of research. Other applications such as biomedical, would benefit from materials that are responsive towards visible light instead of UV light.

To exploit the potential and to bridge the gap between academic research and industry, stability, fatigue and processing techniques should get extra attention as well as adhesion of the coatings with (flexible) substrates. This would provide a way to implement reversible stimuli-responsive photonic polymers in various coating applications.

## **1.6 Aim and outline of this thesis**

This thesis discusses the fabrication of stimuli-responsive LC photonic polymer coatings on flexible substrates. Two main challenges are addressed in this research to implement these polymers in various coating applications. First, using industrial relevant processing techniques, photonic LC coatings are prepared having good alignment and adhesion without the need for additional alignment layers, surface modifications, solvents or surfactants (Chapter 2). Secondly, three routes are investigated to create robust photonic coatings having flexibility, needed for stimuli-responsiveness, and which could be processed using industrially scalable fabrication techniques.

In Chapter 3, hydrogel-like photonic LC coatings are reported, capable to absorb and desorb water from the environment, thereby shifting the reflection band of the photonic structure and thus the color. Surrounded by a sufficiently high environmental humidity, absorption and desorption of water vapor from the air is regulated by temperature variations.

Chapter 4 describes stimuli-responsive Ch-LC elastomer coatings based on dithiols and diacrylates. The responsiveness and color are controlled by tuning the crosslink density and molecular weight between the crosslinks. This control can be used to create both single-layered multi-color patterned and broadband coatings at room temperature. Moreover, the final coatings are able to swell and deswell by several solvents and lose and regain their reflection band by increasing and decreasing the temperature, respectively. The scalability of the coating process is demonstrated by using gravure printing.

Chapter 5 presents a single-layer coating that is transformed into a cell by photo-enforced stratification. A non-polymerized Ch-LC mixture is sandwiched between the substrate and a polymeric top layer. The encapsulated non-polymerized LCs are highly flexible, showing large reflection band shifts induced by only a few degrees of temperature fluctuations.

Finally Chapter 6 discusses further steps to implement the responsive photonic polymers presented in this thesis in various coating applications.

## 1.7 References

- [1] J. Ge, Y. Yin, *Angew. Chemie* **2011**, *50*, 1492.
- [2] A. Seeboth, R. Ruhmann, O. Mühling, *Materials (Basel)*. **2010**, *3*, 5143.
- [3] A. Seeboth, D. Löttsch, R. Ruhmann, O. Muehling, *Chem. Rev.* **2014**, *114*, 3037.
- [4] J. E. Stumpel, D. J. Broer, A. P. H. J. Schenning, *Chem. Commun.* **2014**, *50*, 15839.
- [5] C. I. Aguirre, E. Reguera, A. Stein, *Adv. Funct. Mater.* **2010**, *20*, 2565.
- [6] N. Akamatsu, K. Hisano, R. Tatsumi, M. Aizawa, C. J. Barrett, A. Shishido, *Soft Matter* **2017**, *13*, 7486.
- [7] L. Nucara, F. Greco, V. Mattoli, *J. Mater. Chem. C* **2015**, *3*, 8449.
- [8] I. B. Burgess, M. Lončar, J. Aizenberg, *J. Mater. Chem. C* **2013**, *1*, 6075.
- [9] A. Grinthal, J. Aizenberg, *Chem. Soc. Rev.* **2013**, *42*, 7072.
- [10] H. Chou, A. Nguyen, A. Chortos, J. W. F. To, C. Lu, J. Mei, T. Kurosawa, W. Bae, J. B. Tok, Z. Bao, *Nat. Commun.* **2015**, *6*, 1.
- [11] J. Sun, B. Bhushan, J. Tong, *RSC Adv.* **2013**, *3*, 14862.
- [12] S. Tadepalli, J. M. Slocik, M. K. Gupta, R. R. Naik, S. Singamaneni, *Chem. Rev.* **2017**, *117*, 12705.
- [13] H. Wang, K. Q. Zhang, *Sensors (Switzerland)* **2013**, *13*, 4192.
- [14] T. Lu, W. Peng, S. Zhu, D. Zhang, *Nanotechnology* **2016**, *27*, 1.
- [15] H. Fudouzi, *Sci. Technol. Adv. Mater.* **2011**, *12*.

- [16] Y. Liang, W. Huang, X. Tao, L. Chen, Y. Wu, Y. Azusagawa, <https://www.beautifulchemistry.net/liquid-crystals/> (accessed 28 October 2018) 745.
- [17] D. J. D. Davies, A. R. Vaccaro, S. M. Morris, N. Herzer, A. P. H. J. Schenning, C. W. M. Bastiaansen, *Adv. Funct. Mater.* **2013**, *23*, 2723.
- [18] M. Moirangthem, T. a. P. Engels, J. Murphy, C. W. M. Bastiaansen, A. P. H. J. Schenning, *ACS Appl. Mater. Interfaces* **2017**, *9*, 32161.
- [19] K. Nickmans, D. A. C. van der Heijden, A. P. H. J. Schenning, *Adv. Opt. Mater.* **2019**, *1900592*, 1.
- [20] M. Moirangthem, J. E. Stumpel, B. Alp, P. Teunissen, C. W. M. Bastiaansen, A. P. H. J. Schenning, *Proc. SPIE* **2016**, *9769*, 97690Y.
- [21] A. J. J. Kragt, D. J. Broer, A. P. H. J. Schenning, *Adv. Funct. Mater.* **2018**, *28*, 1.
- [22] H.-S. Kitzerow, C. Bahr, *Chirality in liquid crystals*, Springer-Verlag: New York, 2001.
- [23] J.-W. Wang, B.-Y. Zhang, *Liq. Cryst.* **2013**, *40*, 1550.
- [24] W. Zhang, S. Kragt, A. P. H. J. Schenning, L. T. de Haan, G. Zhou, *ACS Omega* **2017**, *2*, 3475.
- [25] P. Zhang, A. J. J. Kragt, A. P. H. J. Schenning, L. T. de Haan, G. Zhou, *J. Mater. Chem. C* **2018**, *6*.
- [26] R. Parker, Digital thermometer and method of manufacture - US 3861213 A **1975**, 62–66.
- [27] X. Liang, S. Guo, S. Guo, M. Chen, C. Li, Q. Wang, C. Zou, C. Zhang, L. Zhang, H. Yang, *Mater. Horizons* **2017**, *4*, 878.
- [28] X. Liang, C. Guo, M. Chen, S. Guo, L. Zhang, F. Li, S. Guo, H. Yang, *Nanoscale Horizons* **2017**, *2*, 319.
- [29] N. Herzer, H. Guneyusu, D. J. D. Davies, D. Yildirim, A. R. Vaccaro, D. J. Broer, C. W. M. Bastiaansen, A. P. H. J. Schenning, *J. Am. Chem. Soc.* **2012**, *134*, 7608.
- [30] M. Moirangthem, A. P. H. J. Schenning, *ACS Appl. Mater. Interfaces* **2018**, *10*, 4168.
- [31] J. E. Stumpel, D. J. Broer, A. P. H. J. Schenning, *RSC Adv.* **2015**, *5*, 94650.
- [32] H. Wan, X. Li, L. Zhang, X. Li, P. Liu, Z. Jiang, Z. Z. Yu, *ACS Appl. Mater. Interfaces* **2018**, *10*, 5918.
- [33] K. Yao, Q. Meng, V. Bulone, Q. Zhou, *Adv. Mater.* **2017**, *29*, 1.
- [34] R. H. El Halabieh, O. Mermut, C. J. Barrett, *Pure Appl. Chem.* **2004**, *76*, 1445.
- [35] R. Klajn, *Chem. Soc. Rev.* **2014**, *43*, 148.
- [36] S. Kubo, Z.-Z. Gu, K. Takahashi, Y. Ohko, O. Sato, A. Fujishima, *J. Am. Chem. Soc.* **2002**, *124*, 10950.
- [37] S. Kubo, Z. Z. Gu, K. Takahashi, A. Fujishima, H. Segawa, O. Sato, *J. Am. Chem. Soc.* **2004**, *126*, 8314.
- [38] J. Zhao, Y. Liu, Y. Yu, *J. Mater. Chem. C* **2014**, *2*, 10262.
- [39] M. Moritsugu, T. Ishikawa, T. Kawata, T. Ogata, Y. Kuwahara, S. Kurihara, *Macromol. Rapid Commun.* **2011**, *32*, 1546.
- [40] S. Kim, S. Ishii, R. Yagi, Y. Kuwahara, T. Ogata, S. Kurihara, *RSC Adv.* **2017**, *7*, 51978.
- [41] S. Kim, T. Ogata, S. Kurihara, *Polym. J.* **2017**, *49*, 407.





# Chapter 2

## Adhesion and alignment of cholesteric liquid crystalline coatings on flexible substrates

**Abstract.** An easy to produce, industrially viable process is reported that uses a primer layer of a so-called type II photoinitiator to obtain excellent adhesion between plastic substrate and photonic liquid crystalline coatings. Furthermore, a good alignment of the reactive cholesteric liquid crystal (Ch-LC) mixture is obtained using a bar-coating process without alignment layers or surfactants. After photopolymerization, cross-hatch tape tests show a good adhesion of the photonic coating having a reflection band of 50% transmission with almost no scattering. Additionally, we demonstrate the ability to create well-adhering ~100% reflective coatings by coating double layers and the ability to create single layered cholesteric broad band reflectors using solely a reactivity gradient created by the primer layer.

---

This chapter is partially reproduced from: 'Well-Adhering, Easily Producidble Photonic Reflective Coatings for Plastic Substrates' E.P.A. van Heeswijk, J.J.H. Kloos, J. de Heer, T. Hoeks, N. Grossiord, A.P.H.J. Schenning, *ACS Appl. Mater. Interfaces*, 2018, 10, 30008-30013.



## 2.1 Introduction

Photonic coatings based on cholesteric liquid crystals (Ch-LC) can be prepared by photopolymerization of a reactive acrylate mesogenic mixture. Currently, most Ch-LC films are fabricated sandwiched between glass plates.<sup>[1-3]</sup> However, to be able to apply the desired properties to existing exteriors, coatings are far more favorable in industry. Therefore, an increase in interest is observed regarding coated cholesteric reflectors.<sup>[4-6]</sup> For this, glass substrates are covered with thin alignment layers to ensure planar (parallel to the substrate) alignment of the reactive liquid crystals, leaving several non-covalently bound interfaces susceptible for delamination. Besides, optical transparent plastics are used increasingly in industry as a replacement for glass. Weight reduction, toughness, flexibility, transparency, heat resistance and high impact strengths, make for example polycarbonate (PC) a desirable material for windows and roofings in cars, buildings and constructions.<sup>[7]</sup>

Several methods have been developed to functionalize PC surfaces. These methods, however, often require expensive, specialized equipment<sup>[8-10]</sup> or create toxic side-products<sup>[11-13]</sup>. Moreover, most methods are based on chain scissoring of the polycarbonate backbones at the surface.<sup>[14-17]</sup> Thereby, short degraded polymer chains are formed, which form a weak link between the substrate and the coating.<sup>[15-17]</sup>

This chapter reports on a transparent primer deposited on the PC substrate on which the Ch-LC was coated and cured. The primer contains the type II photoinitiator benzophenone (BP). In contrast to the commonly used type I photoinitiators such as commercially available Irgacures, which create radicals by unimolecular bond cleavage, type II photoinitiators initiate polymerization by intermolecular hydrogen abstraction, creating radicals in their near surrounding without breaking C-C bonds of the backbone.<sup>[18]</sup> The covalent bond formed ensures excellent adhesion at the interface between the substrate and the

coating.<sup>[19]</sup> Next to the increased adhesive properties, an excellent alignment of the LC molecules in the polymer network is obtained with an industrially feasible approach, using no alignment layers. It is also demonstrated that this method can be repeated to adhere double layered coatings to fabricate near 100% cholesteric reflective layers and to prepare broadband reflective coatings minimizing successive coating layers without adding additional UV absorbers.<sup>[1,20]</sup>

## 2.2 Experimental details

### Materials

500  $\mu\text{m}$  thick LEXAN<sup>TM</sup> 8040T PC film was kindly provided by SABIC. The chiral dopant **1** (depicted in Figure 2.1) was purchased from BASF, LCs **2**, **4**, **7-9** were purchased from Merck, the LCs **3** and **5** were received from Philips Research Laboratory, the photoinitiator **6** was purchased from Sigma-Aldrich, Irgacure 819 was purchased from Ciba Specialty Chemicals LTD and ethanol from Biosolve.

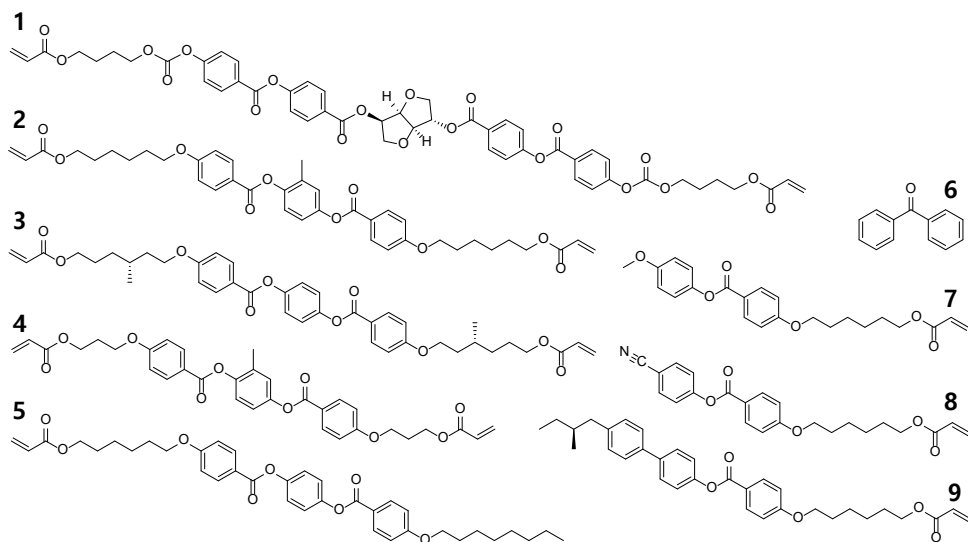


Figure 2.1: Molecular structures of the chemicals used.

## Methods

*Benzophenone (BP) treatment:* 10 wt% (unless stated otherwise) of BP was dissolved in ethanol. The substrate was heated to 40 °C, an approximately 30 cm<sup>2</sup> PC was wetted by 0.25 mL BP solution, and the solvent was allowed to evaporate for 15-20 min.

*Coating procedures:* The treated PC substrates were coated with Ch-LC mixture I at 40 °C using a gap applicator with a 30 μm gap height. The coatings were subsequently photo-polymerized through the substrate in a nitrogen atmosphere at room temperature (RT) using UV light (30 mW/cm<sup>2</sup> in the range of 320-309 nm). Four coating formulations were used in this Chapter. Mixture I for single-layered narrowband coatings, left-handed mixture II and right-handed mixture III for near 100% cholesteric reflective coatings and mixture IV for the formation of a single-layered broadband coating.

*Mixture I:* 3.7 wt% chiral dopant (**1**), 20 wt% crosslinker (**2**), 74.3 wt% monoacrylates (43 wt% **7** and 31.3 wt% **8**) and 2 wt% photoinitiator (BP, **6**).

*Mixture II:* 28 wt% chiral dopant/crosslinker (**3**), 71 wt% monoacrylates (40 wt% **5**, 31 wt% **7**), and 1 wt% photoinitiator (BP, **6**).

*Mixture III:* 36 wt% crosslinker (**4**), 35 wt% chiral dopant/monoacrylate (**9**), 28 wt% monoacrylate (**7**), and 1 wt% photoinitiator (BP, **6**).

*Mixture IV:* 2.5 wt% chiral dopant (**1**), 20 wt% crosslinker (**2**), 77.5 wt% monoacrylates (45 wt% **7** and 32.5 wt% **8**).

*Double-layered coating procedure:* the left-handed mixture II was coated on a treated PC substrate at 70 °C using a gap applicator with a 30 μm gap height. The coating was subsequently photo-polymerized through the substrate in a nitrogen atmosphere at approximately 70 °C using UV light (at an intensity of 30 mW/cm<sup>2</sup> in the range between 320 nm and 390 nm). The coating was again treated with benzophenone as described above. Subsequently, the right-handed mixture III was coated on top, at RT, using again the gap applicator with 30 μm gap height and cured at room temperature similarly to the first coating layer.

## Characterization

*Cross-hatch tape test* was performed for which a cross-hatch pattern was made by a razor blade on which Tesa 4651 tape was applied and pressed firmly. The tape was removed quickly using a little extra force. The remaining coating on the substrate was rated according to the ISO 2409 standards, scaling the adhesion from GT0 to GT5, in which GT0 indicates excellent adhesion and GT5 complete delamination. *Dispersive Raman analysis* were performed on cryo-cutted cross-sections of pretreated PC substrates with a Bruker Senterra dispersive microscope Raman, using a 532 nm laser (20 Mw and 10 Mw) and a 100x objective. *Attenuated total reflection Fourier transfer infrared (ATR-FTIR)* mapping was performed on a Perkin Elmer Spotlight 400 FTIR-imaging system with a germanium ATR crystal. A 200 x 200  $\mu\text{m}^2$  area was measured by individual points with a 1.5  $\mu\text{m}$  distance and a 3  $\mu\text{m}$  spatial resolution. *Optical microscopy* imaging was carried out with an Olympus BX60 or Keyence VHX 5000 microscope. Images were viewed using UV illumination in order to localize benzophenone. *UV-Vis spectroscopy* was performed on a PerkinElmer LAMBDA™ 750 UV/Vis/NIR spectrophotometer equipped with a 150 mm integrating sphere. *Transmission electron microscopy (TEM)* images of ultra-tomed (at -120 °C) cross-sections of PC substrates coated by LC network were made using a FEI Tecnai T12 microscope, with an operating voltage of 100 kV. For *atomic force microscopy (AFM)* analysis, PC substrates coated by the Ch-LC network were cut to size, held between holders and microtomed at RT, the cross-section were characterized with a Bruker Dimension fastscan, using a Quantitative Nanoscale Mechanical (QNM) Mode, with 1 Hz & 0.5 Hz, at RT.

## 2.3 Results and discussion

### Fabrication of the Ch-LC coatings on PC

Ch-LC mixture I was developed to obtain a reflectance peak in the visible light regime and a processing temperature near RT. A paint was created with the

reflection band centered at 660 nm to visualize the alignment capabilities. The PC was pretreated with a BP layer to improve adhesion (see experimental details) and coated with the Ch-LC mixture I, using an easy-to-process bar-coating approach without additional alignment layers. The coating was followed by curing by illumination through the substrate with UV light ( $30 \text{ mW/cm}^2$  in the range of 320-390 nm) at  $40 \text{ }^\circ\text{C}$  for 5 min (Figure 2.2a).

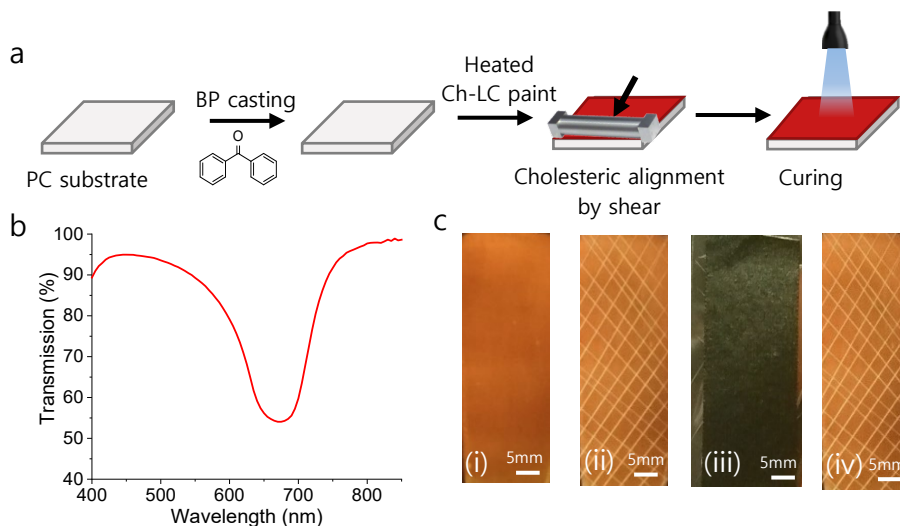


**Figure 2.2:** a) Fabrication method of Ch-LC coatings using an easy-to-process bar-coating technique. b) Transmission spectrum of the Ch-LC coating after the curing process using mixture I. c) Cross-hatch tape test procedure: (i) Ch-LC coating of mixture I on pretreated PC. (ii) Cross-hatch pattern prior to the tape test. (iii) Ch-LC coating covered with a Tesa 4651 tape. (iv) Adhered coating after the rapid removal of the tape showing excellent adhesion (GT0).

The transmission spectrum of an orange-colored Ch-LC coating (Figures 2.2b and 2.2c(i)) showed a Ch-LC reflection band with 50% transmission and almost no scattering, which indicates that the preparation method used results in a planar alignment of the LCs. The photonic coatings were further analyzed by TEM, visualizing typical cholesteric lines, corresponding to the repetitive  $180^\circ$  rotation of the molecular director (Figure 2.3a). The majority of these lines are parallel to each other, meaning that the LCs share a common director. Also, in the two-dimensional (2D) fast Fourier transformed image, a regular spacing of  $0.21 \mu\text{m}$  was observed with a strong directional order, which is in agreement with the

reflection band centered at 660 nm, measured by UV-vis spectroscopy (Figure 2.2b). To investigate the alignment at the substrate and surface interfaces, QNM-AFM measurements were performed on the cross-section of the liquid crystalline films near those interfaces, visualizing again the cholesteric lines (Figure 2.3b). Also here, the aligned Ch-LC phases were observed with only minor defects, for which no alignment layers or surfactants were needed. Using this Ch-LC mixture and the bar-coating technique, shear alone is enough to ensure a proper planar alignment caused by the higher viscosity of the paint as a result of the lack of solvents during application. Most likely, caused by the shear forces between the substrate and the viscous LC mixture, the molecules aligned along a common director, resulting in a well-formed cholesteric reflection band (Figure 2.2b).

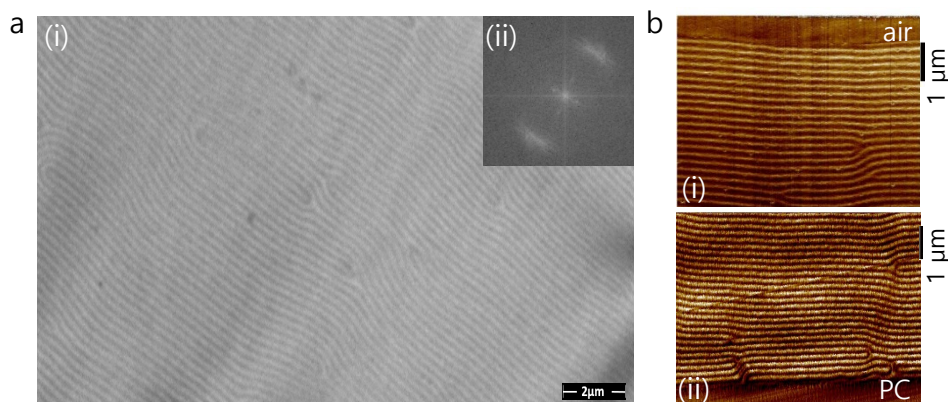


**Figure 2.3:** a) (i) TEM image of the Ch-LC film after photopolymerization in the cholesteric phase. (ii) 2D fast Fourier transformed TEM image. b) QNM-AFM adhesion image of a cross-section of the (i) coating-air interface and (ii) coating-substrate interface of mixture I coating on pretreated PC after photopolymerization in the cholesteric phase.

## Adhesion

To analyze the adhesion of the Ch-LC coating on PC, the crosshatch tape test was performed on the coatings. The reference samples using no primer layer show severe delamination (GT5) when using either Irgacure 819 or BP as the photoinitiator in the LC mixture. Only when a pretreatment of the substrate with 10 wt% BP in ethanol solution was performed to increase the radical

concentration at the PC-coating interface did the adhesion tremendously improve from GT5 to GT0 (Figure 2.2c).

To shed more light on the adhesion of the coating to the PC substrate, several characterization techniques were employed. First, ATR-FTIR mapping of the surface was performed, showing a homogeneous distribution of both BP and PC at the surface, with a relative standard deviation of 4.5% (Figure 2.4a). To gain more insight into the uniformity and thickness of the BP layer formed, OM using UV illumination was used to characterize the cross-section of the PC substrates. Because of the increase in the absorption of UV light of BP with respect to PC, higher concentration of BP will appear lighter in the OM images (Figure 2.4b).

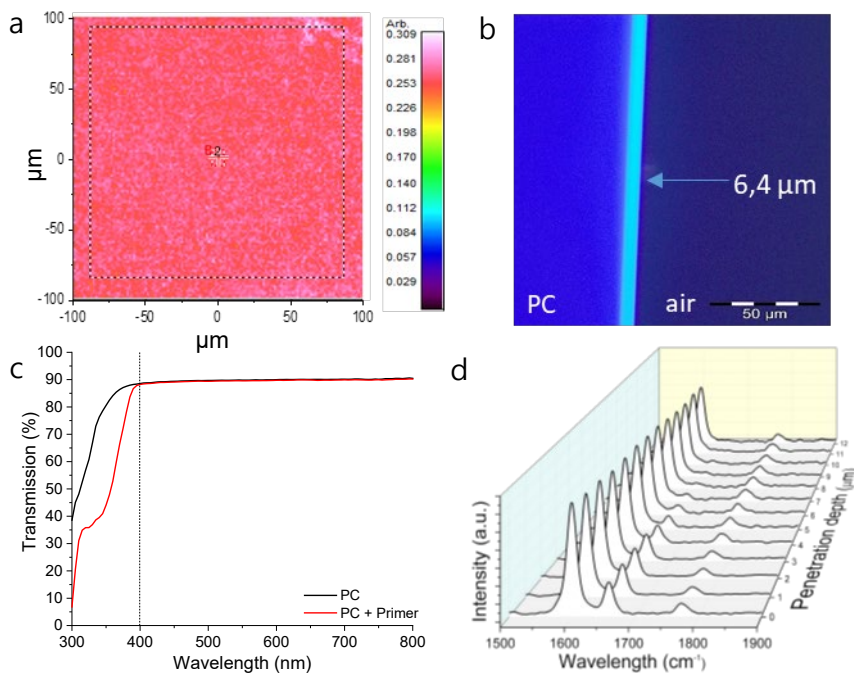


**Figure 2.4:** a) Ratio of BP/PC based on the C=O bonds at 1610 cm<sup>-1</sup> (BP) and 1780 cm<sup>-1</sup> (PC) using ATR-FTIR mapping of the surface of the PC coated with the primer. b) UV-OM image of the cross-sections of PC coated with the primer layer. c) Transmission spectra of pure PC and the PC coated with the primer layer. d) Raman spectra along the cross-section of PC with the primer layer.

A uniform layer thickness of 6.4  $\mu\text{m}$  was evidenced. Note that this thickness is calculated based on the visual evaluation of the brightest parts of the OM image, which might differ from the exact layer thickness. As shown in Figure 2.4c, the optical transparency of the substrate with regard to the visible light region is not influenced by the pretreatment, which is an indication that BP has penetrated in to the PC instead of being crystallized at the surface. This penetration is enabled because of partial swelling of PC in ethanol. To confirm this, cross-sections of the treated PC were made and analyzed by Raman spectroscopy. The phenyl ring stretch of the PC at  $1600\text{ cm}^{-1}$  and the C=O bond of BP at  $1660\text{ cm}^{-1}$  were followed along the cross-section of the PC with a  $1\text{ }\mu\text{m}$  spacing between each measurement. The ratios between the peak areas of the bonds mentioned show that in the BP-rich areas, PC peaks are always present, showing indeed the penetration of BP into the PC substrate (Figure 2.4d). Lowering of the BP concentration in the ethanol solution will lead to both a reduction of the penetration depth and local concentration of BP at the surface. (Figure 2.5).

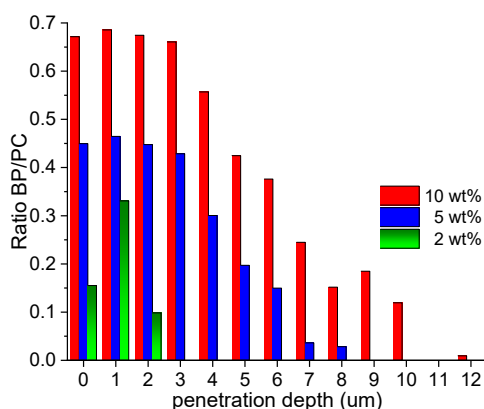


**Figure 2.5:** Ratio between the peak areas measured with Raman spectroscopy of the C=O bond of BP ( $1640 - 1680\text{ cm}^{-1}$ ) and phenyl ring stretch of PC ( $1560 - 1640\text{ cm}^{-1}$ ) for cross-sections of PC films on which BP-ethanol solutions with BP concentrations ranging from 2 wt% to 10 wt% were casted. .



## Broadband reflectors and adhesion of multiple layers

As Ch-LCs reflect only one handedness of circular polarized light, two coating layers with opposite handedness were coated on top of each other to be able to reach near-100% reflection of a specific wavelength. Because the Ch-LC mixtures possess many  $\text{CH}_2$  moieties, these networks are susceptible to hydrogen abstraction as well. Therefore, the first coating layer can serve as a substrate for the second Ch-LC layer. Using the same approach as before, the first coating layer was treated with the BP solution and subsequently coated with the Ch-LC mixture with opposite handedness. Left-handed mixture II and right-handed mixture III were prepared with the reflection bands centered near 900 nm, which would be suitable for IR reflective coatings (Figure 2.6a). The mixtures are based on the mixtures previously used to make near-100% reflective Ch-LC films in cells.<sup>[1]</sup> However, a high brittleness was observed in the coating using these Ch-LC mixtures, causing the LCs to partially break during the cross-hatch tape test, resulting in an overall GT3 classification. Nevertheless, the second coating adheres well (GT0) to the first coating layer (Figure 2.6b).

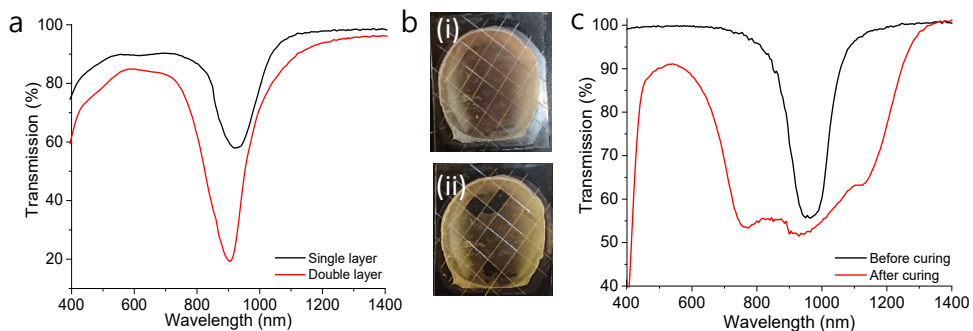


**Figure 2.6:** a) Transmission spectra of the Ch-LC coating containing either a single layer using mixture II or a double layer containing both left- and right-handed Ch-LC mixtures II and III b) photographs of the double layered coating (i) before and (ii) after the cross-hatch tape test. c) Transmission spectra of mixture IV coated on pretreated PC before and after photopolymerization in the cholesteric phase.

It was also investigated if the diffusion of BP can be employed for the formation of broadband reflective coatings. Because of the pretreatment of the substrate with BP, a concentration difference of the photoinitiator is obtained. Using the

diffusion of BP into the coating while curing, a difference in the reaction rate of acrylic polymerization is present throughout the thickness of the coating. In a similar way as with the light intensity gradient, this causes the more reactive species to diffuse to the substrate and the less reactive species to deplete to the air-interface, creating a pitch gradient. To enlarge the concentration difference of BP in the coating, the photoinitiator was removed from the coating mixture, leaving only an initial BP concentration at the substrate-coating interface (mixture IV). To obtain a broadband infrared reflection, mixture IV was coated on a pretreated PC substrate using a BP-in-ethanol concentration of 0.5 wt%. The coating was illuminated through the substrate with UV light ( $3 \text{ mW/cm}^2$  in the range of 320-390 nm) at  $40 \text{ }^\circ\text{C}$  for 20 min, and the sample was post-cured by a high-intensity UV light exposure ( $30 \text{ mW/cm}^2$  in the range of 320-390 nm) at  $40 \text{ }^\circ\text{C}$  for 5 min. Using this approach, a well-aligned single-layer broadband coating was formed, without adding any additional UV absorbers. (Figure 2.6c). A 375 nm increase in the bandwidth is reached during polymerization, resulting in a 500 nm-broad reflection band. Because of a small decrease in the chiral dopant concentration in mixture IV with respect to mixture I, the area of reflected wavelengths is shifted towards 700-1200 nm. This corresponds to the high-intensity IR region of the solar spectrum, which covers the most energetic wavelengths responsible for heating of the environment, making this broadband suitable for transparent heat-reflecting coatings.

## 2.4 Conclusions

In conclusion, a potentially-relevant industrial process was presented to coat aligned acrylic LC monomers to a plastic surface with excellent adhesion. Because of the penetration of BP in the substrate, the acrylic liquid crystalline monomers were grafted from the surface into the network, resulting in a covalently-bound coating. Furthermore, no common alignment layers or surfactants were used in this application process to ensure the alignment of the LCs. Nevertheless, a good

cholesteric alignment was achieved using shear, resulting in reflective functional coatings. Furthermore, the photoinitiator concentration difference created when removing the photoinitiator from the mixture could be used to create well-defined single-layer cholesteric broadband reflective coatings, which may be suitable for smart window applications. This process could be repeated for multiple layers, as long as the substrate surface has protons available for hydrogen abstraction. This interfacial process provides new opportunities for the application of photonic materials on plastic substrates and is applicable for covalent bonding of other polymers to plastic substrates.

## 2.5 References

- [1] H. Khandelwal, R. C. G. M. Loonen, J. L. M. Hensen, A. P. H. J. Schenning, M. G. Debije, *J. Mater. Chem. A* **2014**, *2*, 14622.
- [2] H. Khandelwal, G. H. Timmermans, M. G. Debije, A. P. H. J. Schenning, *Chem. Commun.* **2016**, *52*, 10109.
- [3] L. Wang, H. K. Bisoyi, Z. Zheng, K. G. Gutierrez-Cuevas, G. Singh, S. Kumar, T. J. Bunning, Q. Li, *Mater. Today* **2017**, *20*, 230.
- [4] A. J. J. Kragt, D. J. Broer, A. P. H. J. Schenning, *Adv. Funct. Mater.* **2018**, *1704756*, 1.
- [5] W. Zhang, S. Kragt, A. P. H. J. Schenning, L. T. de Haan, G. Zhou, *ACS Omega* **2017**, *2*, 3475.
- [6] D. Liu, C. W. M. Bastiaansen, J. M. J. den Toonder, D. J. Broer, *Angew. Chemie Int. Ed.* **2012**, *51*, 892.
- [7] D. Katsamberis, K. Browall, C. Iacovangelo, M. Neumann, H. Morgner, *Prog. Org. Coatings* **1998**, *34*, 130.
- [8] S. J. Chang, S. M. Kuo, J. W. Lan, Y. J. Wang, *Artif. Cells, Blood Substitutes, Biotechnol.* **1999**, *27*, 229.
- [9] U. Bora, P. Sharma, S. Kumar, K. Kannan, P. Nahar, *Talanta* **2006**, *70*, 624.
- [10] L. Baumann, K. Schöller, D. de Courten, D. Marti, M. Frenz, M. Wolf, R. M. Rossi, L. J. Scherer, *RSC Adv.* **2013**, *3*, 23317.
- [11] M. Klausner, M. P. Manning, R. F. Baddour, Surface Modification of Polymeric Materials **1990**, 1–3.
- [12] M. Bañuls, F. García-piñón, R. Puchades, Á. Maquieira, *Bioconjug. Chem.* **2008**, *19*, 665.
- [13] J. Tamarit-López, S. Morals, M. J. Bañuls, R. Puchades, Á. Maquieira, *Anal. Chem.* **2010**, *82*, 1954.
- [14] V. VanDelinder, D. R. Wheeler, L. J. Small, M. T. Brumbach, E. D. Spoerke, I. Henderson, G. D. Bachand, *ACS Appl. Mater. Interfaces* **2015**, *7*, 5643.

- [15] B. W. Muir, H. Thissen, G. P. Simon, P. J. Murphy, H. J. Griesser, *Thin Solid Films* **2006**, *500*, 34.
- [16] J. Lub, F. C. M. van Vroonhoven, D. van Leyen, A. Benninghoven, *Polymer*. **1988**, *29*, 998.
- [17] H. van der Wel, F. C. B. M. van Vroonhoven, J. Lub, *Polymer*. **1993**, *34*, 2065.
- [18] N. S. Allen, *J. Photochem. Photobiol. A Chem.* **1996**, *100*, 101.
- [19] J. P. Deng, W. T. Yang, B. Rånby, *J. Appl. Polym. Sci.* **2001**, *80*, 1426.
- [20] D. J. Broer, G. N. Mol, J. A. M. M. van Haaren, J. Lub, *Adv. Mater.* **1999**, *11*, 573.



# Chapter 3

## Humidity-gated temperature-responsive broadband coatings

**Abstract.** This chapter reports on the fabrication of humidity-gated temperature-responsive infrared reflective photonic coatings using an easy-to-process bar-coating technique. At high humidity levels, the hygroscopic cholesteric liquid crystalline polymer is able to absorb water vapor from the air causing swelling of the photonic coating. In turn, the polymer chains of the coating become mobile enough to enable reversible reflection band shifts. In particular, above 45% relative humidity, upon temperature variation between -2 °C and 70 °C, a reversible 420 nm shift of the narrow reflection band is obtained, which is governed by water absorption or desorption. Additionally, the fabrication of a humidity-gated temperature-responsive single-layered broadband IR reflective coatings is demonstrated, which might be suitable for smart windows applications in high relative humidity environments such as greenhouses.

---

This chapter is partially reproduced from: 'Humidity-gated, temperature-responsive photonic infrared reflective broadband coatings. E.P.A. van Heeswijk, J.J.H. Kloos, N. Grossiord, A.P.H.J. Schenning, *J. Mater. Chem. A*, 2019, 7, 6113-6119.

### 3.1 Introduction

Since radiation from the sun is responsible for heating up buildings, automobiles and greenhouses and is partially located in the invisible infrared (IR) part of the spectrum, IR reflective photonic coatings for windows can be used for energy efficient indoor heat control without affecting daylight visibility.<sup>[1]</sup> For battery-free energy efficient windows, a response towards temperature is desired, enabling reflection of heat (near infrared light) during warmer periods, and transmission of heat during cooler periods.<sup>[2]</sup> To avoid interference with visible light, the reflection band should be able to shift to longer wavelengths upon cooling allowing the highest intensity IR light from the sun (around 800-1200 nm) to transmit through the window and contribute to passive heating.

Temperature-responsive materials switching between transparent and scattering or absorbing states, such as hydrogels,<sup>[3,4]</sup> phase changing materials<sup>[5-8]</sup> or polymer composite coatings<sup>[9]</sup> have been developed for temperature-responsive smart window applications. Also static IR reflecting coatings have been studied intensively.<sup>[1]</sup> However, the fabrication of temperature-responsive photonic polymer coatings aiming at reflecting IR light remains a challenge. As discussed in Chapter 1, a coating of a non-crosslinked, oligomeric cholesteric liquid crystalline (Ch-LC) mixture was developed, showing a shift of a narrow IR-reflection band to shorter wavelengths upon temperature increase from 17 °C to 57 °C.<sup>[10]</sup> However, due to the non-crosslinked nature of the coating, cooling to temperatures lower than 16 °C resulted in irreversible reflectivity loss. Cross-linked thermochromic photonic systems based on hydrogels have been reported, for which the narrow reflection bands are able to shift in the visible light range upon heating or cooling of the surrounding water.<sup>[11,12]</sup>

This chapter reports on hygroscopic Ch-LC crosslinked IR-reflective coatings which display a humidity-gated temperature response. Hydrogen-bond containing Ch-LC networks were fabricated and treated with potassium hydroxide (KOH) to create the hygroscopic polymer salts as discussed in Chapter 1. These photonic materials show a reversible shift of the IR reflection band to longer wavelengths upon cooling in atmospheres above 45% relative humidity (RH), and their working mechanism is elucidated. Both narrowband and broadband reflecting coatings could be prepared. These coatings can be easily processed by bar-coating techniques on the flexible polycarbonate (PC) films. The temperature-responsive broadband-reflecting coatings are likely to be of interest for autonomous temperature regulation in greenhouses and tropical environments.

## 3.2 Experimental details

### Materials

500  $\mu\text{m}$  thick LEXAN<sup>TM</sup> 8040T PC film PC and a benzophenone-PC copolymer<sup>†</sup> (XPC) films were kindly provided by SABIC. Liquid crystalline monomers **1**, **3** and **4**, depicted in Figure 3.1, were purchased from Merck. The chiral dopant **2** was obtained from BASF, benzoic acid derivatives **6** and **7** were prepared by Synthron, the photoinitiator benzophenone (BP), dye **5** and KOH pellets were purchased from Sigma Aldrich and the surfactant **8** was purchased from BOC sciences. All solvents were obtained from Biosolve and used without further purification.

Two cholesteric mixtures were used in which the overall crosslink density was kept constant. Ch-CL mixture I was used to prepare the coatings with a narrow reflection band (that is, no pitch gradient was formed). Ch-LC mixture II was used to prepare the coatings with the widened reflection band (i.e. a pitch gradient was formed).



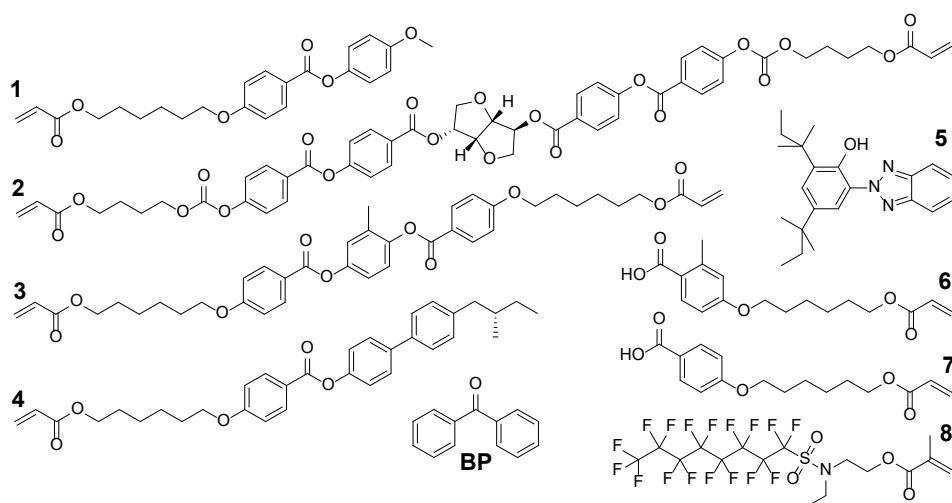


**Figure 3.1:** Molecular structures of chemicals used.

*Ch-LC mixture I:* 37.7 wt% monoacrylate **1**, 2.5 wt% diacrylic chiral dopant **2**, 14.9 wt% diacrylate **3**, 21.7 wt% of both benzoic acid derivatives **6** and **7** and 1.5 wt% photoinitiator BP.

*Ch-LC mixture II:* 14.7 wt% monoacrylate **1**, 15.6 wt% diacrylate **2**, 27.1 wt% monoacrylic chiral dopant **4**, 1.2 wt% dye **5**, 20.4 wt% of both benzoic acid derivatives **6** and **7** and 0.6 wt% surfactant **8**.

## Methods

*Fabrication of the narrowband IR reflective Ch-LC coatings:* approximately 30 cm<sup>2</sup> PC films was wetted at 40 °C by 0.5 ml primer solution of 10 wt% BP and 90 wt% ethanol. The ethanol was allowed to evaporate for 15 minutes. Ch-LC mixture I was applied on the pretreated substrate with a bar-coat applicator having a gap height of 30 μm at room temperature (RT) and illuminated through the substrate at RT for 5 minutes using UV light (30 mW/cm<sup>2</sup> in the range of 320-390 nm). Afterwards, the fully polymerized Ch-LC coatings was submerged in a 1M KOH solution for 10 minutes, rinsed with water and then dried by heating the coating to 70 °C for several minutes.

*Fabrication of the broadband IR reflective Ch-LC coatings:* Approximately 30 cm<sup>2</sup> XPC was wetted by 0.5 ml primer solution of 0.5 wt% BP and 99.5 wt% ethanol at 40 °C. The ethanol was allowed to evaporate for 15 minutes. Ch-LC mixture II was applied on the pretreated substrate with a bar-coat applicator having a gap height of 30 μm at 70 °C and cured through the substrate at 70 °C for 15-20 minutes using UV light (3 mW/cm<sup>2</sup> in the range of 320-390 nm), followed by a 5 minutes post-cure at 70 °C using UV light (30 mW/cm<sup>2</sup> in the range of 320-390 nm). Afterwards, the fully polymerized Ch-LC coatings was submerged in a 1M KOH solution for approximately 30 minutes, rinsed with water and then dried by heating the coating to 70 °C for several minutes.

### **Characterization**

*Attenuated total reflection Fourier transfer infrared (ATR-FTIR)* was measured on a Varian 670-IR spectrometer equipped with a golden gate setup. *UV-Vis spectroscopy* was performed on a PerkinElmer LAMBDA<sup>TM</sup> 750 UV/Vis/NIR spectrophotometer equipped with a 150 mm integrating sphere. Haziness of the coating was measured according to the ASTM standard D-1003-00 and was averaged over 10 different locations of the coating. UV-Vis spectroscopy measurements with temperature and humidity control were performed on a SHIMADZU UV-3102 spectrophotometer equipped with a Linkam temperature control stage in a transparent humidity controlled chamber. All spectra were taken after the coating was held for 5 minutes at the desired temperature for stability of the temperature profile. *Scanning electron microscopy (SEM)* images were obtained from a FEI Thermo Scientific<sup>TM</sup> Quanta<sup>TM</sup> 3D-FEG. The measurement parameters were as follows: acceleration voltage: 5 kilovolt, working distance: 10 mm, and high vacuum. Cross-sections of the sample were prepared by submersion in liquid nitrogen, after which the frozen sample was cut using a razor blade and sputter coated with gold.

### 3.3 Results and discussion

#### Fabrication of the narrowband IR reflective Ch-LC coating

Initially a narrowband hygroscopic Ch-LC coating was prepared to analyze the thermochromic behavior of the coating. To avoid delamination between the plastic substrate and Ch-LC coating, polycarbonate films were pretreated with BP as was described in Chapter 2. The BP type II photoinitiator creates radicals at the substrate interface by hydrogen abstraction, enabling grafting of the acrylate monomers from the substrate. Subsequently, Ch-LC mixture I was coated on the pretreated PC using an easy-to-process bar-coating technique (Figure 3.2a).

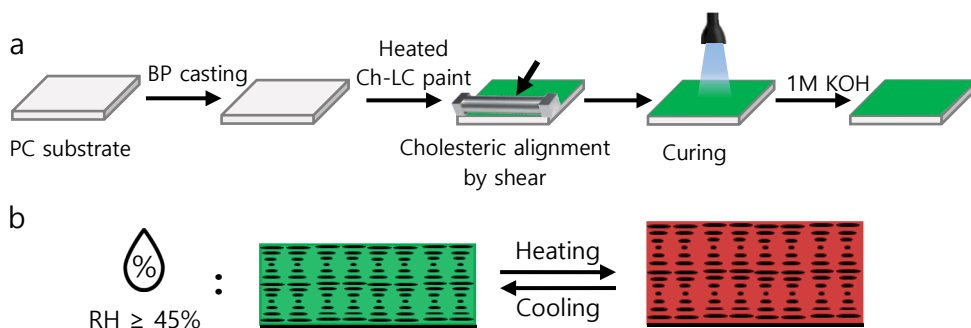


**Figure 3.2:** a) Preparation method for responsive Ch-LC coatings. Pretreatment of the substrate with a primer BP-solution, followed by bar-coating of the Ch-LC mixture and a photopolymerization. Finally, the cured coating was exposed to an alkaline treatment to create the hygroscopic Ch-LC coating. b) Schematic representation of the humidity-gated swelling and deswelling of the Ch-LC coating due to temperature fluctuations.

Using this approach, the necessary cholesteric alignment of the liquid crystals was generated by shear forces, excluding the need for additional alignment layers as discussed in Chapter 2. In order to prepare a hygroscopic polymer, the cured coating was soaked in a potassium hydroxide (KOH) solution to disrupt the hydrogen bonds formed between acidic monomers **6** and/or **7**, creating a polymer potassium salt coating able to absorb water. (Figure 3.2b). FTIR spectra reveal the disruption of the hydrogen bonds (Figure 3.3a).

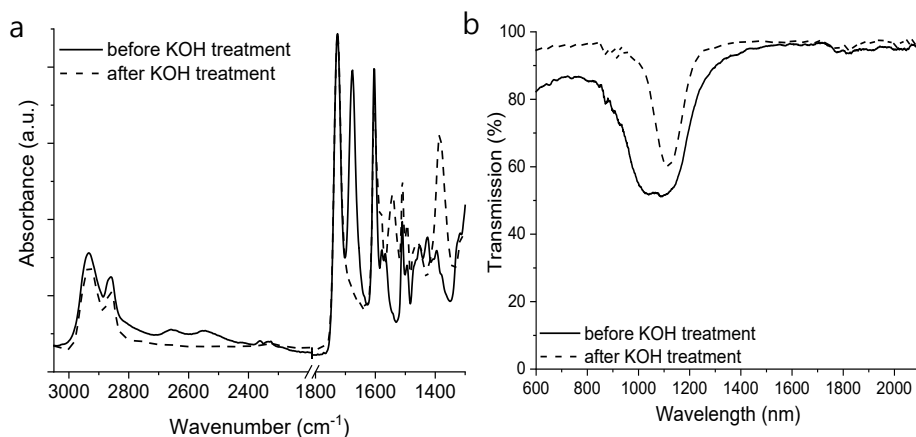


**Figure 3.3:** a) FTIR absorbance spectra of the Ch-LC coating before and after alkaline treatment and subsequent drying. b) Transmission spectra of the Ch-LC coating before and after the alkaline treatment.

In the initial non-activated coating, broad signals between  $2700\text{ cm}^{-1}$  and  $2450\text{ cm}^{-1}$  and a strong signal at  $1680\text{ cm}^{-1}$ , related to the OH-stretching vibration of the hydrogen bonds, are present. After the alkaline treatment, these signals are changed by two others at  $1547\text{ cm}^{-1}$  and  $1388\text{ cm}^{-1}$ , arising from the symmetric and antisymmetric stretching of the carboxylate salts, respectively, showing the disruption of the hydrogen bonds in the coating. Moreover, due to the covalently crosslinked network in the coating caused by the diacrylic monomers 2 and 3, the cholesteric order was maintained after the alkaline treatment as the reflection band remained (Figure 3.3b). Some narrowing and loss in the intensity of the reflection band was observed after the alkaline treatment. However, this slight decline in molecular order is similar to previously reported data for optical humidity sensors based on hydrogen-bonded Ch-LC polymers.<sup>[13,14]</sup> The resulting reflection band of the coating after alkaline treatment is 120 nm broad, measured by full-width at half maximum.

Due to the pretreatment with BP, no delamination between the coating and the PC substrate was observed during submersion of the coating in the alkaline solution. The absorption of water caused the photonic layers to

swell, resulting in an approximately 400 nm red shift of the reflected wavelength. Conversely, drying of the coating induced a blue shift of the Ch-LC reflection band, returning to its original wavelength at 1050 nm.

### **Humidity-gated temperature-responsive narrowband reflector**

To analyze the thermochromic behavior of the coating, transmission spectra at temperatures between 70 °C and -2 °C at 75% RH were taken. By decreasing the temperature of the coating from 30 to -2 °C a reversible red shift of 400 nm from 1150 nm to 1550 nm was obtained (Figure 3.4a). Due to cooling of the coating, locally the dew point of water vapor in air was reached at 16 °C according to the extended Magnus equation. (Equation 3.1).

$$t_d = \frac{B * \left( \ln\left(\frac{RH}{100}\right) + \frac{A * t}{B + t} \right)}{A - \ln\left(\frac{RH}{100}\right) - \frac{A * t}{B + t}} \quad \text{Eq. 3.1}$$

The extended Magnus equation is used for the relationship between the dewpoint and the RH and temperature. The  $t_d$  is the temperature of the dewpoint (°C),  $A$  and  $B$  are coefficients,  $RH$  is the relative humidity (%) and  $t$  is the environmental temperature (°C).<sup>[15]</sup> The coefficients are obtained from literature,  $A = 17.625$  and  $B = 243.04$  °C.<sup>[16]</sup>

Below this dew point temperature, the absorption rate of water into the hygroscopic coating was increased, owing to condensation of the water vapor from the air. This was evidenced by the drastic increase of the slope of the reflection band shift curve near and below the dew point temperature, approximately between 5 °C and 15 °C (Figure 3.4b). Upon heating, water was evaporated from the coating, causing the photonic layers to deswell and the reflection band to return to its original color.

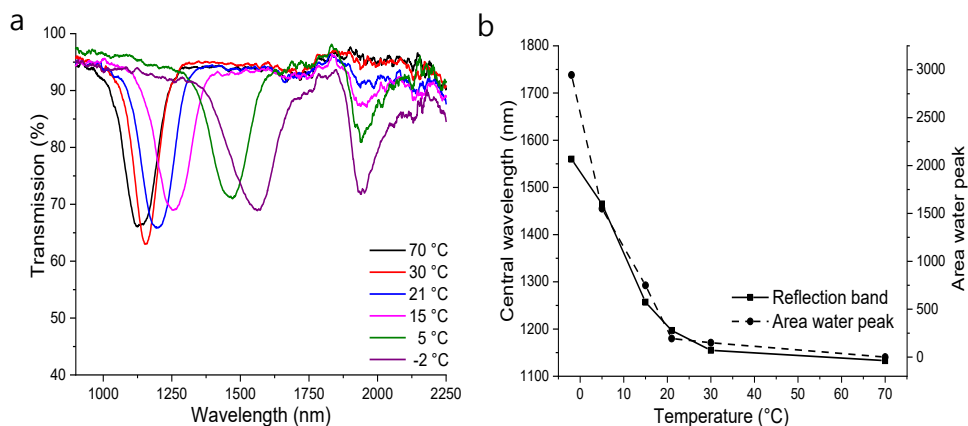


**Figure 3.4:** a) Transmission spectra of the hygroscopic coating prepared from Ch-LC mixture I, measured at various coating temperatures and a constant environmental RH of 75% and temperature of 21 °C. Spectra were measured after the coating was kept at the set temperature for 5 minutes. b) Both the central position of the reflection band and the area of the water absorption peak are plotted versus temperature.

To ensure complete removal of the water from the coating, the coating was heated to 70 °C after every cooling/heating cycle. However, as Figure 3.4a shows, nearly all water was already removed after reaching a temperature of 30 °C since the peak present at 1950 nm, which corresponds to the water absorbance, disappears. To analyze whether the temperature-responsive band-shifting behavior of the coating was solely caused by the absorbance of water, the area of the water absorbance peak was integrated and plotted as a function of the temperature to compare the measured water content with the central position of the reflection band. (Figure 3.4b). As suggested by the similarity of the trends of the two curves, the origin of the temperature response was primarily governed by water uptake of the hygroscopic coating. Only at low temperatures did the curves deviate significantly from each other. This deviation is most likely caused by the formation of a layer of water at the surface of the coating after saturation of the coating itself. This additional layer of water affects the transmission of the IR light (at 1950 nm), but does not result in further swelling and thus shift of the reflection band.

To shed light on the influence of the RH on the thermochromic behavior of the coating, the temperature response of the coating was investigated at different RH's (Figure 3.5). Below 30% RH, no significant shift of the reflection band was observed. At 45% RH, a 137 nm shift of the reflection band was observed when cooling from 21 °C to -2 °C. Increasing the concentration of water vapor in the air resulted in an increase in the maximum shift of the reflection band and an increase of the temperature window within which the coating is responsive. At 60% RH, a 300 nm red shift was achieved between 70 °C and -2 °C and at 75% RH a maximum shift of 420 nm between 70 °C and -2 °C was achieved (*vide supra*).

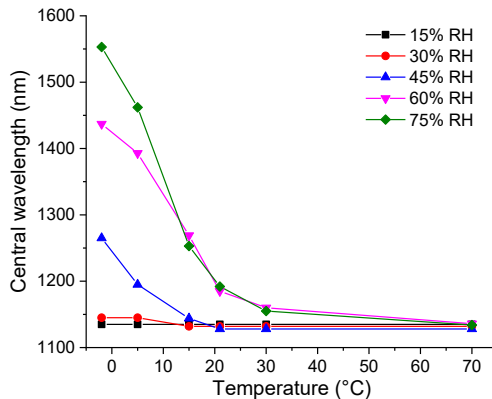


**Figure 3.5:** Central wavelength of the reflection band of the Ch-LC coating measured at different temperatures at various RH's.\* At 45% RH, a significant shift of the reflection band is observed. Decreasing the RH inhibits thermochromic behavior. Increasing the RH from 45% causes an increase in the maximum shift of the reflection band upon temperature variations and an increase in the temperature window in which the coating is responsive. Measurements were taken after the coating was kept at the set temperature for 5 minutes.

This humidity-gated temperature-responsive behavior above 45% RH is most likely due to the decreased dew point at lower RH. For example, at 15% RH the dew point is calculated to be -7 °C. Therefore, these temperature-responsive coatings are especially interesting for heat reflecting windows in higher RH climates, such as greenhouses.<sup>[17]</sup>

### **Fabrication of the broadband IR reflective Ch-LC coating**

To create a broader reflection band, a pitch gradient was created.<sup>[18]</sup> By partial diffusion of the photoinitiator from the substrate-coating interface into the coating during photopolymerization, a concentration difference of radicals throughout the thickness of the coating should be created. Due to depletion-induced diffusion of the monomers, this inhomogeneity of radicals creates a difference in chiral dopant concentration, needed for broadband formation.<sup>[19]</sup> During the diffusion process, faster reacting diacrylic monomers diffuse towards the areas with a higher polymerization rate due to increased local depletion of those monomer by polymerization, while slower reacting monoacrylic monomers counter diffuse towards areas with a lower polymerization rate. To optimize the broadband formation, some changes were made during the fabrication process to aid monomer diffusion during photopolymerization (i and ii) and improve adhesion of the coating to the substrate (iii), as described below.

(i) Since the acidic LCs **6** and **7** were still hydrogen-bonded during the polymerization reaction, their reactivity was comparable to that of a diacrylic monomer. In order to sufficiently differentiate between the reactivity of the various monomers, the diacrylic chiral dopant **2** was exchanged for a monoacrylic chiral dopant **4**, keeping the crosslink density constant by adjusting the monoacrylic *versus* diacrylic ratio.

(ii) The ability to obtain a gradient in polymerization rate and a widened reflection band by partial diffusion of the photoinitiator BP from the substrate interface into the coating was demonstrated in Chapter 2. To establish enough time for diffusion of the monomers, the photo-curing intensity was lowered by a factor of 10, the initial concentration of BP applied during pretreatment was lowered by a factor of 20 and no BP was present in the Ch-LC mixture. Moreover, UV-light absorbing dye **5** was added to enhance the light intensity gradient, amplifying the polymerization



rate gradient.<sup>[19]</sup> At the substrate interface, the concentration of radicals in the coating was high with respect to the air-interface. Therefore, the diacrylate **3** and the acidic LCs **6** and **7** could diffuse towards the substrate, leaving room for the monoacrylic chiral dopant to counter diffuse towards the coating-air interface.

(iii) Lowering of the BP concentration was needed to ensure a low enough reaction rate so that the monomers were able to sufficiently diffuse prior to polymerization. However, adhesion between the coating and the substrate was compromised when the BP concentration in the primer solution was lowered to 0.5 wt%. To ensure sufficient adhesion of the coating to the substrate after base treatment, PC-benzophenone copolymer XPC was used as a substrate, which contained 10 mol% covalently bound non-diffusible BP groups.

After polymerization, similar to the procedure used to prepare the narrowband reflectors, the coating was soaked in an alkaline solution to disrupt the hydrogen bonds. Figure 3.6a shows the transmission spectra of the 400 nm-broad reflection band of the Ch-LC coating after KOH treatment.

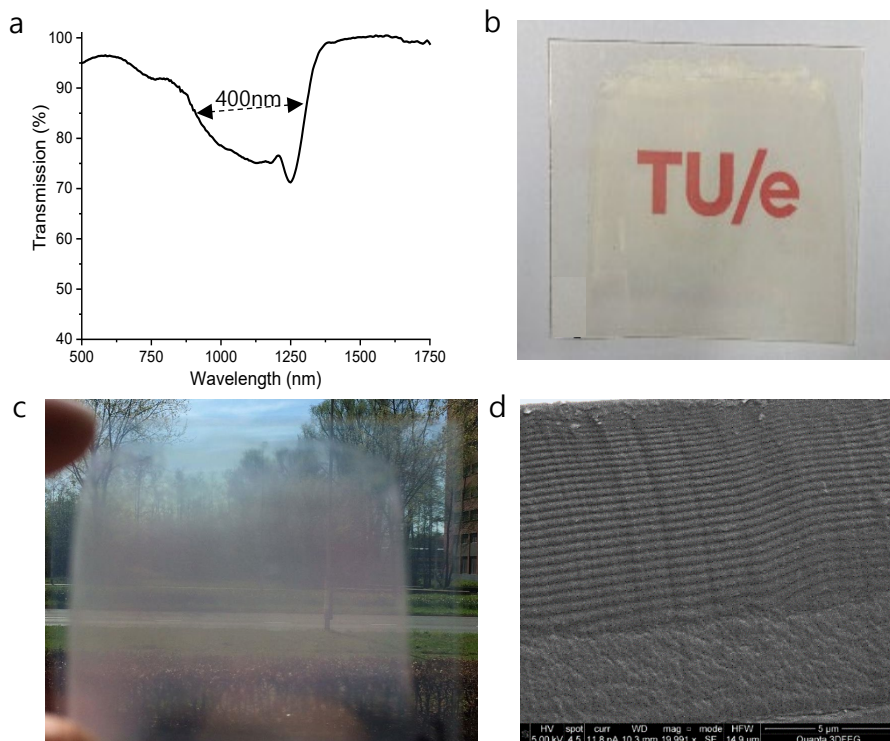


**Figure 3.6:** a) Transmission spectra of the Ch-LC coating prepared from Ch-LC mixture II, after the alkaline treatment. The hygroscopic coating has a bandwidth of approximately 400 nm, measured at full-width half-maximum as is indicated by the dashed line. b) Photograph of the coating and substrate covering the TU/e logo, showing excellent transmission of the visible light. c) Photograph of the coating and substrate in front of a window, showing the effect of haze. d) SEM image of the cross-section of the coating. Cholesteric lines are easily visible with the larger pitches at the bottom (substrate interface) and the smaller pitches at the top (air interface). In between the cholesteric aligned film and the substrate, an area of disordered polymer is visualized, which has a constant thickness across the coating.

Comparing with the bandwidth of the Ch-LC coating without a pitch gradient (Figure 3.4a), with the bandwidth of the Ch-LC coating with a pitch gradient, the width had increased by a factor of 3.3. Figure 3.6b and 3.6c show photographs of the coating covering the TU/e logo and the view through a window to the outside, respectively. The TU/e logo is clearly visible behind the coating showing excellent transmission of the broadband coating for visible light. Looking outside the window through the coating, haze ( $40\% \pm 3\%$ , measured by UV-Vis spectroscopy) caused by forward

scattering was observed. SEM images of the coating cross-section (Figure 3.6d) clearly shows a pitch gradient, with the largest pitches near the substrate interface as expected, due to the lower concentration of chiral dopant. In addition to the well-ordered cholesteric lines displaying only a few defects, a non-aligned layer sandwiched between the aligned Ch-LC network and the substrate was observed. This non-aligned layer most likely causes the haziness of the coating. BP diffusion through the coating is likely to cause Ch-LC alignment disruption during photopolymerization, because the concentration of this non-mesogenic molecule is too high. The haziness limits these coatings for smart window applications in office buildings, for example, since the outside view would be adversely affected. However, for applications in the greenhouse industry, windows are desired that generate more diffuse light (*via* forward scattering) for optimal crop growth. In this case, diffuse light penetrates through the leaf canopy to the middle layers of the crop, resulting in increased photosynthesis.<sup>[20]</sup>

### **Humidity-gated temperature-responsive broadband reflector**

At a fixed 75% RH, transmission spectra were taken at various temperatures to analyze the thermochromic behavior of the coating (Figure 3.7a). The central position of the widened reflection band had an approximate red shift of 400 nm upon decrease of the temperature from 30 °C to 2 °C (Figure 3.7b). Note that this temperature-triggered red shift is similar to the shift exhibited by the narrowband reflector shown in Figure 3.4a. Alongside the red shift of the reflection band upon cooling, the shape of the reflection band was also affected by the temperature: upon cooling from 15 °C to 5 °C and 2 °C, the short wavelength portion of the reflection band displays an intensity reduction, due to a loss of the Ch-LC alignment.

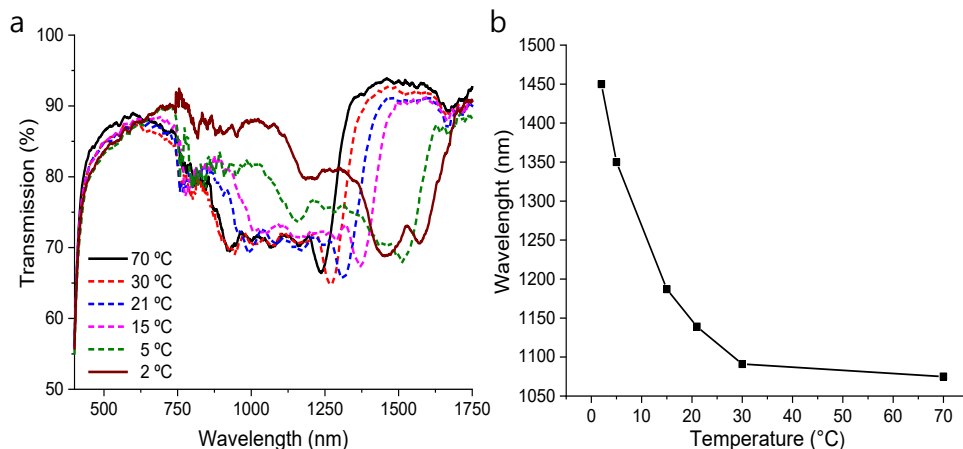


**Figure 3.7:** a) Transmission spectra of the broadband Ch-LC coating at 75% RH and various temperatures. Spectra were measured after the coating was kept at the set temperature for 5 minutes. b) The central wavelength of the reflection band plotted as a function of temperature. Note that the central position is difficult to determine by the full-width half-maximum method, since the width of the reflection band is ill defined.

The loss of alignment for the smaller pitches is caused by the gradient of the local crosslink density coming from the enrichment in diacrylic (with respect to monoacrylic) monomers towards the coating-substrate interface (with respect to the coating-air interface). Due to the monoacrylic nature of the chiral dopant, the smallest pitches are formed in the area of lower crosslink density. Therefore, these smaller pitches showed a greater decline in molecular order upon swelling with respect to the more crosslinked areas of the higher pitches.

To analyze the time needed for the coating to absorb water from the environment, the coating was rapidly cooled down from 70 °C to 5 °C and kept isothermal. Afterwards, the coating was rapidly heated to 70 °C to assess the time needed for desorption of the water present in the coating. The environmental RH was kept constant at 75% throughout the entire cycle. Figure 3.8a shows the central wavelength shifts of the broadened reflection band during the isothermal stages. In the first 10 minutes, the coating absorbs most of the water, as shown by the rapid reflection band

shift from approximately 1080 nm to 1325 nm. After these initial 10 minutes, the reflection band slowly continues to absorb water, causing disorder in the smaller Ch-LC helix pitch, shifting therefore the central position of the reflection band further, similar to the reflection bands shown in Figure 3.7a. After heating from 5 °C to 70 °C, the central wavelength recovered its original position within a few minutes. Alternating heating and cooling of the coating for a least 10 times at 75% RH shows good reversibility of the shift of the IR reflection band (Figure 3.8b).

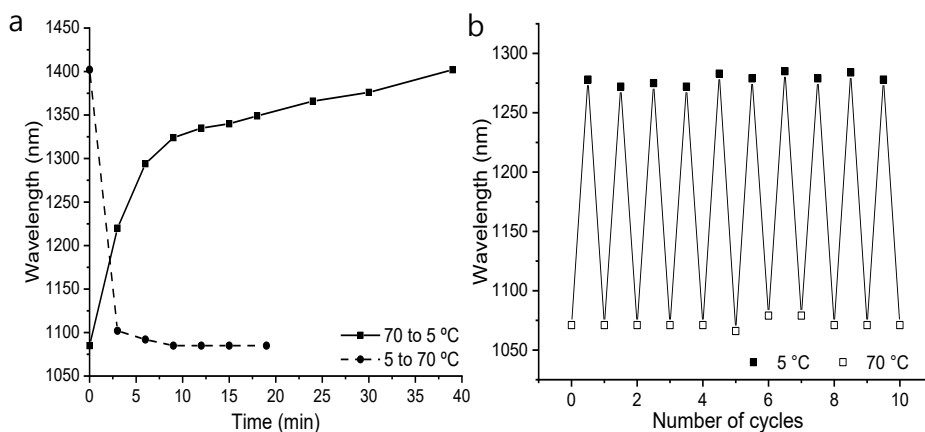


**Figure 3.8:** a) Central wavelength of the broad reflection band after the coating was heated (dashed) or cooled (solid) at 50 °C/min and kept isothermal at 75% RH. Spectra were measured every 3 minutes with t=0 at the start of the cooling or heating ramp. b) Central wavelength of the reflection band after keeping the coating isothermal for 5 minutes during 10 cycles of heating and cooling at 75% RH.

### 3.4 Conclusions

In this chapter, the successful fabrication process for humidity-gated temperature-responsive coatings using an easy-to-process bar-coating technique was reported and the working mechanism of its responsive behavior was elucidated. At 75% RH, heating or cooling of the coatings result in a blue shift or red shift of the Ch-LC reflection band of a maximum of 420 nm, respectively. This temperature-responsive shift is caused by the

absorbance of water vapor from the air into the coating at lower temperatures, swelling the photonic layers.

Furthermore, a Ch-LC broadband was created by diffusion of the photoinitiator from the substrate into the polymerizing coating. For these coatings, a ~400 nm band shift was obtained as well, demonstrating the ability to reflect heat at higher temperatures, while allowing heat to be transmitted through the coating at lower temperatures. These coatings are potential candidates for heat-regulating windows in climates where the humidity is higher than 60%, such as tropical environments and greenhouses. Furthermore, modifying the chiral dopant concentration to a (narrow) reflection band in the visible light, aesthetic or other humidity-gated temperature-responsive applications can be considered as well.

### 3.5 Notes and references

‡ Copolycarbonate film substrate, comprising a copolycarbonate of bisphenol A and 10 mol% of 4,4'-dihydroxybenzophenone,  $M_w$  of 21000-23000 g/mol as determined by GPC using bisphenol A polycarbonate standards, phenol end-capped as described in WO2015-193862

\* Transmission spectra of the coating at all temperatures and RH mentioned are reported in the supporting information of the article corresponding to this chapter.

- [1] H. Khandelwal, A. P. H. J. Schenning, M. G. Debije, *Adv. Energy Mater.* **2017**, *7*, 1.
- [2] H. Khandelwal, R. C. G. M. Loonen, J. L. M. Hensen, A. P. H. J. Schenning, M. G. Debije, *J. Mater. Chem. A* **2014**, 14622.
- [3] Y. Zhou, Y. Cai, X. Hu, Y. Long, *J. Mater. Chem. A* **2014**, *2*, 13550.
- [4] Y. S. Yang, Y. Zhou, F. B. Yin Chiang, Y. Long, *RSC Adv.* **2016**, *6*, 61449.
- [5] X. Liang, S. Guo, S. Guo, M. Chen, C. Li, Q. Wang, C. Zou, C. Zhang, L. Zhang, H. Yang, *Mater. Horizons* **2017**, *4*, 878.
- [6] S. Grynning, F. Goia, B. Time, *Energy Procedia* **2015**, *78*, 85.
- [7] A. Seeboth, R. Ruhmann, O. Mühlring, *Materials (Basel)*. **2010**, *3*, 5143.
- [8] L. Wang, H. K. Bisoyi, Z. Zheng, K. G. Gutierrez-Cuevas, G. Singh, S. Kumar, T. J. Bunning, Q. Li, *Mater. Today* **2017**, *20*, 230.
- [9] F. Guo, S. Chen, Z. Chen, H. Luo, Y. Gao, T. Przybilla, E. Spiecker, A. Osvet, K. Forberich, C. J. Brabec, *Adv. Opt. Mater.* **2015**, *3*, 1524.

- [10] W. Zhang, S. Kragt, A. P. H. J. Schenning, L. T. de Haan, G. Zhou, *ACS Omega* **2017**, *2*, 3475.
- [11] Y. Takeoka, M. Watanabe, *Langmuir* **2003**, *19*, 9104.
- [12] M. Chen, L. Zhou, Y. Guan, Y. Zhang, *Angew. Chemie - Int. Ed.* **2013**, *52*, 9961.
- [13] N. Herzer, H. Guneyso, D. J. D. Davies, D. Yildirim, A. R. Vaccaro, D. J. Broer, C. W. M. Bastiaansen, A. P. H. J. Schenning, *J. Am. Chem. Soc.* **2012**, *134*, 7608.
- [14] J. E. Stumpel, D. J. Broer, C. W. M. Bastiaansen, A. P. H. J. Schenning, *Proc. SPIE* **2014**, *9137*, 1.
- [15] M. G. Lawrence, *Am. Meteorol. Soc.* **2005**, 225.
- [16] O. A. Alduchov, R. E. Eskridge, *J. Appl. Meteorol.* **1996**, *35*, 601.
- [17] C. Stanghellini, J. Dai, F. Kempkes, *Biosyst. Eng.* **2011**, *110*, 261.
- [18] D. J. Broer, J. Lub, G. N. Mol, *Nature* **1995**, *378*, 467.
- [19] D. J. Broer, G. N. Mol, J. A. M. M. van Haaren, J. Lub, *Adv. Mater.* **1999**, *11*, 573.
- [20] S. Hemming, T. Dueck, J. Janse, F. van Noort, *Acta Hortic.* **2008**, *801*, 1293.







# Chapter 4

## Thiol-acrylic elastomer responsive photonic coatings

**Abstract.** The functional and responsive properties of elastomeric materials highly depend on crosslink density and molecular weight between crosslinks. In this chapter, an in-situ structure property characterization method is reported by monitoring the structural color change in a photonic elastomeric material. The photonic materials are prepared in a two-step polymerization process. The step-growth polymerization process can be monitored by following the photonic reflection band red shift, enabling to program the molecular weight between the crosslinks. These processes can be locally controlled creating both single-layered multi-color patterned and broadband reflective coatings at room temperature. The scalability of the coating process is further demonstrated by using a gravure printing technique. Additionally, due to the elastomeric nature of the polymer network, the final coatings are made responsive towards specific solvents and temperature. Here the responsiveness and color is controlled by tuning the polymer network structure.

---

This chapter is partially reproduced from: 'Tunable photonic materials via monitoring step-growth polymerization kinetics by structural colors. E.P.A. van Heeswijk, N. Grossiord, A.P.H.J. Schenning (submitted)

## 4.1 Introduction

Elastomeric polymers have been investigated intensively over the past years for the creation of stimuli-responsive materials. In particular, the combination of the anisotropic nature of liquid crystals (LCs) and the flexibility of elastomer networks have proven to be an excellent combination for shape memory films<sup>[1,2]</sup>, soft actuators<sup>[3-7]</sup> and stimuli-responsive materials<sup>[8-11]</sup>. Having control over the polymerization reaction by controlling crosslink density and molecular weight between crosslinks is highly desired to create optimal functionality, flexibility and strength in the material.<sup>[12-17]</sup>

In recent studies, LC elastomer films are frequently prepared with siloxane oligomers or by Michael addition chain extension reactions of diacrylic LC monomers.<sup>[18]</sup> Especially the latter, involving Michael addition, has received a lot of interest recently, due to the large variety of reactive mesogens that are available.<sup>[1-5,8,12,13,19,20]</sup> By controlling the network formation, a large variety of stimuli-responsive shape and color changing materials with desired functional properties can be obtained.<sup>[21]</sup>

For the creation of color contrast in a single layer, cholesteric LC (Ch-LC) materials are typically first illuminated through a mask, after which they are heated to affect the helical twisting power (HTP) or heated above the cholesteric to isotropic phase transition temperature.<sup>[22,23]</sup> However, reports about the responsive behavior of elastomeric multi-colored polymer coatings remain scarce.<sup>[11]</sup>

LC elastomers with well-defined responsive properties require a specific oligomeric chain length, needing additional polymerization and analysis steps for the oligomers before the coatings are formed. In this chapter, a method is reported that gives in-situ feedback for thiol-acrylic Michael addition polymerization kinetics by structural coloration. Using this approach, oligomers are prepared during the coating process, avoiding the need for pre-polymerization before coating application. Moreover, both single-layered multi-

color patterned and broadband coatings are formed at room temperature (RT), without the requirement for additional heating and the scalability of the coating process is further demonstrated using a gravure printing technique. Additionally, photonic elastomer Ch-LC coatings are made dual-responsive towards specific solvents and temperature in which responsiveness and color is controlled by tuning the crosslink density and molecular weight between the crosslinks.

## 4.2 Experimental details

### Materials

500  $\mu\text{m}$  thick LEXAN™ 8040T polycarbonate (PC) film was kindly provided by SABIC. 36  $\mu\text{m}$ -thick biaxially-oriented polyethylene terephthalate (PET) substrates (Tenolan® OCN0003) were purchased from SABIC Snijuni BV. Benzophenone (BP), triethylamine (TEA), 2,2'-(ethylenedioxy)diethanethiol (**1**) and liquid crystal **3**, depicted in Figure 4.1, were purchased from Merck. Chiral dopant **2**, was received from BASF. The solvents 1-methoxy-2-propanol and cyclopentanone were purchased from Merck as well.

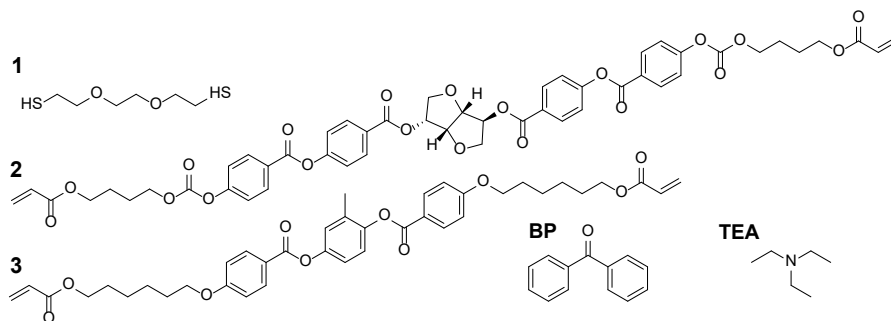


**Figure 4.1:** Molecular structures of chemicals used.

The Ch-LC mixtures contained 20 wt% monomer dithiol **1**, 1 wt% photoinitiator BP, 2 wt% catalyst TEA and varying concentrations of the LC monomer **3**, and the chiral dopant **2**, depending on the color desired for the coating. Initial blue coatings contained 7 wt% chiral dopant **2** / 70 wt% LC monomer **3**. Initial green

coatings contained 5 wt% chiral dopant **2** / 72 wt% LC monomer **3**. Initial red coatings contained 4 wt% chiral dopant **2** / 71 wt% LC monomer **3**.

## Methods

*Ch-LC cells:* a Ch-LC monomer mixture was coated on a glass plate at RT using a gap applicator with a 30  $\mu\text{m}$  gap height. A second glass plate was added on top of the coating to avoid evaporation. The glass plates were pressed together and sheared to regain proper Ch-LC alignment.

*Patterned coatings (Bar-coating):* Ch-LC monomer mixtures were coated on a flexible PC substrate at RT (*i.e.* 20  $^{\circ}\text{C}$ ) using a gap applicator with a 30  $\mu\text{m}$  gap height. Patterned coatings were partially cured by a masked photopolymerization using an Omnicure<sup>®</sup> S2000 UV lamp at an intensity of 3  $\text{mW}/\text{cm}^2$  for 80 seconds. Afterwards, the uncured areas of the coating were allowed to react via thiol-Michael addition for 0-180 min. Subsequently, the coating was fully cured into a network via photopolymerization using again the same illumination setup at an intensity of 30  $\text{mW}/\text{cm}^2$  for 5 minutes. For the preparation of coatings exhibiting more than two colors, additional successive masked photopolymerization steps took place before the coating was completely cured. The complete procedure was performed at RT.

*Broadband coating:* Ch-LC monomer mixtures were coated on a flexible PC substrate at RT using a gap applicator with a 30  $\mu\text{m}$  gap height. The coatings were partially cured by an Omnicure<sup>®</sup> S2000 UV source at 0.4  $\text{mW}/\text{cm}^2$  for 45 seconds. Subsequently, the coating was allowed to react further via thiol-Michael addition. After 180 min, the coating was fully cured using photopolymerization the same illumination setup at 30  $\text{mW}/\text{cm}^2$  for 300 seconds. The complete coating procedure was performed at RT.

*Gravure printing:* Ch-LC monomer mixtures were dissolved in a 1:1 mass ratio in cyclopentanone. The ink was printed at a speed of 0.5 m/s on flexible PET substrates using an IGT F1 printability tester in a gravure printing mode.

Afterwards, the solvent was allowed to evaporate for approximately 2 min at 50 °C. The coatings were partially cured by masked photopolymerization using an Omnicure® S2000 UV source at 30 mW/cm<sup>2</sup> for 40 seconds. The multi-colored coatings were allowed to react further via thiol-Michael addition and cured afterwards in a second illumination step (30 mW/cm<sup>2</sup>, 300 sec). Non-patterned coatings were directly cured for 300 seconds at an intensity of 30 mW/cm<sup>2</sup>.

### Characterization

*UV-Vis spectroscopy* was performed on a PerkinElmer LAMBDA™ 750 UV/Vis/NIR spectrophotometer equipped with a 150 mm intergrading sphere. *Gel permeation chromatography (GPC)* was performed on a Shimadzu Prominence-I LC-2030C high-performance liquid chromatography (HPLC) equipped with photodiode array and refractive index detectors. Polystyrene (PS) standards and a 1 mL/min CHCl<sub>3</sub> flow rate were used. *Nuclear magnetic resonance (NMR)* spectra were recorded on a 400 MHz Bruker AVANCE™ III HD spectrometer with tetramethyl silane used as an internal standard. *Scanning electron microscopy (SEM)* images were obtained from a JEOL JSM-7800F microscope using an acceleration voltage of 5 kV, a working distance of 6 mm and high vacuum. To obtain a larger SEM image, several SEM images were stitched together using a 67% overlap between every image. Cross-sections of the sample were prepared by cryotomy at -120 °C, 200 nm and 0.2 mm/s, followed by stabilization at room temperature for at least 30 min. Prior to SEM imaging, a Pt/Pd sputter coating of 5 nm in thickness was applied with a JEOL 208HR sputter coater. *Contact angle measurements* were performed on a KRÜSS Drop Shape Analysis System DSA30 using the sessile drop method. Surface free energy was calculated according to the Owens, Wendt, Rabel and Kälble method.<sup>[24,25]</sup> 10 droplets of each ethylene glycol (Fisher Scientific, 99% purity) and water (Milli-Q) were used. Diiodomethane was not used since it swelled the coating.

### 4.3 Results and discussion

Ch-LC mixtures consisting of dithiols and diacrylates, photoinitiator and base-catalyst (Figure 4.1) were prepared. For the formation of the elastomeric Ch-LC coatings, a two-step thiol-acrylic polymerization mechanism was used after bar-coating the Ch-LC mixture, which oriented the LCs uniformly by shear alignment.<sup>[26]</sup> In the first polymerization step, only chain extension of the monomers occurs by linear step growth polymerization. Afterwards, the linear oligomers are cured to form a polymer network (Figure 4.2).

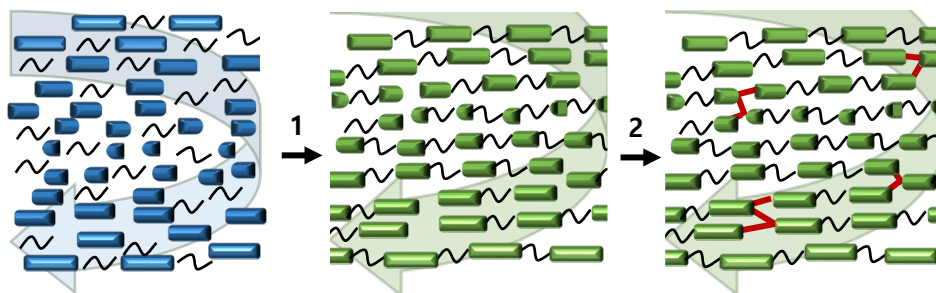


**Figure 4.2:** Schematic representation of the two phases of the coating preparation. In step 1 only chain extension occurs by a base-catalyzed polymerization reaction. In step 2 a network is formed by crosslinking the acrylic end groups.

To exclude network formation in the first polymerization step, a base-catalyzed polymerization mechanism is used. During this polymerization, which is often referred to as a Michael addition reaction, diacrylic monomers are bifunctional resulting in the formation of oligomers through chain extension. For the second polymerization step, in which a network is formed, the oligomers are photopolymerized. Radicals formed cause homo-polymerization of the acrylic endgroups, causing the acrylates to serve as crosslinkers.<sup>[27]</sup>

#### **Monitoring in-situ step growth polymerization by structural color changes**

Remarkably, when the Ch-LC mixtures were coated, a color change over time was observed, which is normally not observed when solely using free radical polymerization (FRP). However, for chiral dopants, it is known that the helical

twisting power depends on the surrounding environment.<sup>[28,29]</sup> Since this approach allows for linear chain extension of the monomer and excludes rapid network formation, the chiral dopant might be able to respond to its slowly polymerizing matrix. In this case, the oligomerization causes a red shift of the reflection band (Figure 4.2), which, according to Equation 4.1, indicates a decrease of the helical twisting power during the Michael addition reaction.

$$\lambda_{refl} = \frac{n_{av}}{HTP*[C]} \quad \text{Eq. 4.1}$$

Where  $\lambda_{refl}$  is the central wavelength of the reflection band,  $n_{av}$  is the average refractive index,  $HTP$  is the helical twisting power of the chiral dopant and  $[C]$  is the concentration of the chiral dopant. To study the relation between the Ch-LC reflection band and the growing polymer chains, a Ch-LC monomer mixture was prepared with an initial blue reflection band. To avoid evaporation of monomers or the catalyst during polymerization, the monomer mixture was prepared in a glass cell and LC alignment was obtained using shear. Figure 4.3a shows the Ch-LC reflection band of the film at various thiol-Michael addition reaction times and reveals a significant red shift as the reaction progresses. After 4 hours at RT, the reflection band has shifted from blue (440 nm) to red (650 nm), keeping a good LC alignment. Continuing the Michael addition reaction allows for a slight additional red shift of the reflection band. However, scattering starts to increase and, after a full day of polymerization, the Ch-LC alignment becomes focal conic, as indicated by the broadening of the reflection band (Figure 4.3a).

Besides the reflection band, the degree of polymerization (DP) and conversion were determined by GPC and NMR, respectively. An increase in chain length and conversion is clearly observed during the time period of the Ch-LC band shift, linking the growing polymer chains to the color shift and enabling the ability to predict the oligomer length based on the structural coloration of the film (Figure 4.3b). Photographs of the films are included in the figure to show the corresponding colors. In Figure 4.3c the DP is plotted as a function of the



conversion showing a typical step-growth kinetic curve thus indicating chain growth by the Michael addition reaction.

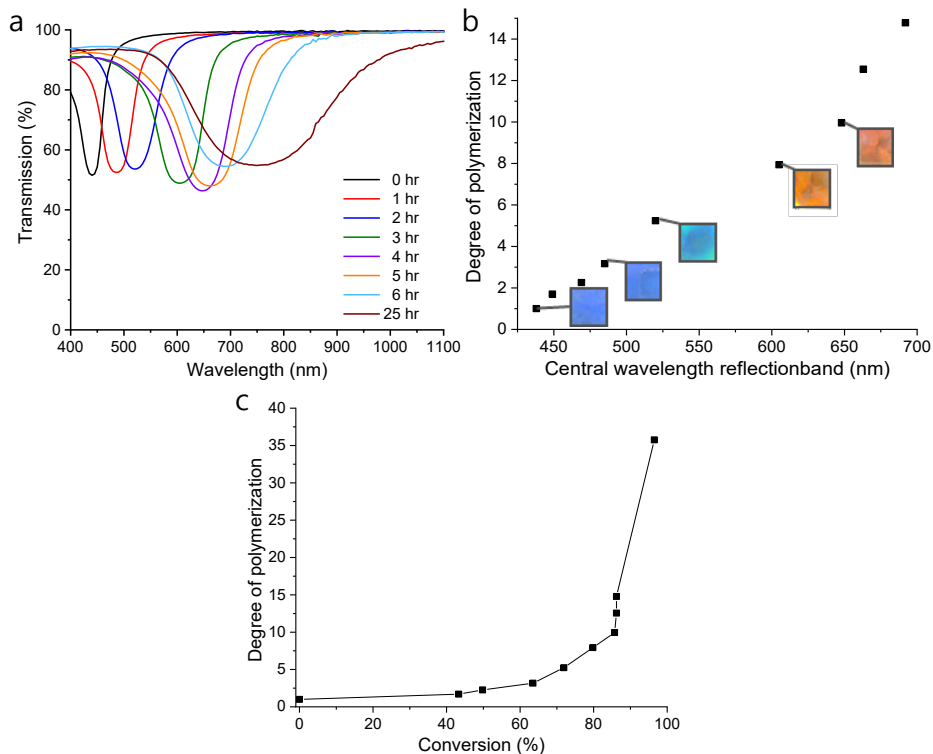


**Figure 4.3:** a) Transmission spectra of the Ch-LC reflection band at various times during the base-catalyzed polymerization reaction. Photographs of the films are shown in the squares. b) Evolution of the degree of polymerization of the films with respect to the central wavelength of the reflection band. Photographs of the films (taken at a 90° angle) are shown in the squares. c) Evolution of the degree of polymerization of the films with respect to the conversion showing the typical step-growth kinetics curve.

After photopolymerization-induced crosslinking, a red shift of the reflection band is no longer observed. Therefore, the Ch-LC reflection band can be 'frozen in' at any time. Using this structural color in situ analytical method, the crosslink density and molecular weight between crosslinks can be controlled by Michael addition reaction times and initial monomer composition.

### Patterned Ch-LC coatings

With the knowledge obtained above, multi-colored patterns were formed in a single-layered coating prepared by bar coating (Figure 4.4a). Using a successive masked UV light illumination, exposed areas of the coating were cured by FRP, while the unexposed areas kept reacting via the thiol-Michael addition. Figure 4.4b shows a triple colored image in which the blue background was cured immediately using UV light (80 sec, 30 mW/cm<sup>2</sup>) while the green and red areas were cured after allowing those areas to linearly polymerize at RT for an additional 40 minutes and 4 hours, respectively. A proper alignment of the Ch-LC causes the coating to be transparent for wavelengths outside of the reflection band, as is visualized by Figure 4.4c.

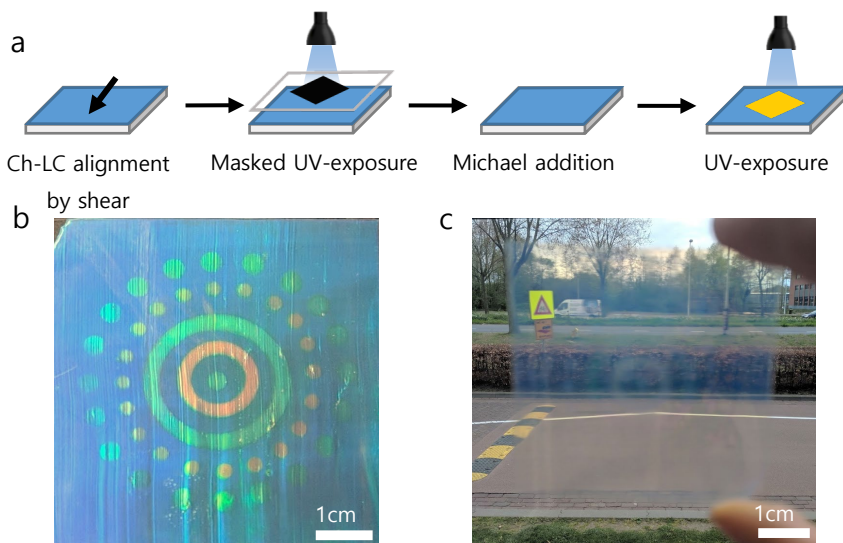


**Figure 4.4:** a) Schematic representation of the preparation procedure for the patterned photonic coatings. b) Ch-LC triple pattern formed by dual mask-exposure of a single layered coating. The blue backgrounds was cured directly after bar-coating, the green areas were cured after approximately 40 minutes and red areas were cured after 4 hours. c) The triple colored pattern (b) in front of a window, showing good transmission of the coating indicating good alignment of the LCs.

To demonstrate scalability of the coatings, multicolor coatings were prepared by gravure printing. The Ch-LC mixture was dissolved in cyclopentanone to tune the viscosity and printed on a black PET substrate at a speed of 0.5 m/s. The solvent

was evaporated and the ink was cured by UV-light exposure ( $30 \text{ mW/cm}^2$ , 5 min). By adjusting the time between ink preparation and printing, a specific network density and therefore color can be obtained (Figure 4.5a).

Using again a masked UV-exposure step (Figure 4.4a), patterns were created, having a Ch-LC color contrast (Figure 4.5b and 4.5c). The 45 nm shift between the reflection band of the butterfly (548 nm) and the background (593 nm) was achieved after 30 minutes of linear step-growth polymerization between the masked and non-masked exposure.

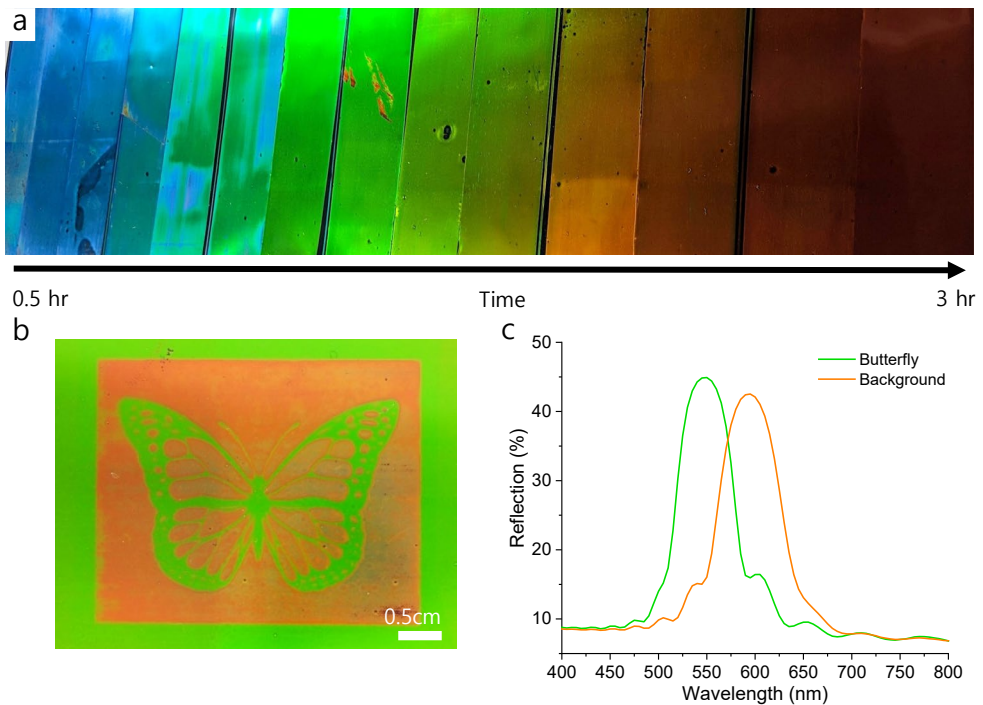


**Figure 4.5:** a) Coated black substrates using 1 batch of ink, showing the changing color of the ink over time from 0.5 to 3 hours. b) Photograph of a gravure printed photonic coating showing a Ch-LC green butterfly and edges and an orange background. c) Reflection spectra of the gravure printed patterned butterfly and background.

### Broadband Ch-LC coatings

The control over network formation in the lateral direction can also be translated into control of network formation throughout the coating thickness. By allowing

only network formation at the top of the coating, while prohibiting light to penetrate sufficiently to the other side of the coating (*i.e.* bottom), monomers are able to linearly extend at the bottom. There, the pitch will increase gradually due to the Michael addition reaction of the reactive chiral dopant, creating a broad reflection band throughout the thickness of the overall coating. Using this approach, a gradient in the pitch and thus a single layered broad Ch-LC reflection band can be formed. Using again a dual-light exposure approach, the coating was initially exposed to UV light with a low intensity ( $0.4 \text{ mW/cm}^2$ ) for 45 sec, in order to create a (partial) network at the illuminated side (*i.e.* top) of the coating. The remaining monomers/oligomers were allowed to react via the Michael addition reaction for at least 4 hours. Finally, the coating was fully cured for 300 sec using UV light with a high ( $30 \text{ mW/cm}^2$ ) intensity (Figure 4.6a). Figure 4.6b shows the widening of the reflection band. The black line in the figure corresponds to the narrowband formed after the coating was directly cured into a network using high intensity UV light. The dashed line corresponds to the broadband formed after the dual light exposure, broadening the reflection band from 120 nm to 400 nm. A SEM image of the cross-section of the coating (Figure 4.6c) shows that the small pitches are indeed formed at the air interface, on the right hand side, and that the pitch size gradually increases along the cross-section of the coating, as expected.

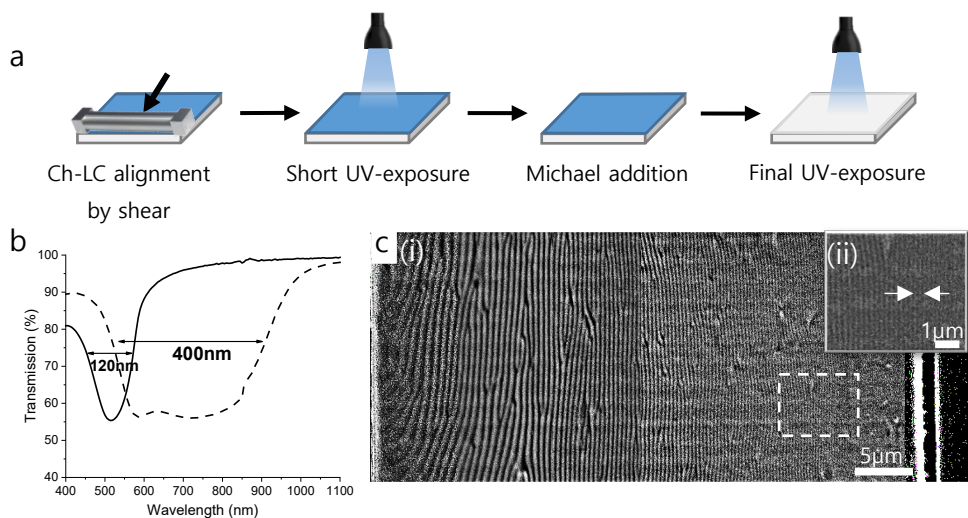


**Figure 4.6:** a) Schematic representation of the preparation procedure for the broadband coatings. b) Transmission spectra of coatings, directly cured (solid) and unmasked dual exposure (dashed) showing band widening of the Ch-LC reflection band. c) (i) SEM image of a cross-section of the broadband coating with the air interface at the right side. (ii) Enlarged image of the dashed rectangle showing the smaller pitches present in the coating.

### Stimuli-responsiveness of the Ch-LC coatings

Due to the increased flexibility of the elastomeric network formed, the final coatings are able to reversibly swell and de-swell with several solvents such as acetone. (Table 4.1).

**Table 4.1:** Analyzed solvent categorized based on their ability to swell the coatings.

Swelling solvents	Non-swelling solvents
Diiodomethane	Water
Toluene	Ethanol
Acetone	n-Hexane
Chloroform	Ethylene glycol
<i>N</i> -Methyl-2-pyrrolidone (NMP)	Methanol
Tetrahydrofuran (THF)	Isopropanol
Ethylacetate	Butan-1-ol
Acetonitrile	
Xylene	
Dimethylsulfoxide (DMSO)	

With a surface free energy (SFE) of  $18.6 \pm 3.5$  mN/m and 2% polarity, these coatings are very apolar. Therefore, the coating is less swollen by polar solvents. When calculating the Hansen parameters of the different solvents used,<sup>[30]</sup> it becomes clear that the swelling behavior of the coating cannot be described by one single set of such parameters. It is believed that different interactions are causing various solvents to swell the coating, which are not necessarily captured by the Hansen parameters.

Swelling of the coating leads to expansion of the cholesteric helix (e.g. pitch), which in turn results in a red shift of the Ch-LC reflection band (Eq. 4.1) in which the responsiveness and color is controlled by the crosslink density and molecular weight between the crosslinks. Figure 4.7 shows a multi-colored coating on glass, prepared by masked illumination as discussed before, revealing a flower. The flower disappears when soaked in acetone, which is fully reversible when the coating is dried. Due to the swelling of the coating, the reflection band shift towards the infrared, making the pattern invisible to the human eye. Due to the denser network formation in the blue region, the wetted coating remained slightly blue. Different designs can also cause a change in visible colors (blue-red) or the appearance of a pattern when the initial reflection band is located in the UV light regime (Figure 4.8).

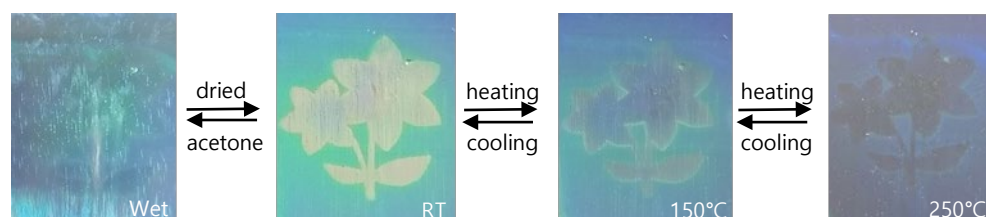


**Figure 4.7:** Patterned coating on glass showing dual responsiveness towards solvents and temperature. The coating was soaked in acetone (left), resulting in the disappearance of the pattern. The same coating was heated (right) to 150 °C and 250 °C showing the reversible disappearance of first the red color and subsequently the green color.

In addition to the responsiveness towards solvents, the coatings formed were able to undergo a reversible Ch-LC to isotropic transition visualized by the loss and reappearance of color at elevated temperatures (Figure 4.7). Heating the

coating to 150 °C, the reflection band of areas that have the largest average molecular weight between crosslinks (yellow-red) disappears first. Increasing the temperature further, areas with a smaller average molecular weight between crosslinks disappear as well. As is shown in Figure 4.7, blue areas, which possess the lowest molecular weight between crosslinks, do not fully lose their reflection band even at 250 °C.

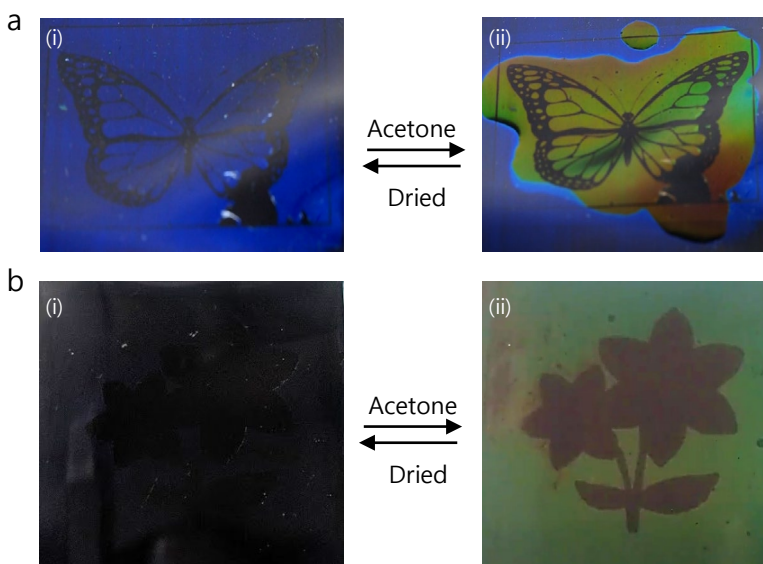


**Figure 4.8:** a) A Ch-LC/isotropic blue butterfly coating on a flexible PET substrate in the dry state (i) and swelled with acetone (ii), showing a reversible red shift of the reflection band. b) A Ch-LC/isotropic patterned coating on a flexible PET film with the Ch-LC reflection band in the UV regime when dry (i) and in the visible light when swelled with acetone (ii). For the Ch-LC/isotropic contrast, the coatings were heated the isotropic phase after the masked illumination and cured at these elevated temperatures.

To study the relationship between molecular weight before crosslinking, the crosslinking itself and the temperature, coatings with an initial red color were kept at room temperature and polymerized via the Michael addition reaction for 0, 1, 3 and 24 hours after which they were cured by photopolymerization. Before curing, the molecular weight was measured and after curing the temperature responsiveness was determined by heating and cooling the coating while measuring the transmission spectra of the coating. Figure 4.9 shows the

transmission spectra of the coatings. For all coatings, a reversible temperature response was obtained, which caused the reflection band to disappear at higher temperatures. As the molecular weight before network formation increases (from 1000 g/mol to 7500-18100 g/mol), the temperature needed for the reflection band to disappear decreased slightly (from >200 °C to 150 °C). Besides, as shown before, the photonic reflection band has red shifted with increasing chain length. Hence by monitoring the shift of the photonic color, the final responsive behavior of the coating can be predicted and controlled. Note that the temperature remains quite high, making these temperature responses less suitable for many plastic substrates and coating applications which rely on outdoor environmental temperatures. A way to significantly lower the temperature is to eliminate the network formation. In a non-crosslinked coating, disappearance of the reflection band is already observed at temperatures below 100 °C. However, this coating is sticky, and increasing the temperature further than 80 °C leads to an irreversible loss of the Ch-LC alignment.



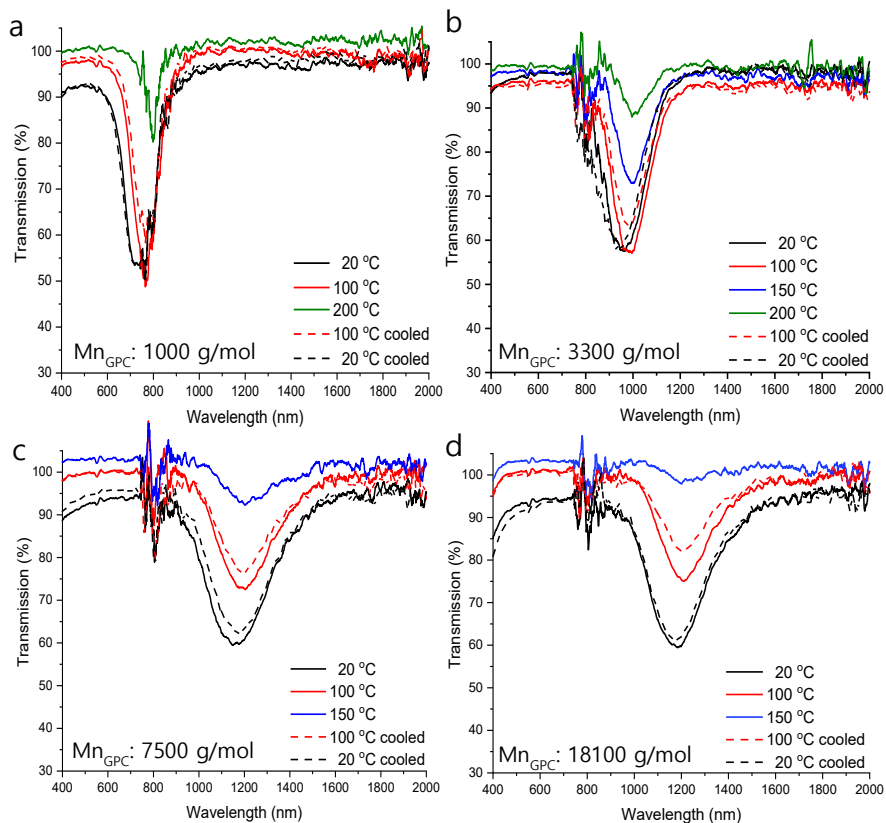


**Figure 4.9:** Transmission spectra of the Ch-LC reflection bands after photopolymerization of the different molecular weight polymer coatings obtained by thiol-Michael addition reaction for a) 0 hours, b) 1 hour, c) 3 hours, and d) 24 hours. The molecular weight mentioned in the graphs corresponds to the molecular weight (by GPC) after the 1<sup>st</sup> step of the process, *i.e.* the thiol-Michael addition. In all graphs, the solid lines correspond to heating cycles and the dashed lines correspond to cooling cycles.

## 4.4 Conclusions

An in-situ characterization method is reported in which Michael addition polymerization kinetics are coupled to structural coloration variations. A two-step polymerization approach was used, in which the oligomers and the network were formed both during the coating deposition process at room temperature. Initially, monomers were linearly chain extended by the Michael addition reaction causing a red shift of the reflection band. Over time, the reaction was monitored by the

visual color change of the coating. Subsequently, the linear chain lengths or desired colors were 'frozen in' by network formation due to photopolymerization.

With this new method, we have shown the ability to control chain extension versus network formation locally by creating both patterns with multiple colors and broadband reflecting coatings, widening the reflection band from 120 to 400 nm. Moreover, we demonstrated the ability to scale these materials using gravure printing techniques, for which the coatings were printed on flexible PET substrates, again creating multi-colored images. These dual-responsive photonic elastomer coatings show a reversible swelling behavior towards several solvents, and are able to lose their reflection band at elevated temperatures in a reversible manner. Apart from the coatings shown here, this in-situ two-step polymerization approach gives a new method to tune functional (optical) and responsive properties and opens up potential routes for the fabrication of camouflage and anti-counterfeit materials, broadband IR reflective coatings and the in-situ analyses of prepolymer lengths.

## 4.5 References

- [1] Z. Wen, M. K. McBride, X. Zhang, X. Han, A. M. Martinez, R. Shao, C. Zhu, R. Visvanathan, N. A. Clark, Y. Wang, K. Yang, C. N. Bowman, *Macromolecules* **2018**, *51*, 5812.
- [2] K. Nickmans, D. A. C. van der Heijden, A. P. H. J. Schenning, *Adv. Opt. Mater.* **2019**, *1900592*, 1.
- [3] C. P. Ambulo, J. J. Burroughs, J. M. Boothby, H. Kim, M. R. Shankar, T. H. Ware, *ACS Appl. Mater. Interfaces* **2017**, *9*, 37332.
- [4] A. H. Gelebart, M. M. Bride, A. P. H. J. Schenning, C. N. Bowman, D. J. Broer, *Adv. Funct. Mater.* **2016**, *26*, 5322.
- [5] T. Guin, M. J. Settle, B. A. Kowalski, A. D. Auguste, R. V. Beblo, G. W. Reich, T. J. White, *Nat. Commun.* **2018**, *9*, 1.
- [6] H. Zeng, O. M. Wani, P. Wasylczyk, R. Kaczmarek, A. Priimagi, *Adv. Mater.* **2017**, *29*, 1.
- [7] A. Merekalov, H. Finkelmann, A. Sa, *Macromol. Rapid Commun.* **2011**, *32*, 671.
- [8] T. J. White, D. J. Broer, *Nat. Mater.* **2015**, *14*, 1087.
- [9] A. J. J. Kragt, D. J. Broer, A. P. H. J. Schenning, *Adv. Funct. Mater.* **2018**, *1704756*, 1.
- [10] V. S. R. Jampani, D. J. Mulder, K. R. De Sousa, A. H. Gélébart, J. P. F. Lagerwall, A. P. H. J. Schenning, *Adv. Funct. Mater.* **2018**, *28*.

- [11] A. J. J. Kragt, N. C. M. Zurbier, D. J. Broer, A. P. H. J. Schenning, *ACS Appl. Mater. Interfaces* **2019**, *11*, 28172.
- [12] M. Barnes, R. Verduzco, *Soft Matter* **2019**, *15*, 870.
- [13] T. H. Ware, Z. P. Perry, C. M. Middleton, S. T. Iacono, T. J. White, *ACS Macro Lett.* **2015**, *4*, 942.
- [14] M. Kashima, H. Cao, H. Liu, Q. Meng, D. Wang, F. Li, H. Yang, *Liq. Cryst.* **2010**, *37*, 339.
- [15] M. Bispo, D. Guillon, B. Donnio, H. Finkelmann, *Macromolecules* **2008**, *41*, 3098.
- [16] H. Finkelmann, In *Polymer Liquid Crystals*; Ciferri, A.; Krigbaum, W. R.; Meyer, R. B., Eds.; 1982; pp. 35–62.
- [17] Z. Cheng, H. Cao, D. Zhao, W. Hu, W. He, X. Yuan, J. Xiao, H. Zhang, H. Yang, *Liq. Cryst.* **2011**, *38*, 9.
- [18] S. W. Ula, N. A. Traugutt, R. H. Volpe, R. R. Patel, K. Yu, C. M. Yakacki, *Liq. Cryst. Rev.* **2018**, *6*, 78.
- [19] J. M. Boothby, T. H. Ware, *Soft Matter* **2017**, *13*, 4349.
- [20] W. Hu, M. Chen, Q. Wang, L. Zhang, X. Yuan, F. Chen, H. Yang, *Angew. Chemie - Int. Ed.* **2019**, *58*, 6698.
- [21] M. T. Brannum, A. M. Steele, M. C. Venetos, L. S. T. J. Korley, G. E. Wnek, T. J. White, *Adv. Opt. Mater.* **2019**, *7*, 1801683.
- [22] P. Zhang, A. J. J. Kragt, A. P. H. J. Schenning, L. T. de Haan, G. Zhou, *J. Mater. Chem. C* **2018**, *6*.
- [23] D. C. Hoekstra, K. Nickmans, J. Lub, M. G. Debije, A. P. H. J. Schenning, *ACS Appl. Mater. Interfaces* **2019**, *11*, 7423.
- [24] D. K. Owens, R. C. Wendt, *J. Appl. Polym. Sci.* **1969**, *13*, 1741.
- [25] D. H. Kaelble, *J. Adhes.* **1970**, *2*, 66.
- [26] E. P. A. van Heeswijk, J. J. H. Kloos, J. De Heer, T. Hoeks, N. Grossiord, A. P. H. J. Schenning, *ACS Appl. Mater. Interfaces* **2018**, *10*, 30008.
- [27] C. E. Hoyle, C. N. Bowman, *Polym. Chem.* **2010**, *49*, 1540.
- [28] M. J. Cook, M. R. Wilson, *J. Chem. Phys.* **2000**, *112*, 1560.
- [29] G. H. Brown, *Advances in Liquid Crystals*, 1976.
- [30] C. M. Hansen, In *Hansen Solubility Parameters: A User's Handbook*, 2007; pp. 1–26.





# Chapter 5

## Encapsulated single-substrate photonic reflectors

**Abstract.** A temperature-responsive photonic coating on a flexible substrate was prepared by a photoinduced phase-separation process. In this coating, a low molecular weight cholesteric liquid crystal mixture was encapsulated between the substrate and an in-situ formed protective top layer. The temperature-responsive coating structure and composition were investigated in detail, revealing a thick top coat. The adhesion of the coating was improved by providing walls to anchor the top coat to the substrate.

---

This chapter is partially reproduced from: 'Paintable encapsulated body-temperature-responsive photonic reflectors with arbitrary shapes' E.P.A. van Heeswijk, T. Meerman, J. de Heer, N. Grossiord, A.P.H.J. Schenning, *ACS Appl. Polym. Mater.*, 2019, (accepted manuscript)

## 5.1 Introduction

The high mobility of low molecular weight liquid crystalline (LC) molecules enables large and fast reflection band shifts when exposed to environmental changes such as temperature variations. Often low molecular weight cholesteric-LC (Ch-LC) mixtures are sandwiched between two glass plates or foils, creating a stimuli-responsive photonic cell.<sup>[1-4]</sup> To create mechanically-robust coatings, it is usually desirable to crosslink LCs, which usually comes at the expense of the amplitude and/or speed of the optical response.<sup>[5]</sup> Various approaches have been studied to overcome this restriction, including polymer dispersed LC films<sup>[6,7]</sup> and hydrogel-like<sup>[8,9]</sup> (Chapter 3) or elastomeric LC photonic coatings<sup>[10,11]</sup> (Chapter 4).

Recently, we<sup>[12]</sup> and others<sup>[13]</sup> have reported on paintable temperature-responsive Ch-LC reflectors encapsulated in a single flexible polymer substrate. These polymer coatings consist of microscale polymer containers filled with a Ch-LC solution created by a two-stage polymerization-induced phase separation method<sup>[14]</sup> using a mask. The reflectivity of coatings changed over a large temperature range.

In this report, we used phase-separated Ch-LC coatings to create fast temperature-responsive photonic coatings, which need only 1 °C temperature difference to experience a 100 nm blue shift of their photonic reflection band. If one uses the difference between room temperature and skin temperature, a red to green shift occurred within seconds. Additionally, the phase-separation of the coating was investigated in detail, by comprehensive optical and confocal characterizations of the coating structure and composition revealing a relatively thick top coating. Substrates were also used that contained trays, avoiding the use of a mask exposure step during the coating process. These trays could be created by 3D printing allowing to produce arbitrary-shaped patterned photonic coatings with enhanced adhesion and a highly sensitive temperature-responsivity using an easy-to-use one-stage bar-coating technique.

## 5.2 Experimental details

### Materials

500  $\mu\text{m}$  thick LEXAN™ 8040T polycarbonate (PC) film was kindly provided by SABIC. Etched PC substrates were purchased from Philips. Black (*i.e.* RAL 9005) polylactic acid (PLA) filament was purchased from Ultimaker. Bisphenol A dimethacrylate (**1**), isobornyl methacrylate (**2**), LC mixture MLC-2138 and chiral dopant S811 (**5**) were purchased from Merck. Irgacure 819 (**3**) and Tinuvin-328 (**4**) were purchased from Ciba Specialty Chemicals LTD. The molecular structures are depicted in Figure 5.1.

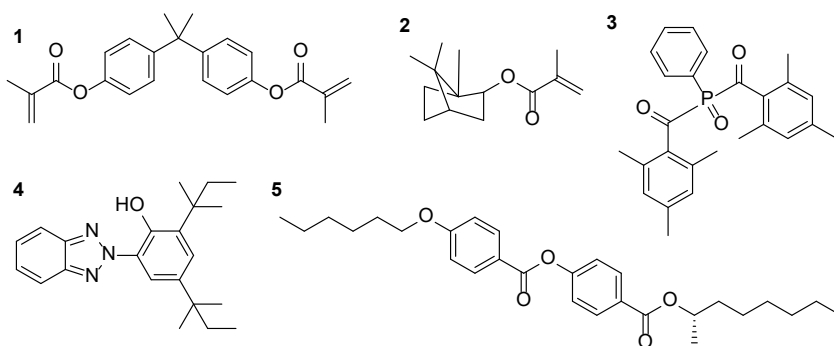


**Figure 5.1:** Molecular structures of chemicals used. The Ch-LC component of the mixture contains mesogenic mixture MLC-2138, for which the molecular structures are unknown, and was doped with the chiral mesogen **5**.

### Methods

*Temperature-responsive paint (Ch-LC mixture)* contains 4 wt% crosslinker (**1**), 45.5 wt% monoacrylate (**2**), 0.5 wt% photoinitiator (**3**), 0.3 wt% dye (**4**), 15 wt% chiral dopant (**5**), and 34.7 wt% MLC-2138.

*Temperature-responsive coating procedure:* the Ch-LC mixture was spread on a PC substrate using an 80  $\mu\text{m}$  wire-wound rod. The coating was cured in a nitrogen atmosphere at 42  $^{\circ}\text{C}$  using 0.8  $\text{mW}/\text{cm}^2$  UV light (320-390 nm) for 20 min. The coatings were post-cured with 30  $\text{mW}/\text{cm}^2$  UV light (320-390 nm) for 5 min.

*3D printed substrates:* PLA substrates were printed using an ultimaker 3 3D printer and black PLA filament. The substrates have a total thickness of 2 mm and an



average layer height of 200  $\mu\text{m}$ . All layers except the final layer are completely filled with the printed polymer. In the final layer, only the veins and contour of the butterfly were printed as is shown schematically in Figure 5.2.



**Figure 5.2:** Schematic drawing separating the layers of the 3D printed butterfly. All layers except the final layer are completely filled with the printed polymer. In the final layer, only the veins and contour of the butterfly were printed (black), serving as the walls, leaving the white areas in the wings open to be filled with ink.

## Characterization

*UV-Vis spectroscopy* was performed on a PerkinElmer LAMBDA 750 UV/Vis/NIR spectrophotometer equipped with a 150 mm intergrading sphere. *Differential scanning calorimetry* (DSC) measurements were performed on a TA Instruments Q 2000 using a heating ramp of 5  $^{\circ}\text{C}/\text{min}$ . *Optical microscopy (OM)* was done with a VHX-5000 KEYENCE digital microscope used in bright field. *Scanning electron microscopy (SEM)*: a JEOL JSM-7800F SEM was used to characterize some of the samples. The settings used were: high vacuum, 10 kV acceleration voltage, 10 mm working distance, backscatter electron detector. Cross-sections of the samples (coating and substrate) were made by cryo-cutting. For SEM analysis, a 6 nm thick layer of Pd/Pt was sputtered at the surface of the samples. *Raman spectroscopy* measurements were performed on a Bruker SENTERRA dispersive Raman microscope. A confocal line scan was measured starting at the surface and measured every 5  $\mu\text{m}$ , using a 532 nm laser, 100x objective, 10 scans per step. The confocal resolution is  $\sim 20 \mu\text{m}$ .

### 5.3 Results and discussion

#### Body-temperature-responsive reflector

Photo-stratified Ch-LC coatings were fabricated using a mixture of acrylic monomers **1** (4 wt%) and **2** (46 wt%) and a mesogenic mixture (50 wt%). Acrylic monomers **1** and **2** were used to build up the hard top polymer layer.<sup>[12]</sup> Cross-linker **1** was added to enhance the rigidity of the polymer layer formed. Monoacrylate **2** was chosen because of its non-volatile low-viscous nature. Furthermore, it remains transparent after polymerization while the glass transition temperature of poly-**2** of 110 °C is sufficiently high to create a hardened top coating. To increase the depletion-induced diffusion of the acrylic monomers to the top, UV-absorbing dye **4** was added in the mixture as well. For the formation of the mesogenic Ch-LC phase with a large temperature response near room temperature, *i.e.*, between 17 °C and 49 °C, a ratio of 70 wt% MLC-2138 to 30 wt% chiral dopant was used. Below 17 °C, a smectic phase was obtained, and above 49 °C the mixture became isotropic. Because of the smectic to cholesteric LC phase transition temperature ( $T_{S-Ch}$ ) of the LCs in the coating, cooling at a temperature just above the  $T_{S-Ch}$  causes unwinding of the helical alignment, which results in a strong pitch increase and red shift of the reflection band. By adjusting the composition of the mesogenic mixture, the phase transition temperatures and the width of the Ch-LC temperature window could be tuned (Figure 5.3).

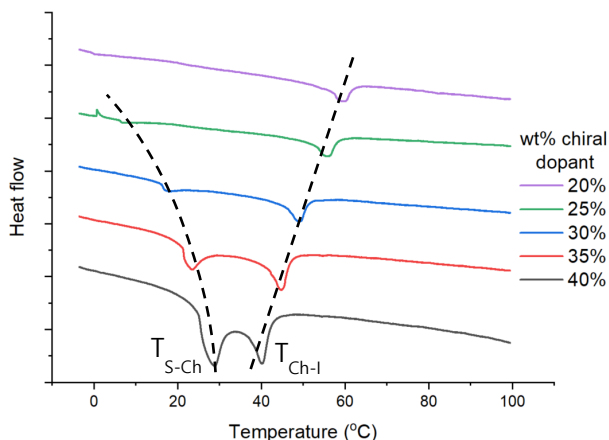


**Figure 5.3:** DSC diagrams of the mesogenic mixtures varying the chiral dopant (**5**) concentration in the mesogenic mixture. Increasing the chiral dopant leads to narrowing of the Ch-LC window by the increasing  $T_{S-Ch}$  and decreasing cholesteric to isotropic phase transition, which is indicated by the dashed lines.

We first prepared a photonic coating without trays to study the temperature-responsive optical properties. The combined mixture of acrylic monomers and non-polymerizable LCs (Ch-LC mixture) was coated on a flexible PC substrate. Polymerization of the acrylate monomers caused photo-induced phase-separation of the polymer formed and the non-reactive mesogens. As a result, although the initial paint is fully transparent, removal of non-liquid crystalline monomers allowed for the formation of a Ch-LC phase in between the polymer layer formed and the substrate, which is schematically shown in Figure 5.4a. Figure 5.4b and 5.4c show photographs of the final coating, revealing the formation of a Ch-LC phase, as evidenced by the red or green coating coloration. A reversible red to green color change can be achieved on the flexible substrate by solely using the difference between room temperature (namely 24 °C) and skin temperature (namely 33 °C). Moreover, because of the maintained mobility of the LCs, shifting of the reflection band occurs in a matter of seconds.

Close to the  $T_{S-Ch}$ , cooling of a single degree causes the reflection band of the coating to red shift for 100 nm, *i.e.* from 726 nm to 826 nm, caused by the rapid unwinding of the helix (Figure 5.4d and 5.4e). A total reflection band blue shift of 330 nm was observed when heating the coating from 22 °C to 45 °C.

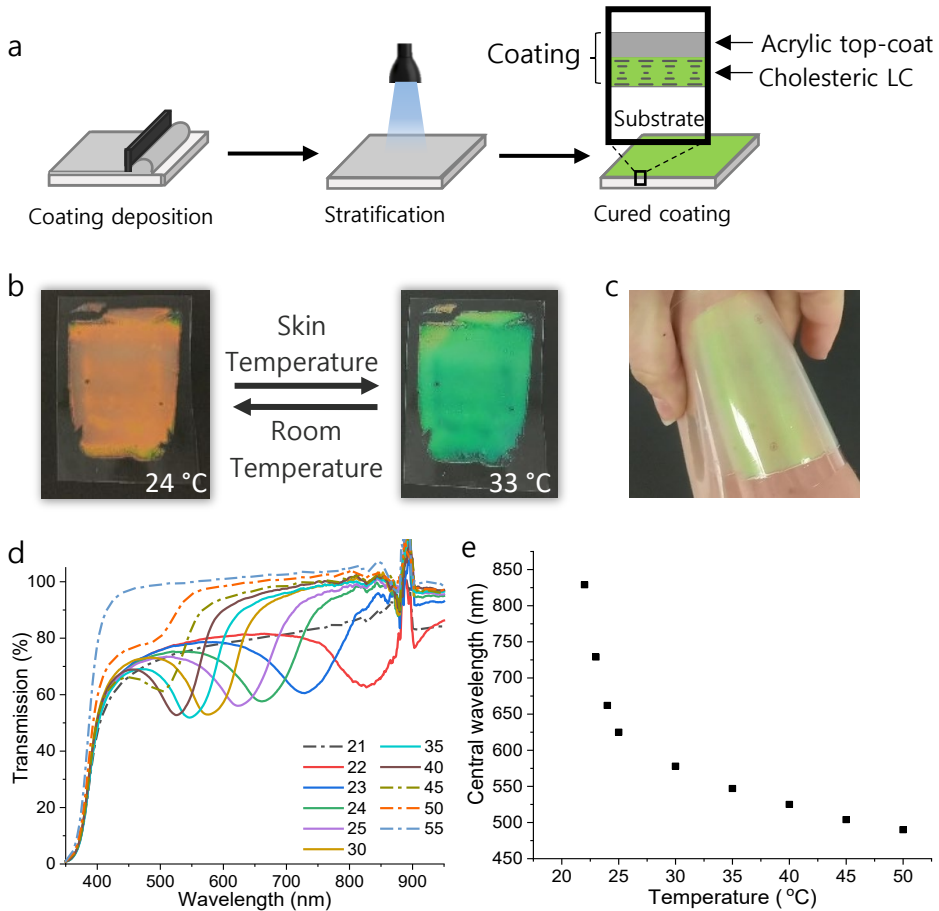


**Figure 5.4:** a) Schematic representation of the fabrication method for the stratified coating via bar-coating and photopolymerization (based on visual of reference [19]). The cured coating depicts the ideal case when polymerization occurs subsequently to the depletion induced diffusion. b) Photographs of the coating at room temperature (namely 24 °C) and skin temperature (namely 33 °C). c) Photograph of the coating heated by the skin, showing the flexibility of the coating and the substrate d) Transmission spectra of the coating at various temperatures, showing the cholesteric reflection bands of the coating between 22 °C and 45 °C. Below and above these temperatures, the coatings becomes smectic and isotropic, respectively. e) Central wavelength of the reflection bands shown in (d) displayed at various temperatures showing the temperature-responsive curve of the coating.

To study the internal structure of the stratified temperature-responsive photonic coating, cross-sections were analyzed by a variety of techniques. Note that due to non-polymerized LC mesogens present in the coating, the analysis of the cross-section of the coatings is challenging. Figure 5.5 shows both optical microscopy (OM) and scanning electron microscopy (SEM) images of cross-sections of the

coating. Remarkably, in the OM image (Figure 5.5a), a narrow color-reflective layer is present, indicating a photonic Ch-LC alignment sandwiched between the PC substrate and a thicker top-layer. Analyzing a cross-section of the coating using SEM (Figure 5.5b), similar layers are found, for which the top layer (1) has a thickness of  $\sim 32 \mu\text{m}$  and the Ch-LC layer a thickness of  $\sim 5 \mu\text{m}$ . The  $37 \mu\text{m}$  thick coating has sufficiently phase-separated to lead to the creation of a continuous photonic Ch-LC inside the final coating, as is evidenced by the detection of a reflection band by UV-Vis spectroscopy (Figure 5.4c), it nevertheless seems that the polymerization of the acrylic monomers took place before a perfect acrylic : LC bilayer structure could be formed. Because initially a ratio of 50/50 wt% acrylic monomers *versus* LC mesogens was used, theoretically a much thicker Ch-LC phase of approximately  $18 \mu\text{m}$  would be expected inside the phase-separated cell structure. Therefore, the top layer (1) most likely contains significant amounts of non-reactive LC mesogens as well, which do not contribute to the photonic reflection band. By use of confocal Raman spectroscopy, the ratio between the peak area at  $2190\text{-}2250 \text{ cm}^{-1}$  corresponding to CN moieties in the mesogenic mixture and the peak area at  $2800\text{-}3028 \text{ cm}^{-1}$  corresponding to the  $\text{CH}_2$  of monomer **2** moieties was used to calculate the composition of the material through the thickness of the coating (Figure 5.5c). Since the  $\text{CH}_2$  moieties of monomer **2** overlapped with the  $\text{CH}_2$  vibrational signals of the LC mixture and the PC substrate, calibration curves were made to separate the peak areas using known ratios between the polymer formed and LCs and known ratios between the vibrational signals at  $869\text{-}907 \text{ cm}^{-1}$  and  $2800\text{-}3028 \text{ cm}^{-1}$  of the PC substrate. Although at a penetration depth between  $0 \mu\text{m}$  (*i.e.* coating-air interface) and  $25 \mu\text{m}$ , more polymer seemed to be present with respect to the LC mesogens, still a significant number of LC mesogens was found at these penetration depths corresponding to layer 1 in Figure 5.5b. Measuring further into the coating, the polymer : LC ratio decreased. Above penetration depths of  $35 \mu\text{m}$ , only signals from the PC substrate and LCs were identified, indicating indeed a layer dominantly made of LC mesogens, as observed in Figure 5.5a and 5.5b. Note that

the thickness of the coating is approximately 37-40  $\mu\text{m}$ . However, during Raman analysis, LC signals were measured at penetration depths of 45  $\mu\text{m}$ , which is most likely caused by the confocal resolution of the equipment ( $\sim 20$   $\mu\text{m}$ ) or leakage of LCs during sample preparation of the cross-sections of the coating.

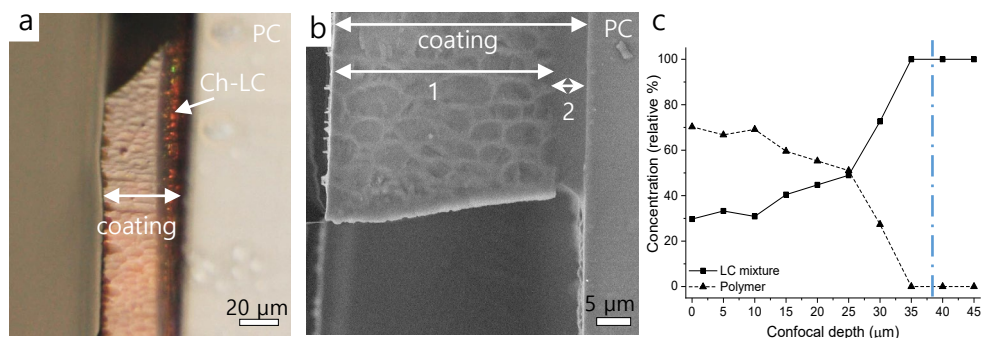


**Figure 5.5:** a) OM image of a cross-sections of the stratified coating showing a narrow red reflective layer in between the PC and a non-reflective top-layer. b) SEM image of a cross-section of the coating, showing again a narrow layer in between the PC and the top-layer. In this case, the LCs are no longer present due to the need for vacuum in the SEM chamber. In both images, part of the coating was lost during sample preparation. c) Ratio between polymer formed and LC mixture using Raman spectroscopy. The blue dashed line indicates the thickness of the coating observed in (b).

## Temperature-responsive coatings on substrates with trays

To see whether the Ch-LC mixture can also be coated and stratified on substrate with trays, a PC substrate with rectangular boxes of  $60 \times 20 \times 20 \mu\text{m}^3$  (length  $\times$  width  $\times$  height), separated by  $2 \mu\text{m}$  thick walls was prepared by etching. Using this approach, walls are composed of PC, avoiding the need for masked-illumination steps (Figure 5.6a). Note that the height of the walls is smaller than the  $40 \mu\text{m}$  thickness of the coating. However, since the thickness of the photonic layer is approximately  $5 \mu\text{m}$  (*vide infra*), the acrylic polymer layer should be anchored to the wall-architecture after stratification. Again, the Ch-LC mixture was applied to the substrate and polymerized similarly to the ones discussed in Figure 5.4. Photographs of the coating (Figure 5.6b) reveal that trays are not visible with the naked eye. The resulting coating shows a good alignment as illustrated by the red reflective color. Temperature-responsive behavior is similar to the coating without trays (Figure 5.4). Upon heating the coating reversibly blue shifts from red to green within seconds, after which it becomes isotropic at temperatures higher than  $50 \text{ }^\circ\text{C}$ . Figure 5.6c shows an optical microscope image of the substrate before and after stratification. The photonic reflection of the Ch-LC mesogens in the coating was only present inside the rectangular boxes of the substrate (Figure 5.6c(ii)), which indicated that the walls are most likely connected to the acrylic polymer top layer. Macroscopically, the adhesion of the coatings was significantly enhanced. While coatings without these wall structures are easily movable across the substrate by rubbing, these coatings are far more resistant toward such displacement.

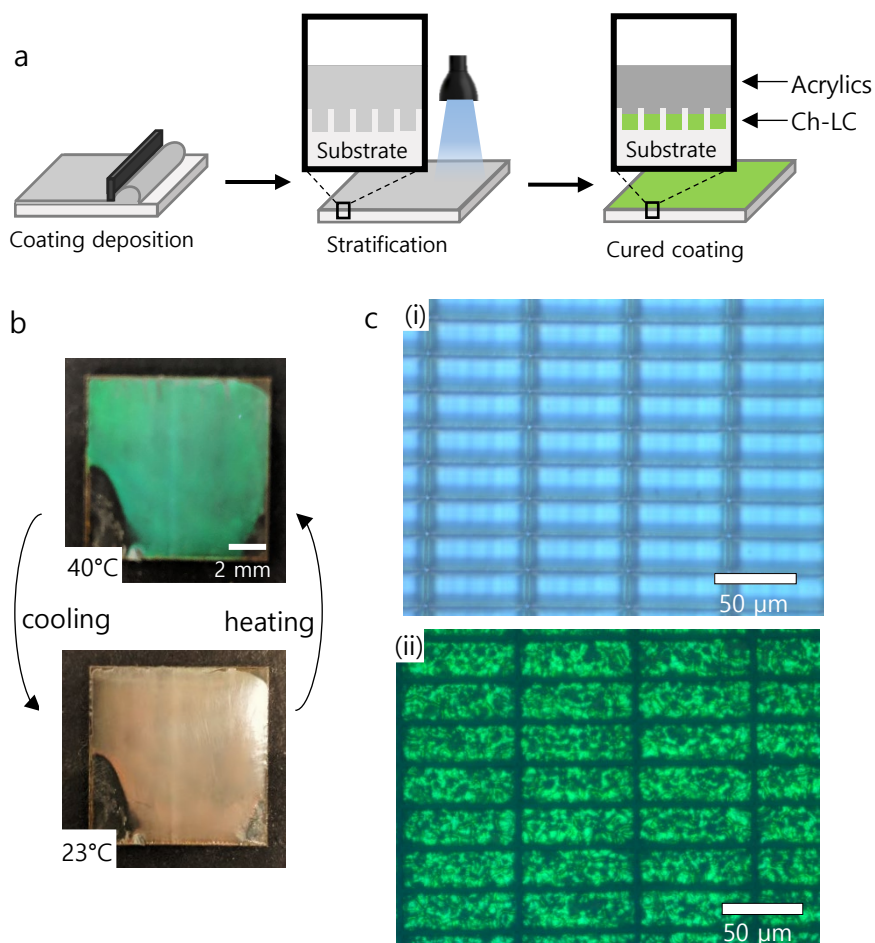


**Figure 5.6:** a) Fabrication method of the coatings, using substrates with walls. b) Photographs of the coating at room temperature (namely 23 °C) and heated to 40 °C. c) OM images of the structured substrates showing the laser etched rectangular boxes ( $60 \times 20 \times 20 \mu\text{m}^3$  (length, width and height), with a wall thickness of 2 μm), (i) before the coating was applied and (ii) after the substrate was coated, showing the reflective material inside the etched boxes,

As a next step 3D printing was used to create tray structures of any desired shape that can be filled with the Ch-LC mixture. In this case, a butterfly was 3D printed from black PLA polymer filament. All layers except the final one were completely filled by the PLA polymer, serving as the 2 mm thick substrate. The final ~200 μm thick layer contained trays in the wing while printing only the veins and contour of the butterfly, serving as the walls (Figure 5.2). Subsequently, the ink (Ch-LC mixture) was applied using bar-coating and was exposed to light to induce



the stratification. Figure 5.7 shows the printed butterfly coated with the temperature-responsive paint at various temperatures. As the layer thickness of the walls had increased and the coating covered the entire substrate (*i.e.* including the veins and edge), the final coating had an increase in thickness of  $\sim 200 \mu\text{m}$ . Nevertheless, after the fabrication process, again a well-aligned encapsulated Ch-LC layer was obtained on the PLA substrate, as was evidenced by the structural coloration of the butterfly. The coating was heated and cooled, showing again a similar reversible temperature-responsive behavior similar as shown before (Figure 5.4 and 5.6), with a reversible blue shift of the reflection band upon heating between  $22 \text{ }^\circ\text{C}$  and  $\sim 50 \text{ }^\circ\text{C}$ , shifting the color from outside the visible spectrum (IR light) at  $22 \text{ }^\circ\text{C}$  to green at  $40 \text{ }^\circ\text{C}$  within seconds. Also in this case, the coating can be rubbed without movement of the coating across the substrate, indicating that the open spaces in the wings are filled partially with the photonic Ch-LC mesogens, anchoring the acrylic polymer top layer to the veins and edge.

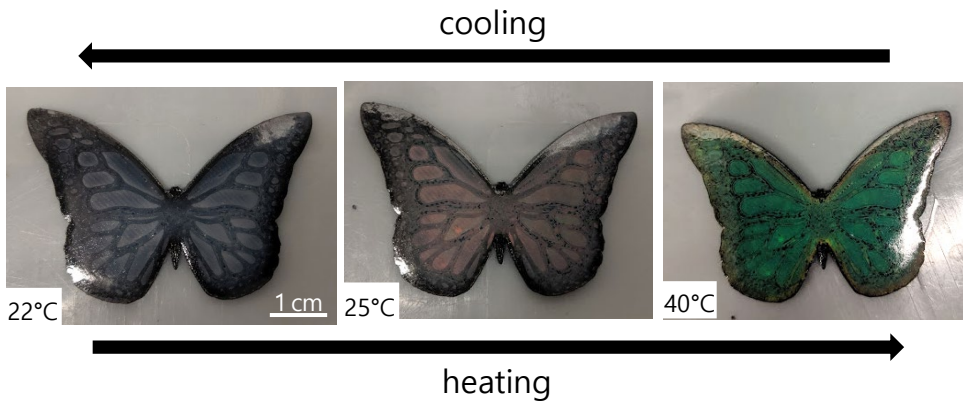


**Figure 5.7:** 3D printed butterfly (polymer: PLA). The veins have an additional printed layer with respect to the rest of the butterfly. Heating the coating, causes a reversible photonic color change of the Ch-LC mesogens

## 5.4 Conclusions

Photo-induced phase-separation was used to create temperature-responsive encapsulated Ch-LC coatings on flexible substrates. Using mesogenic components having a smectic to cholesteric phase transition temperature, coatings were

fabricated, needing only a few seconds and 1 °C temperature difference to shift the reflection band 100 nm and a total reflection band shift of 330 nm while heating from 22 °C to 45 °C.

Subsequently the linkage between the substrate and the polymer top layer was studied by creating walls from the substrate increasing the coating adhesion. Moreover, a butterfly with walls was 3D-printed and coated with the temperature-responsive paint, showing the ability to coat arbitrary-shaped substrates with the temperature-responsive paint. The Ch-LC mixture can be easily aligned in the trays giving clear visible structural colors. These coatings displayed enhanced adhesion and a similar temperature-responsive behavior as the coatings prepared without walls. Various other processes relying on stamping or selective material addition or removal can be thought of as well to produce defined structured substrate surfaces. Such photonic reflectors with arbitrary shapes are potentially interesting for sensors, surfaces with tunable aesthetics or anti-counterfeit labels, which might require sensitivity to small temperature variations close to room- or body temperature and reaction times within seconds.

## 5.5 References

- [1] M. E. McConney, V. P. Tondiglia, J. M. Hurtubise, L. V. Natarajan, T. J. White, T. J. Bunning, *Adv. Mater.* **2011**, *23*, 1453.
- [2] L. V. Natarajan, J. M. Wofford, V. P. Tondiglia, R. L. Sutherland, H. Koerner, R. A. Vaia, T. J. Bunning, *J. Appl. Phys.* **2008**, *103*.
- [3] H. Khandelwal, G. H. Timmermans, M. G. Debije, A. P. H. J. Schenning, *Chem. Commun.* **2016**, *52*, 10109.
- [4] <https://www.hallcrest.com/products/healthcare-thermometers/forehead-anesthesia/clinitrend> - accessed on 30-08-2019.
- [5] E. P. A. Van Heeswijk, J. J. H. Kloos, J. De Heer, T. Hoeks, N. Grossiord, A. P. H. J. Schenning, *ACS Appl. Mater. Interfaces* **2018**, *10*, 30008.
- [6] Y. Bashtyk, O. Bojko, A. Fechan, P. Grzyb, P. Turyk, *Mol. Cryst. Liq. Cryst.* **2017**, *642*, 41.
- [7] S. S. Lee, B. Kim, S. K. Kim, J. C. Won, Y. H. Kim, S. H. Kim, *Adv. Mater.* **2015**, *27*, 627.
- [8] N. Herzer, H. Guneysu, D. J. D. Davies, D. Yildirim, A. R. Vaccaro, D. J. Broer, C. W. M. Bastiaansen, A. P. H. J. Schenning, *J. Am. Chem. Soc.* **2012**, *134*, 7608.

- [9] E. P. A. van Heeswijk, J. J. H. Kloos, N. Grossiord, A. P. H. J. Schenning, *J. Mater. Chem. A* **2019**, *7*, 6113.
- [10] A. J. J. Kragt, N. C. M. Zuurbier, D. J. Broer, A. P. H. J. Schenning, *ACS Appl. Mater. Interfaces* **2019**, *11*, 28172.
- [11] W. Zhang, S. Kragt, A. P. H. J. Schenning, L. T. de Haan, G. Zhou, *ACS Omega* **2017**, *2*, 3475.
- [12] H. Khandelwal, E. P. A. van Heeswijk, A. P. H. J. Schenning, M. G. Debije, *J. Mater. Chem. C* **2019**, *7*, 7395.
- [13] A. Ranjkesh, T.-H. Yoon, *ACS Appl. Mater. Interfaces* **2019**, *11*, 26314.
- [14] R. Penterman, S. I. Klink, H. de Koning, G. Nisato, D. J. Broer, *Nature* **2002**, *417*, 55.





# Chapter 6

## Technology assessment

**Abstract.** This chapter describes the technology assessment of the developed stimuli-responsive photonic coatings in this thesis. Limitations and approaches to further improve the coatings described are discussed as well as the challenges that need to be addressed to make these coatings commercially viable.

## 6.1 Introduction

Various kinds of responsive photonic polymer coatings have been described in this thesis. Stimuli-responsive cholesteric liquid crystalline (Ch-LC) polymer coatings were developed having hydrogel-like (Chapter 3) or elastomeric (Chapter 4) properties and non-polymerized cholesteric liquid crystals were encapsulated in a single substrate cell (Chapter 5). In the first chapter, industrial feasibility was already briefly touched upon. This chapter considers the extent to which the objectives of this thesis have been achieved and which challenges need to be addressed to implement these materials in various coating applications.

## 6.2 Processability and scalability

Throughout the research presented in this thesis, several processing techniques were used to prepare lab-scale coatings on flexible substrates. These well-aligned Ch-LC samples were prepared by bar-coating techniques using gap-applicators and wire-wound rods. These techniques were chosen since they are potentially scalable using industrially relevant methods. Gap applicators may be replaced by slot-die coating and wire-wound rods have been used to mimic brush applicators. Methods that are more difficult to upscale, such as spin-coating or opening of cell made films, were avoided in this research. In Chapter 4, preliminary research was done to coat the Ch-LC materials via a roll-to-roll gravure printing technique, using a gravure test-setup. Although some steps of the process (*e.g.* curing) are not yet done in a continuous fashion, the ability to create a film and to align the LCs in the film using transfer of the ink from the anilox roll to the flexible substrate at 0.5 m/s was demonstrated. Another deposition technique often used in industry is spray-painting. Using this technique, it was recently demonstrated that a Ch-LC mixture can be self-aligned on conventional oriented polyamide 6 films or other stretched polymers.<sup>[1]</sup>

Further optimization of the (acrylic-based) coating processability and scalability can focus on the requirement of the inert atmosphere during curing. In oxygen-rich environments, initiating and propagating radicals are scavenged and converted to peroxy radicals, which inhibits propagation of acrylic polymerization.<sup>[2-4]</sup> In Chapter 4, thiols were added to the mixture to create an elastomer network. These thiol functional monomers are known to enable film curing in oxygen-rich environments as the peroxy radical generated can abstract a thiol hydrogen to generate thiyl radicals that can in turn propagate through addition or chain transfer reactions.<sup>[2,5]</sup> Addition of a small quantity of thiols (or amines) to other acrylic-based LC systems might eliminate the need for nitrogen environments in those systems as well.<sup>[6]</sup>

Another option could rely on the use of oxetane-functional instead of acrylic-functional monomers. Due to the cationic ring-opening polymerization, oxetanes are not sensitive to the oxygen inhibition observed in free-radical polymerization. Hoekstra *et al.* already demonstrated the ability to create printed Ch-LC films by using these monomers that are curable in an oxygen-rich environment.<sup>[7]</sup> However, oxetanes cannot be used in combination with carboxylic acid functional monomers (Chapter 3), as they act as a chain transfer agent during the cationic ring-opening polymerization reaction.

### 6.3 Lifetime of the photonic coatings

Depending on the application, photonic coatings may require reversible responsive functionalities over a longer period of time. Especially for outdoor applications, like smart windows, which preferably have a lifetime of at least ten years, temperature cycling and sun light are likely to accelerate the coating degradation. In particular UV radiation is known to degrade polymer materials, reducing their lifetime significantly.<sup>[8-10]</sup>

To protect coatings against light degradation, UV absorbers are often used as additives. In the coatings prepared in Chapter 3 and 5, such UV absorbers are



already present, which might enhance the lifetime of the photonic polymers. Moreover, the coatings would benefit from the absorbance of UV light by the window when the coating is applied on the inside. The hydrogel-like coatings discussed in Chapter 3, would, in case of an application in the greenhouse industry, be placed inside of the greenhouse to benefit from the high-humidity and simultaneously gain protection from UV light by the polycarbonate (PC) window panels.

Other coating applications, such as labels or sensors might not need long term outdoor stability, but will require for instance a good scratch resistance. For the encapsulated Ch-LC coatings an additional transparent scratch resistant protective layer would not cause a decrease in the responsiveness. However, for the photonic systems that require a solvent to swell (Chapter 3 and 4) the coating, coverage of the coating will unavoidably cause a loss of responsiveness. Keeping the mechanical resistance of such coatings in mind, fully-cured networks were designed. However, a more detailed study regarding the mechanical resistance of these coatings should be carried out.

#### **6.4 Opportunities for encapsulated photonic single substrate cells**

In Chapter 5, coatings were prepared in which non-reactive Ch-LC mixtures were encapsulated between the substrate and an in-situ formed polymer top layer. While only the temperature-responsive behavior of these Ch-LC systems was reported, responses to other stimuli have not been addressed yet. Electrical responsiveness can be obtained by introducing interdigitated indium tin oxide electrodes on a glass substrate.<sup>[11,12]</sup> Using interdigitated electrodes on a flexible substrate (Figure 6.1) may allow for the formation of electrically responsive flexible Ch-LC substrates.

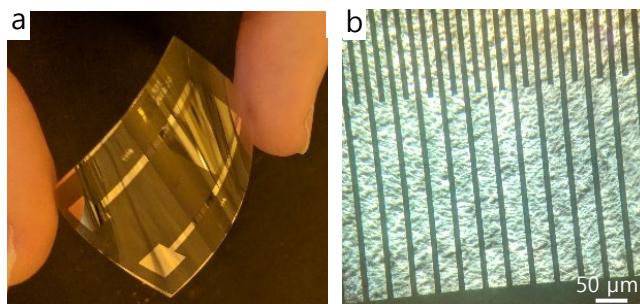


**Figure 6.1:** a) Photograph of the interdigitated gold electrode on a flexible polyetherimide substrate b) Optical microscope image of the interdigitated pattern showing the interdigitated structure coated with a Ch-LC mixture.

### Printing photonic single substrate cells

Designing a printing procedure for Ch-CL droplets forming each an individual encapsulated cell could potentially be interesting for the formation of pixelated photonic structures. Ink-jet printing of droplet with, for instance, different colors would allow for multi-color images. Preliminary research reveals that printing of such droplets is possible: the Ch-LC mixture used in Chapter 5 was ink-jet printed on PC substrates and stratified as discussed in the previous chapter (Figure 6.2a). Due to the small volume that can be jetted (*i.e.* tens to hundreds of  $\mu\text{L}$ ), it was necessary to apply multiple passes (overprinting) to obtain a final drop height of approximately  $60 \mu\text{m}$ . Since the ink is not drying during the printing process, the smaller droplets were merged into a final droplet. Figure 6.2b shows a photograph of the final droplets formed, which show coloration, indicating the formation of the Ch-LC phase. After analyzing the droplets between cross-polarizers (Figure 6.2c), although bright reflective spots were found in the image, other areas remained relatively dark, which most likely cause the coloration of the entire droplets to be less bright. Nevertheless, upon heating and cooling above the isotropic phase transition and back, the coloration was reversibly regained, needing no additional stimuli to induce Ch-LC realignment.

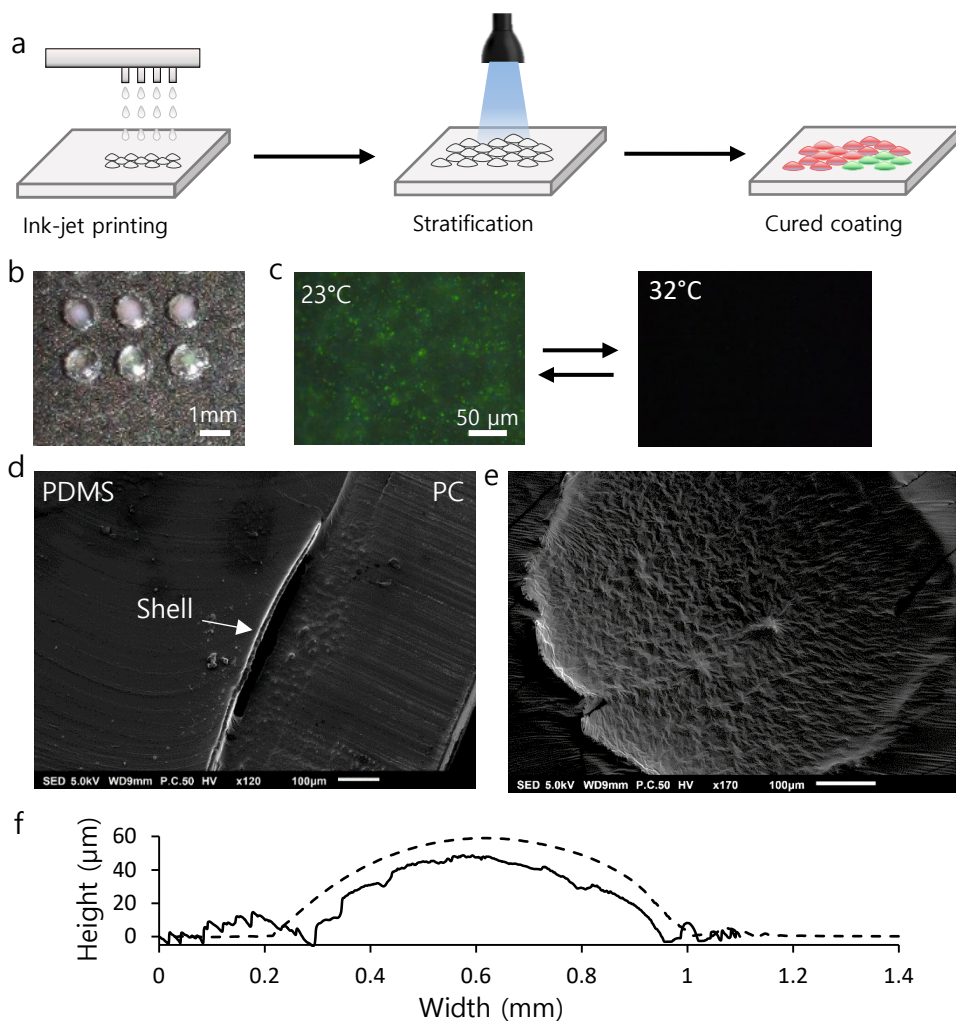


**Figure 6.2:** a) Fabrication method of the printed and stratified droplets. b) Photograph of the droplets having a red or green reflection band. c) Reflective optical microscope image through cross-polarizers showing reversible loss of color when heated. d) Scanning electron microscopy image of the cross-section of the droplet encapsulated in between polydimethylsiloxane (PDMS) and the substrate, showing the polymerized shell of the droplet. e) SEM image of the inside of the polymerized shell. PDMS was cured on top of the droplet, subsequently the PDMS was peeled of the PC substrate after which the shell remained attached to the PDMS. f) Height profile measurements of the inner and outer side of the shell using a Dektak profilometer.

A cross-section of a droplet (Figure 6.2d), showed a shell thickness of 15 μm. The inner side of the shell showed a rough surface, which could be the cause of the inhomogeneous coloration, since the roughness might cause focal conic

alignment at these surfaces (Figure 6.2e). The height profile of the inside and outside of the shell showed a similar thickness and roughness as was observed by SEM analyses (Figure 6.2f).

Further optimization of these droplets is needed, which could be achieved for example by tuning the roughness of the drop shell interior, the stratification parameters and the coating formulation. Improvements may also be observed when droplets with desired dimensions can be fabricated from a single ink-jet printed droplet or the use of other printing techniques such as screen printing, allowing to process droplets with increased dimensions.

### **Secondary reactions in the photonic single substrate cells**

Polymer stabilized LC cells have been often used to create reversible temperature and electrical-responsive photonic systems with programmed optical properties.<sup>[13–17]</sup> It would be interesting to create such systems in single-substrate cells, providing additional stimuli-responses and resistance towards mechanical wear.<sup>[18]</sup> The network formed inside the cell could potentially provide a linkage between the substrate and the top-layer without the need for walls and the lifetime of the coating might be increased by decreasing leakage. Since the free-radical polymerization (FRP) of acrylic functional groups is already used for the formation of the stratified cells, this polymerization reaction cannot be used for the formation of a polymer stabilized environment inside the LC cells. As already mentioned in paragraph 6.2, oxetane-functional monomers react via cationic ring-opening polymerization (C-ROP), meaning that, theoretically, these monomers can be initiated after the FRP has been used to form the single substrate cell-architecture.

In a preliminary study, we observed that when two different photoinitiators (**4**) and (**8**), depicted in Figure 6.3a, were added to an approximately 50/50 wt% acrylic/oxetane monomeric mixture, FRP and C-ROP could be initiated independently. The C-ROP photoinitiator (**4**) was not affected by light above 380

nm. When illuminating the acrylic/oxetane blend containing both photoinitiators with 405 nm light, the FRP was initiated, without initiating the C-ROP. Afterwards, UV light below 380 nm could be used to initiate the C-ROP, which might create a polymer-stabilized system inside the cell formed (Figure 6.3b).

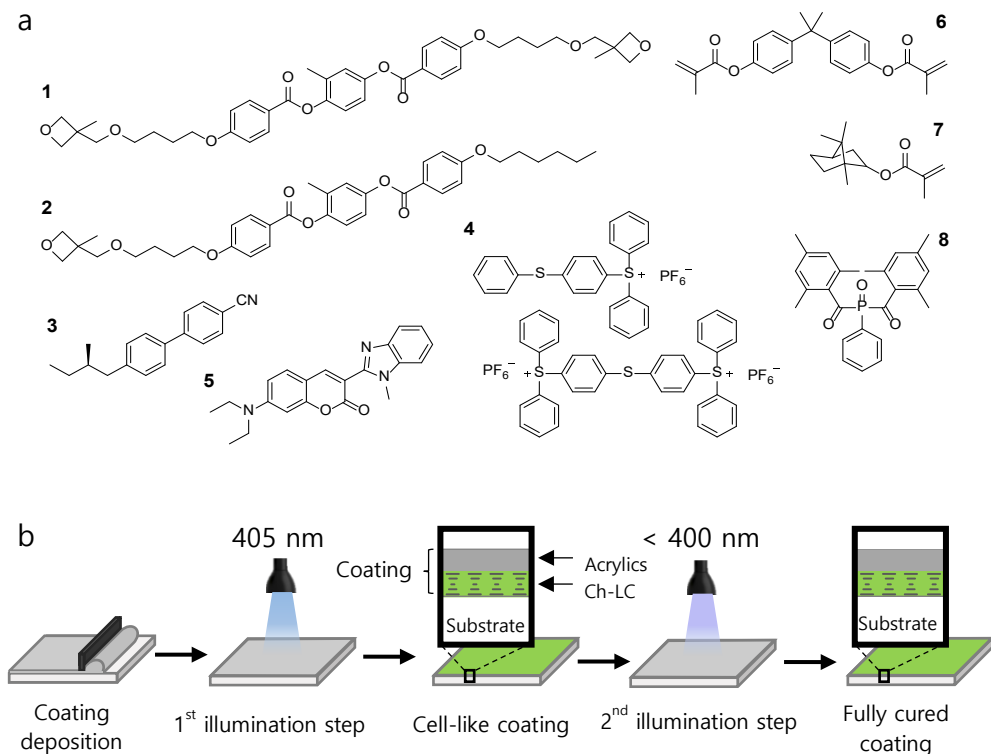


**Figure 6.3:** a) Molecular structures of the monomers used. b) Fabrication method for the ideally formed polymer stabilized single substrate cell using a dual-illumination step.

Initially, a large quantity of oxetane based LCs were used in the mixture to investigate the ability to align and cure the LCs independently to the acrylate monomers. Using a mixture containing 16.1 wt% monomer **1**, 16.1 wt% monomer **2**, 15.2 wt% chiral dopant **3**, 2.5 wt% photoinitiator **4**, 5 wt% monomer **6**, 44.5 wt% monomer **7** and 0.5 wt% photoinitiator **8** and various amount of light-absorber **5**, single substrate cells were fabricated using the dual-illumination approach. Initially, dye **5** was not added to investigate the ability to stratify the

cell without light gradient enhancement. As Figure 6.4a shows, after the first illumination step, the coating becomes colored. Since the oxetanes were not cured yet at this stage, the colored coating is temperature-responsive, resulting in the reversible loss of the reflection band after heating above the isotropic phase transition temperature (*i.e.* 42 °C,  $T_{Ch-I}$ ).

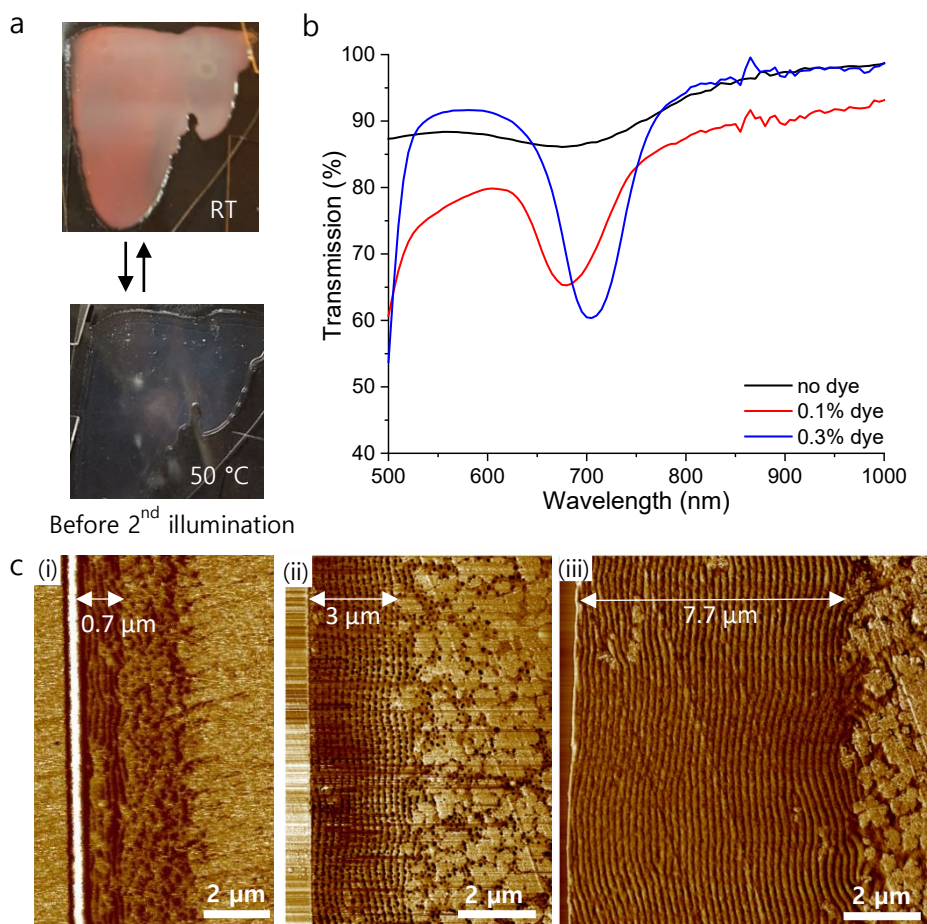


**Figure 6.4:** a) Photographs of the coating before the second illumination step, showing the temperature responsiveness of the coating before network formation of the oxetane functional monomers. b) Transmission spectra of the final coatings. Increasing the dye content causes an increase in the reflection band intensity and decrease of scattering. c) AFM images of the cross-sections of the final coatings having a dye content of (i) 0 wt%, (ii) 0.1 wt%, (iii) 0.3 wt%.

After the second illumination step, the temperature responsiveness was lost due to the tight network formation of the oxetane functional monomers. Optimizing the chemical composition and crosslink density would be needed to obtain stimuli-responsive behavior after the second curing step. However, in this case, the network formed allowed for the formation of cross-sections without severe leakage, enabling the study of the thickness and alignment of the photonic layer. Transmission spectra show that the intensity of the reflection band was very low (Figure 6.4b). After analyses of the cross-section using atomic force microscopy (AFM) (Figure 6.4c(i)), it became clear that the thickness of the aligned cholesteric phase was only 0.7  $\mu\text{m}$ , which is not adequate for the formation of a well-defined Ch-LC reflection band. When 0.1 wt% of dye **5** was added to the mixture, aiming to improve the phase-separation by enhancing the light gradient, the reflection band intensity and the thickness of the aligned cholesteric phase (Figure 6.4c(ii)), was improved. Increasing the dye **5** content further to 0.3 wt%, the phase-separation was even further improved, resulting in a 7.7  $\mu\text{m}$  thick aligned cholesteric phase (Figure 6.4c(iii)). Also, a higher intensity of the reflection band and a diminished scattering were observed. These results show that it is in principle possible to create polymer stabilized liquid crystal single substrate cells with a defined photonic reflection band. Such systems allow further programming of the optical performance of photonic materials even further.

## 6.5 Conclusions

This thesis described the fabrication of a varied set of responsive photonic polymer coatings based on different working principles. Special attention was given to the adhesion of the coatings to the substrate and in all chapters scalability was kept in mind while designing the fabrication methods of the coatings. By further developing these photonic coatings as discussed in this chapter, it is foreseen that this will lead to stimuli-responsive materials which

could potentially be implemented in the fields of smart windows, sensors, aesthetics and security labels.

## 6.6 References

- [1] R. C. P. Verpaalen, M. G. Debije, C. W. M. Bastiaansen, H. Halilović, T. A. P. Engels, A. P. H. J. Schenning, *J. Mater. Chem. A* **2018**, *6*, 17724.
- [2] M. E. Whitely, J. L. Robinson, M. C. Stuebben, H. A. Pearce, M. A. P. McEnergy, E. Cosgriff-Hernandez, *acs Biomater. Sci. Eng.* **2017**, *3*, 409.
- [3] C. Decker, A. D. Jenkins, *Macromolecules* **1985**, *18*, 1241.
- [4] F. A. Rueggeberg, D. H. Margeson, *J. Dent. Res.* **1990**, *69*, 1652.
- [5] A. K. O'Brien, N. B. Cramer, C. N. Bowman, *J. Polym. Sci. Part A Polym. Chem.* **2006**, *44*, 2007.
- [6] K. Nickmans, D. A. C. van der Heijden, A. P. H. J. Schenning, *Adv. Opt. Mater.* **2019**, *1900592*, 1.
- [7] D. C. Hoekstra, K. Nickmans, J. Lub, M. G. Debije, A. P. H. J. Schenning, *ACS Appl. Mater. Interfaces* **2019**, *11*, 7423.
- [8] E. Yousif, R. Haddad, *Springerplus* **2013**, *2*, 1.
- [9] S. Chatani, C. J. Kloxin, C. N. Bowman, *Polym. Chem.* **2014**, *5*, 2187.
- [10] B. Littlejohn, K. M. Heeger, T. Wise, E. Gettrust, M. Lyman, *J. Instrum.* **2009**, *4*, 1.
- [11] R. Penterman, S. I. Klink, H. De Koning, G. Nisato, D. J. Broer, *Nature* **2002**, *417*, 55.
- [12] D. Liu, N. B. Tito, D. J. Broer, *Nat. Commun.* **2017**, *8*, 1.
- [13] H. Khandelwal, G. H. Timmermans, M. G. Debije, A. P. H. J. Schenning, *Chem. Commun.* **2016**, *52*, 10109.
- [14] H. Khandelwal, R. C. G. M. Loonen, J. L. M. Hensen, M. G. Debije, A. P. H. J. Schenning, *Sci. Rep.* **2015**, *5*, 11773.
- [15] C. V. Rajaram, S. D. Hudson, L. C. Chien, *Chem. Mater.* **1996**, *8*, 2451.
- [16] I. Dierking, *Adv. Mater.* **2000**, *12*, 167.
- [17] X. Chen, S. Jose, Encapsulated polymer network liquid crystal material, device and application - US 8801964 B2 **2014**.
- [18] I. E. Heynderickx, D. J. Broer, Optical temperature indicator - EP0701594 B1 **2001**.





# Samenvatting

## Responsieve fotonische polymeercoatings

Op bijna alle materialen in onze dagelijkse omgeving worden coatings aangebracht om oppervlaktes te beschermen of een mooier uiterlijk te geven. De meeste coatings zijn echter statisch, wat betekent dat ze niet reageren op prikkels uit de omgeving. De laatste jaren werd de vraag naar oppervlaktes die reageren op invloeden uit de omgeving steeds prominenter in de academische wereld en industrie. Om dit te kunnen realiseren worden cholesterische vloeibaar kristallijne polymeren gezien als veelbelovende eendimensionale fotonische materialen. De spiraalvormige organisatie van de cholesterische vloeibare kristallen veroorzaakt een selectieve reflectie van licht waarvan de golflengte van het gereflecteerde licht bepaald wordt door de draaisterkte van de spiraal.

Dit proefschrift richt zich op het ontwikkelen van responsieve coatings gemaakt van cholesterische vloeibaar kristallijne polymere netwerken, aangebracht op flexibele substraten. Deze coatings zijn in staat hun selectieve reflecterende kleur te veranderen als gevolg van bijvoorbeeld verschillen in temperatuur of vochtigheid of door in contact te komen met bepaalde vloeistoffen. Eerst werd voor een goede uitlijning en aanhechting van de vloeibaar kristallijne coatings gezorgd zonder de noodzaak voor extra uitlijnlagen, oppervlakte modifacaties van het substraat, of oplosmiddelen. Om dit te bewerkstelligen werden de cholesterische vloeibare kristallen op het substraat uitgelijnd met behulp van een applicator met een opening van een definieerbare gewenste hoogte. Een groot voordeel van deze techniek is de goede schaalbaarheid voor eventuele industrialisatie. Om de hechting van de coating te vergroten, werd het oppervlak van het substraat voorbehandeld met de foto-initiator benzofenon, waardoor covalente bindingen tussen het substraat en de coating mogelijk werden.

Vervolgens werden er drie routes onderzocht om robuuste, responsieve fotonische coating te verkrijgen, waar ook hier gewerkt werd met technieken met een goede opschaalbaarheid. In de eerste route werden temperatuurgevoelige coatings ontwikkeld met behulp van hydrogelachtige fotonische vloeibare kristallen. Deze coatings konden water uit de omgeving absorberen en desorberen, waardoor de reflectieband en dus de structurele kleur verschoof. Bij een hoge luchtvochtigheid werd de absorptie en desorptie van waterdamp uit de lucht gereguleerd door temperatuursveranderingen. Bovendien werd de breedte van de reflectieband van de coating vergroot tot 400 nm, waardoor een aanzienlijk deel van het infrarood gebied in het zonlichtspectrum werd bedekt, welke deels verantwoordelijk is voor warmte. Dergelijke materialen zijn potentieel interessant voor energiezuinige regeling van binnenwarmte, waarbij het infrarood licht gereflecteerd wordt tijdens warmere periodes en doorgelaten wordt tijdens koelere periodes.

Daarnaast werden coatings ontwikkeld op basis van cholesterische vloeibaar kristallijne elastomeren, welke reageren op bepaalde vloeistoffen en temperatuursveranderingen. Door dithiolen en diacrylaten te gebruiken, werden vloeibare kristallijne groepen in de hoofdketen van de polymeren opgenomen waardoor een minder dicht verknoopt netwerk werd gecreëerd ten opzicht van polymeren waar ze als zijtakken aan de hoofdketen vast zitten. De stapgroei polymerisatiekinetiek kon eenvoudig gevolgd worden door een zichtbare kleurverandering. Bovendien konden er meerdere kleuren in de coating gecreëerd worden door gedeeltelijke blootstelling van de coating aan UV licht door een masker en vervolgens, na een gedefinieerde rustperiode, een volledige uitharding van het netwerk door blootstelling van de coating aan UV licht zonder masker. Door het masker te vervangen door lage intensiteit UV licht kan op een zelfde manier ook met deze materialen een breedband reflectieve coating gemaakt worden. Met behulp van een testopstelling voor diepdruk, een rol naar rol druktechniek op hoge snelheid, werden goed uitgelijnde gepatroneerde coatings bereid met opnieuw industrieel relevante processen. Deze coatings vertoonden

omkeerbare kleurveranderingen bij hoge temperaturen (150-200 °C) en tijdens zwellen van de coating met verschillende vloeistoffen.

In de laatste route die in dit onderzoek werd bestudeerd werd een stratificatie proces gebruikt om niet responsieve cholesterische vloeibaar kristallijne moleculen tijdens de polymerisatie in te klemmen tussen een polymere toplaag en het substraat. Vanwege de onoplosbaarheid van de polymeren die gevormd worden tijdens de polymerisatie en het niet polymeriseerbare vloeibaar kristallijne mengsel vindt er een fasescheiding plaats en vormt het polymeer een dekkende laag op de vloeibare kristallen die voor robuustheid van de coating zorgde. Omdat de cholesterische vloeibare kristallen niet worden gepolymeriseerd werden grote verschuivingen van de reflectieband waargenomen bij temperatuursveranderingen van slechts enkele graden. Vervolgens werd de hechting van de coating aan het substraat verbeterd door wanden te creëren om de polymere toplaag aan het substraat te verankeren.

Concluderend laat dit proefschrift zien dat responsieve vloeibaar kristallijne fotonische polymere coatings geproduceerd kunnen worden op flexibele substraten met behulp van industrieel relevante processen. De coatings vertonen een goede uitlijning en hechting, en verschillende methodes zijn onderzocht om responsief gedrag in de coatings te introduceren. Deze materialen tonen het brede scala aan mogelijkheden voor de fotonische vloeibaar kristallijne polymeren in coatings met verschillende toepassingen zoals kleur veranderende verven, optische sensoren, authenticiteit indicatie en slimme infrarood reflecterende ramen.



# Acknowledgements

In the past four years I have worked with amazing people, who helped me to create and to finish the work presented in this thesis. I hope to have shown my sincere gratitude throughout all these years. Nevertheless, I would like to use these pages of my thesis to thank those people ones more.

Allereerst wil ik mijn promotoren prof. Albert Schenning en prof. Dick Broer bedanken voor alle steun en advies in de afgelopen jaren. Albert, jouw positieve insteek in alle meetings die we hebben gehad was vaak precies wat ik nodig had. Je enthousiasme voor de resultaten van het onderzoek en alles wat er binnen SFD gebeurt is erg aanstekelijk en heeft ervoor gezorgd dat ik altijd met veel plezier verder kon werken. Dick, bedankt voor je bereidheid om tijd te maken voor alle vragen die ik voor je had in de afgelopen jaren. Het was erg fijn om af en toe de lopende projecten met je te kunnen bespreken, wat altijd weer leidde tot nieuwe en interessante ideeën, waarvan er ook heel wat terug te vinden zijn in dit proefschrift.

Ik wil mijn copromotor dr. Nadia Grossiord graag bedanken voor alle tijd, advies en medewerking die ze heeft geleverd tijdens mijn PhD traject. Het maakte niet uit hoe druk je het had, ik kon altijd met vragen bij je terecht en je hebt ervoor gezorgd dat de samenwerking tussen SABIC en de universiteit soepel is verlopen. We hebben talloze onderwerpen samen uitgezocht en ik wil je nogmaals bedanken voor de hele fijne samenwerking.

I would also like to thank the committee members, prof. Cor Koning, dr. Catarina Esteves, prof. Chris Bowman and dr. Michael Debije for taking the time to carefully read the manuscript and give useful comments and suggestions. Cor, jij hebt een grote rol gespeeld in de aanzet tot mijn PhD carrière. Zelfs voorafgaand aan dit traject was je ervan overtuigd dat het me goed af zou gaan. Je belangtelling naar de voortgang van het project als ik je tegenkwam tijdens DPD of de coating

cursus was erg motiverend. Michael, thank you for your willingness to answer all kinds of questions and to discuss the ongoing projects. I enjoyed working with you on the OGO projects and even more the board games evenings you organized within SFD.

Tijdens mijn PhD heb ik ook twee masterstudenten mogen begeleiden. Joey en Sterre, jullie zijn op dezelfde dag begonnen aan jullie eindprojecten en gingen als een echte jut en jul aan het werk. Jullie goede inzet en harde werk hebben hoofdstuk 3 en 6 mogelijk gemaakt, bedankt daarvoor. Het is goed om te zien dat jullie beide een PhD zijn begonnen binnen MMP en SFD en ik ben ervan overtuigd dat daar in een paar jaar twee mooie proefschriften uit voort zullen komen.

I am grateful to all the people in SABIC, who helped me with all kinds of analyses during the last four years. Thank you Toob, Jos, Lanti, Julia, Ramon, Jan, Ruud and students Mattieu and Noémie for all your help. Also many thanks to Theo Hoeks, Rieko van Heerbeek and Andre van Zyl, for all the feedback during the progress meetings and the many approvals granted for the research, publications and conferences.

I would like to thank all current and past members of SFD and the ones we adopted from upstairs for the great atmosphere, the discussions and collaborations. Special thanks go to Tom en Marjolijn. Bedankt voor alles wat jullie voor mij hebben geregeld de afgelopen jaren! Aan diegenen die de term collega's zijn gepasseerd. Lieve vrienden, jullie zijn te gek! Ik ga het zeker missen dat ik niet meer dagelijks met jullie zit opgescheept.

Ik wil ook graag mijn paranimfen bedanken. Stijn, wat fijn dat je in de drukke tijd van het afronden van je thesis en het opstarten van je eigen bedrijf ook mijn paranimf wilt zijn. We zijn bijna tegelijk aan onze PhD begonnen en hebben daardoor alle mijlpalen samen doorlopen, het was super dat we samen naar Amerika mochten voor de conferentie. Hoe hard jij kan werken (en feesten) is

ongekend en heeft me erg gemotiveerd. Gilles, wat was ik blij toen je besloot om ook een PhD project te starten binnen SFD. Na al die jaren samen te hebben gestudeerd waren we nu ook collega's, dat hadden we goed geregeld. Ik kon altijd mijn hart bij je luchten en het was fijn om een collega en sfeermaker in de buurt te hebben die me zo goed kent! Bedankt en succes met het laatste stukje van je PhD.

Aan alle lieve vrienden en familie. Bedankt! Jullie zijn in een woord geweldig! Alle weekendjes weg, uitjes, feestjes, terrasjes en spelletjesavonden hebben ervoor gezorgd dat deze jaren omgevlogen zijn! Dat er nog maar vele mogen volgen.

Papa en mama bedankt voor al jullie onvoorwaardelijke steun in de afgelopen jaren en de constante aanmoediging. Erik en Anne, Karin en Rüd, wat leuk dat ik vorig jaar maar liefst vier keer tante mocht worden van jullie prachtige kinderen. En wat leuk dat er binnenkort nog een neefje of nichtje bij gaat komen.

Bas, wat hebben we een enorm druk en super mooi jaar achter de rug met als hoogtepunt onze bruiloft. Bedankt voor je oneindige support en liefde, zonder jou was het allemaal nooit gelukt.





# Curriculum Vitae

Ellen van Heeswijk was born on July 22<sup>nd</sup>, 1992, in Oijen (NL). After graduating from high school at the Titus Brandsmalyceum in Oss in 2010, she moved to Eindhoven to study Chemical Engineering at the Eindhoven University of Technology (TU/e). In April 2015, she successfully defended her master thesis titled: 'An Isocyanate-free approach to waterborne polyurethane dispersions for coating applications'. After an industrial internship at DSM Coating Resins she received her Master's degree in the same year. She then joined the group of 'Stimuli-responsive Functional Materials and Devices' at the same university for her PhD on responsive photonic polymer coatings for plastic substrates based on cholesteric liquid crystals, under supervision of prof.dr. Albert Schenning and in close collaboration with industry (SABIC). The most important results of this research are summarized in this thesis.



# List of Publications

## Publications related to this thesis

- E.P.A. van Heeswijk, J.J.H. Kloos, J. de Heer, T. Hoeks, N. Grossiord, A.P.H.J. Schenning, Well-adhering, Easily Producidble Photonic Reflective Coatings for Plastic Substrates, *ACS Applied Materials and Interfaces* 2018, 10, 35, 3008-30013
- E.P.A. van Heeswijk, A.J.J. Kragt, N. Grossiord, A.P.H.J. Schenning, Environmentally responsive photonic polymers, *Chemical Communications*, 2019, 55, 20, 2880-2891
- E.P.A. van Heeswijk, J.J.H. Kloos, N. Grossiord, A.P.H.J. Schenning, Humidity-gated, temperature-responsive photonic infrared reflective broadband coatings, *Journal of Materials Chemistry A*, 2019, 7, 11, 6113-6119
- E.P.A. van Heeswijk, N. Grossiord, A.P.H.J. Schenning, Tunable photonic materials via monitoring step-growth polymerization kinetics by structural colors, (submitted)
- E.P.A. van Heeswijk, T. Meerman, J. de Heer, N. Grossiord, A.P.H.J. Schenning, Paintable encapsulated body-temperature-responsive photonic reflectors with arbitrary shapes, *ACS Applied Polymer Materials*, 2019 (accepted manuscript)
- H. Khandelwal, E.P.A. van Heeswijk, A.P.H.J. Schenning, M.G. Debije, Paintable temperature-responsive cholesteric liquid crystal reflectors encapsulated on a single flexible polymer substrate, *Journal of Materials Chemistry C*, 2019 7, 7395-7398

- N. Grossiord, E.P.A. van Heeswijk, A.P.H.J. Schenning, T. Hoeks, A. van Zyl, Toolbox to design responsive photonic liquid crystal network coatings on flexible substrates, (submitted)

### **Patents related to this thesis**

- F. di Lena, R. Groote, N. Grossiord, E.P.A. van Heeswijk, Methods for grafting liquid crystalline coatings onto polymer surfaces, WO 2018/122719 A1
- N. Grossiord, E.P.A. van Heeswijk, J.J.H. Kloos, A.P.H.J. Schenning, High-humidity, Temperature-responsive film and self-regulating window using the film, application number 18205371.0-1210

### **Other publications**

- M. Hendriks, J. ter Schiphorst, E.P.A. van Heeswijk, G. Koçer, C. Knie, D. Bléger, S. Hecht, P. Jonkheijm, D.J. Broer, A.P.H.J. Schenning, Re- and preconfigurable multistable visible light responsive surface topographies, *Small*, 2018, 14, 50, 7, 1803274
- G. Filonenko, J.A.M. Lugger, C. Liu, E.P.A. van Heeswijk, M.M.R.M. Hendrix, M. Weber, C. Muller, E.J.M. Hensen, R.P. Sijbesma, E.A. Pidko, Tracking local mechanical impact in heterogeneous polymer with direct optical imaging, *Angewandte Chemie – International Edition* 2018, 57, 50, 16385-16390
- S. Ma, E.P.A. van Heeswijk, B.A.J. Noordover, R.J. Sablong, R.A.T.M. van Bentem, C.E. Koning, Isocyanate-free approach to water-borne polyurea dispersions and coatings, *ChemSusChem*, 2018, 11, 1, 149-158